A Dissertation

entitled

An Investigation Into the Fate of a C5'-Uridinyl Radical

by

Matthew W. Ellis

Submitted to the Graduate Faculty as partial fulfillment of the requirements for the

Doctor of Philosophy Degree in

Medicinal Chemistry

_____
Dr. Amanda Bryant-Friedrich, Committee Chair

_____
Dr. Paul Erhardt, Committee Member

_____
Dr. Zahoor Shah, Committee Member

_____
Dr. Hermann von Grafenstein, Committee Member

_____
Dr. Peter Andreana, Committee Member

_____
Dr. Amanda Bryant-Friedrich, Dean
College of Graduate Studies

The University of Toledo

December 2017

Copyright 2017, Matthew W. Ellis

This document is copyrighted material. Under copyright law, no parts of this document may be reproduced without the expressed permission of the author.

An Abstract of

An Investigation Into the Fate of a C5'-Uridinyl Radical

by

Matthew W. Ellis

Submitted to the Graduate Faculty as partial fulfillment of the requirements for the
Doctor of Philosophy Degree in
Medicinal Chemistry

The University of Toledo

December 2017

Constituents of the endogenous exposome include reactive oxygen species, which cause oxidative damage to nucleic acids, proteins, and lipids. It has been shown that such damage to RNA plays a role in the initiation of neurodegenerative diseases, such as Alzheimer's. To investigate this phenomenon at the molecular level, the synthesis of a modified uridine was improved upon and subjected to photolytic activation, generating a C5'-uridinyl radical mimicking the hydrogen atom abstraction normally observed under conditions of oxidative stress. This was accomplished using a *tert*-butyl ketone at the C5' position, which undergoes Norrish Type I cleavage. Studies were performed under anaerobic conditions in the presence or absence of reductant at varying pH to emulate the diversity of the cellular environment, and it was found that the base release product uracil was predominant. Aerobic conditions were also utilized, which led to the formation of a C5' aldehyde. The C5'-uridinyl radical precursor was further derivatized for its incorporation into oligoribonucleotides. Development of a new automated RNA synthesis method in the 5′ to 3′ direction using 5′ H-phosphonates was initiated. This included the synthesis of the building blocks required for the method development.

“God, grant me the serenity to accept the things I cannot change,

courage to change the things I can,

and wisdom to know the difference.”

- Reinhold Niebuhr

# Acknowledgements

I would like to thank everyone I worked with in the lab for their encouragement and support. I especially want to single out everyone who helped work on my projects in one way or another; Mariah Pasternak, who helped with both synthesizing more precursor and HPLC work, Chris DeRosa and Audrey Corcoran, who helped in the adenosine and cytidine synthesizes, Elijah Harter, who helped with various synthetic schemes, and Akrimah, who will be continuing my project. I would also like to thank Dr. Kim for all his help with NMR and Dr. Prestwich for her guidance on the LCMS.

I want to express my gratitude to everyone who served on my committee; Dr. Erhardt, Dr. Shah, Dr. von Grafenstein, and Dr. Andreana. Thank you for the support in class, the advice, answering chemistry questions, and writing recommendation letters.

Thank you Dr. Amanda. Without you, this would not have happened. You always take the time to speak with students and really care about their success. Thank you for stopping to talk to me after that medicinal chemistry exam nearly five years ago. You didn't know me beyond being one of your almost 200 students, but you still took the time to invest in me. From there you mentored me, built me up, and helped lead me to where I am today. You encouraged me to grow as a person, not just a chemist, and I cannot thank you enough.

Lastly, though not least, I would like to thank my many friends and family for all their support, especially that of my husband Mark.

# Table of Contents

Abstract ..... iii

Acknowledgements ..... v

Table of Contents ..... vi

List of Tables ..... ix

List of Figures ..... x

List of Schemes ..... xiii

List of Abbreviations ..... xiv

List of Symbols ..... xvi

1 Introduction and Background ..... 1

1.1 Endogenous Exposome ..... 1

1.2 Organic Chemistry as a Tool in the Study of RNA Damage ..... 10

1.2.1 Radical Precursors ..... 10

1.2.2 Oligoribonucleotide Synthesis ..... 13

2 Results and Discussion ..... 18

2.1 5' Uridinyl Radical Precursor Synthesis ..... 18

2.2 5' Uridinyl Radical Precursor Photolysis ..... 22

2.3 5' Uridinyl Radical Mechanism ..... 27

2.4 5' Uridinyl Radical Precursor H-Phosphonate Synthesis ..... 28

2.5 H-Phosphonate Monomer Syntheses ..... 30

2.5.1 Overview of 5' H-Phosphonate Synthesis.....30

2.5.2 Uridine 5' H-Phosphonate Synthesis.....32

2.5.3 Cytidine 5' H-Phosphonate Synthesis.....32

2.5.4 Adenosine 5' H-Phosphonate Synthesis.....36

2.5.5 Guanosine 5' H-Phosphonate Synthesis.....37

3 Conclusions….....43

4 Future Work….....45

5 Experimental Procedures.....50

5.1 Materials, Methods, and Equipment.....50

5.2 Synthesis of Novel Compounds.....52

5.2.1 ((3a*R*,4*R*,6*R*,6a*R*)-6-(2-isobutyramido-6-oxo-1,6-dihydro-9*H*-purin-9-yl)-2,2-dimethyltetrahydrofuro[3,4-*d*][1,3]dioxol-4-yl)methyl isobutyrate.....52

5.2.2 1-((2*R*,3*R*,4*S*,5*R*)-4-(bis(4-methoxyphenyl)(phenyl)methoxy)-3-hydroxy-5-(1-hydroxy-3,3-dimethyl-2-oxobutyl)tetrahydrofuran-2-yl)pyrimidine-2,4(1*H*,3*H*)-dione.....53

5.2.3 1-((2*S*,3*R*,4*R*,5*R*)-4-acetoxy-3-(bis(4-methoxyphenyl)(phenyl)methoxy)-5-(2,4-dioxo-3,4-dihydropyrimidin-1(2*H*)-yl)tetrahydrofuran-2-yl)-3,3-dimethyl-2-oxobutyl phosphonate triethylammonium salt……..…..55

5.2.4 ((2*R*,3*R*,4*R*,5*R*)-3-(bis(4-methoxyphenyl)(phenyl)methoxy)-4-((*tert*-butyldimethylsilyl)oxy)-5-(2,4-dioxo-3,4-dihydropyrimidin-1(2*H*)-yl)tetrahydrofuran-2-yl)methyl phosphonate triethylammonium salt .....57

5.3 Photolysis of **96** .....58

5.3.1 Anaerobic Photolysis ..... 58

5.3.2 Aerobic Photolysis ..... 59

A Appendix ..... 60

References ..... 87

# List of Tables

2.1 5' Uridinyl Radical Precursor Synthetic Optimization .....19

2.2 Preliminary Anaerobic 5' Uridinyl Radical Product Distribution.....21

# List of Figures


1-1 Hydroxyl Radical Lesions....2

1-2 Singlet Oxygen Lesions....3

1-3 Formaldehyde Cross-Links....5

1-4 Alkylation Lesions....5

1-5 Halogenation Lesions....7

1-6 Nitration Lesions....7

1-7 Chemical Elucidation Lesions....9

1-8 Norrish Type I Cleavage....12

1-9 Sarcin/Ricin Loop RNA....14

1-10 Formation of 5' Aldehyde....17

2-1 RP-HPLC Results for Anaerobic Photolysis of 5' Uridinyl Radical Precursor....23

2-2 Conversion of 5' Uridinyl Radical Precursor to Uracil under Anaerobic Conditions....23

2-3 RP-HPLC Results for Aerobic Photolysis of 5' Uridinyl Radical Precursor....25

2-4 Guanosine Protecting Groups....38

5-1 ((3a*R*,4*R*,6*R*,6a*R*)-6-(2-isobutyramido-6-oxo-1,6-dihydro-9*H*-purin- 9-yl)-2,2-dimethyltetrahydrofuro[3,4-*d*][1,3]dioxol-4-yl)methyl isobutyrate....52

5-2 1-((2*R*,3*R*,4*S*,5*R*)-4-(bis(4-methoxyphenyl)(phenyl)methoxy)-3-hydroxy-5-(1-hydroxy-3,3-dimethyl-2-oxobutyl)tetrahydrofuran-2-yl)pyrimidine-2,4(1*H*,3*H*)-dione....53

5-3 (2*R*,3*R*,4*R*,5*S*)-4-(bis(4-methoxyphenyl)(phenyl)methoxy)-5-(3,3-dimethyl-2-oxo-1-(phosphonooxy)butyl)-2-(2,4-dioxo-3,4-dihydropyrimidin-1(2*H*)-yl)tetrahydrofuran-3-yl acetate ....55

5-4 ((2*R*,3*R*,4*R*,5*R*)-3-(bis(4-methoxyphenyl)(phenyl)methoxy)-4-((*tert*-butyldimethylsilyl)oxy)-5-(2,4-dioxo-3,4-dihydropyrimidin-1(2*H*)-yl)tetrahydrofuran-2-yl)methyl phosphonate triethylammonium salt ....57

A-1 $^{1}$H NMR for **92** ....61

A-2 $^{13}$C NMR for **92** ....62

A-3 HRMS for **92** ....63

A-4 $^{1}$H NMR for **93** ....64

A-5 $^{13}$C NMR for **93** ....65

A-6 HRMS for **93** ....66

A-7 $^{1}$H NMR for **94** ....67

A-8 $^{13}$C NMR for **94** ....68

A-9 $^{31}$P NMR for **94** ....69

A-10 HRMS for **94** ....70

A-11 $^{1}$H NMR for **95** ....71

A-12 $^{13}$C NMR for **95** ....72

A-13 $^{31}$P NMR for **95** ....73

A-14 HRMS for **95** ....74

A-15 Mass Data for pH 7.0 Aerobic Photolysis Run....75
A-16 Mass Data for pH 3.5 Aerobic Photolysis Run....76
A-17 Mass Data for 11.8 min, pH 7.0 Aerobic Photolysis Run....77
A-18 Mass Data for 11.5 min, pH 3.5 Aerobic Photolysis Run....78
A-19 Mass Data for 12.9-13.3 min, pH 7.0 Aerobic Photolysis Run....79
A-20 Mass Data for 12.9-13.3 min, pH 3.5 Aerobic Photolysis Run....80
A-21 Mass Data for 14.2 min, pH 7.0 Aerobic Photolysis Run....81
A-22 Mass Data for 14.1 min, pH 3.5 Aerobic Photolysis Run....82
A-23 Mass Data for 23 min, pH 7.0 Aerobic Photolysis Run....83
A-24 Mass Data for 24 min, pH 3.5 Aerobic Photolysis Run....84
A-25 Mass Data for 41.0 min, pH 7.0 Aerobic Photolysis Run....85
A-26 Mass Data for 40.9 min, pH 3.5 Aerobic Photolysis Run....86

# List of Schemes


1-1 Adenosyl 4' Radical Mechanism....12

1-2 3'-Deoxy-2'-ketouridine Termini Formation....14

2-1 Synthesis of 5' Uridinyl Radical Precursor....19

2-2 Preliminary Anaerobic 5' Uridinyl Radical Formation....21

2-3 Proposed Mechanism of 5' Uridinyl Radical....26

2-4 Synthesis of Uridine 5' H-Phosphonate Radical Precursor....29

2-5 Synthesis of Uridine 5' H-Phosphonate....31

2-6 Attempted Synthesis of Cytidine 5' H-Phosphonate....33

2-7 Attempted Synthesis of Adenosine 5' H-Phosphonate....35

2-8 Attempted Synthesis of Guanosine 5' H-Phosphonate Using Benzoyl Protecting Groups....39

2-9 Attempted Synthesis of Guanosine 5' H-Phosphonate Using Isobutyryl Protecting Groups....40

2-10 Attempted Synthesis of Guanosine 5' H-Phosphonate Using a Combination of Isobutyryl and Benzoyl Protecting Groups....41

4-1 Proposed Automated RNA Synthesis Approach....47

4-2 Synthesis of Modified Sarcin/Ricin Loop RNA....48

4-3 Photolysis of Modified Sarcin/Ricin Loop RNA....49

# List of Abbreviations

$^{1}$H NMR .....Proton NMR
$^{13}$C NMR .....Carbon NMR
$^{31}$P NMR .....Phosphorus NMR
A.....Adenosine
Ac.....Acetate
ACN .....Acetonitrile
ATP .....Adenosine Triphosphate
Bz .....Benzoyl
BzCl .....Benzoyl Chloride
C.....Cytidine
C2.....Carbon 2
C4.....Carbon 4
C5.....Carbon 5
C6.....Carbon 6
CPG.....Controlled Pore Glass
d.....Doublet
dd.....Doublet of Doublets
DCM .....Dichloromethane
DMAP .....4-Dimethylaminopyridine
DMSO .....Dimethyl Sulfoxide
DMTrCl.....Dimethoxytrityl Chloride
DNA .....Deoxyribonucleic Acids
EA .....Ethyl Acetate
ESI.....Electrospray Ionization
EtOH .....Ethanol
FaPy .....4,6-diamino-5-formamidopyrimidine
FaPyA .....FaPyAdenosine
G.....Guanosine
GSH .....Reduced Glutathione
GSSG .....Oxidized Glutathione
GUA.....Guanosine, Uridine, Adenosine
HPLC .....High-Performance Liquid Chromatography
HRMS .....High Resolution Mass Spectrometry
Ibu .....Isobutyryl
IR.....Infrared
LCMS.....High-Performance Liquid Chromatography-Mass Spectrometry
m .....Multiplet
MeOH .....Methanol

mRNA .....Messenger Ribonucleic Acids
MS.....Mass Spectrometer
NMR .....Nuclear Magnetic Resonance
nt .....Nucleotide
P (III).....Trivalent Phosphorus
P (V).....Pentavalent Phosphorus
Pyr.....Pyridine
O.....Oxygen
OPC.....Oligonucleotide Purification Cartridge
q.....Quadruplet
Q-TOF.....Quadrupole Time-of-Flight
RNA .....Ribonucleic Acids
RP-HPLC .....Reverse Phase-HPLC
rRNA.....Ribosomal Ribonucleic Acids
s.....Singlet
SAM.....S-Adenosyl Methionine
sep .....Septet
siRNA .....Small Interfering RNA
t .....Triplet
*t*-BuLi.....*Tert*-Butyllithium
TBAF .....Tetrabutylammonium Fluoride
TBATB .....Tetrabutylammonium Tribromide
TBDMSCl.....*Tert*-Butyldimethylsilyl Chloride
TBDMSCN .....*Tert*-Butyldimethylsilyl Cyanide
TEA.....Triethylamine
TEA·3HF .....Triethylamine Trihydrofluoride
TEAA.....Triethylammonium Acetate
TEAB .....Triethylammonium Bicarbonate Buffer
TFA.....Trifluoroacetic Acid
THF.....Tetrahydofuran
TLC.....Thin Layer Chromatography
TMSCl .....Trimethylsilyl Chloride
tRNA.....Transfer Ribonucleic Acids
U.....Uridine
UV.....Ultraviolet Light

# List of Symbols

≥ .....Greater than or equal to
'.....Prime
°C .....Degrees Celsius

α .....Alpha
ß.....Beta
∂.....Chemical Shift

Å.....Angstrom
µL.....Microliter
µm .....Micrometer
cm.....Centimeter
eq.....Equivalent
hr .....Hour
hν.....Energy
J .....Coupling Constant
L .....Liter
M .....Molar
mAU.....Milli Absorption Unit
min .....Minute
mL .....Milliliter
mM.....Millimolar
mmol .....Millimole
mv .....Millivolt
Mz .....Magnetic Field Strength
m/z.....Mass per Charge
N.....Normal
nm .....Nanometer
nmol .....Nanomole
W.....Watt

$Ac_2O$.....Acetic Anhydride
$AgNO_3$.....Silver Nitrate
$CDCl_3$.....Dueterated Chloroform
$CH_3COOH$ .....Acetic Acid
$CoCl_2$.....Cobalt(II) Chloride

H.....Hydrogen
$H^+$ .....Proton
$H_2O$ .....Water
$H_2O_2$ .....Hydrogen Peroxide
HCl.....Hydrochloric Acid
HO• .....Hydroxy Radical
HOBr.....Hypobromous Acid
HOCl.....Hypochlorous Acid
HOO• .....Hydroperoxy Radical
$K_3Fe(CN)_6$.....Potassium Ferricyanide
KCN .....Potassium Cyanide
$KHSO_5$ .....Potassium Peroxymonosulfate
MeOH-$d_4$.....Dueterated Methanol
NaOH .....Sodium Hydroxide
$Na_2IrCl_6$.....Iridic Sodium Chloride
$NEt_3$.....Triethylamine
$O_2$ .....Oxygen
$O_2$•-.....Superoxide Radical Anion
$PCl_3$ .....Phosphorous Trichloride

# Chapter 1

# Introduction and Background

## 1.1 Endogenous Exposome

The concept of the exposome was first introduced by Christopher Wild as a way to complement human genomics relative to investigating chronic diseases. The exposome can be defined as the culmination of environmental constituents the body comes in contact with, as well as the biological responses they elicit, from conception to death [1]. The definition was reintroduced in 2014 to include 'endogenous processes' to highlight the way the body reacts to environmental pressures and the complex chemistries resulting from the biochemical reactions that happen in our body like glycolysis and oxidative respiration [2]. Within the scope of the endogenous exposome, this project relates specifically to ribonucleic acids, or RNA.

RNA is transcribed from deoxyribonucleic acids (DNA) and in turn translates to proteins. Unlike DNA, RNA is usually single stranded and resides predominantly in the cytosol of the cell. Due to this, RNA is more susceptible to damage, primarily oxidative. RNA is also susceptible to alkylation, halogenation, and nitration. When RNA gets

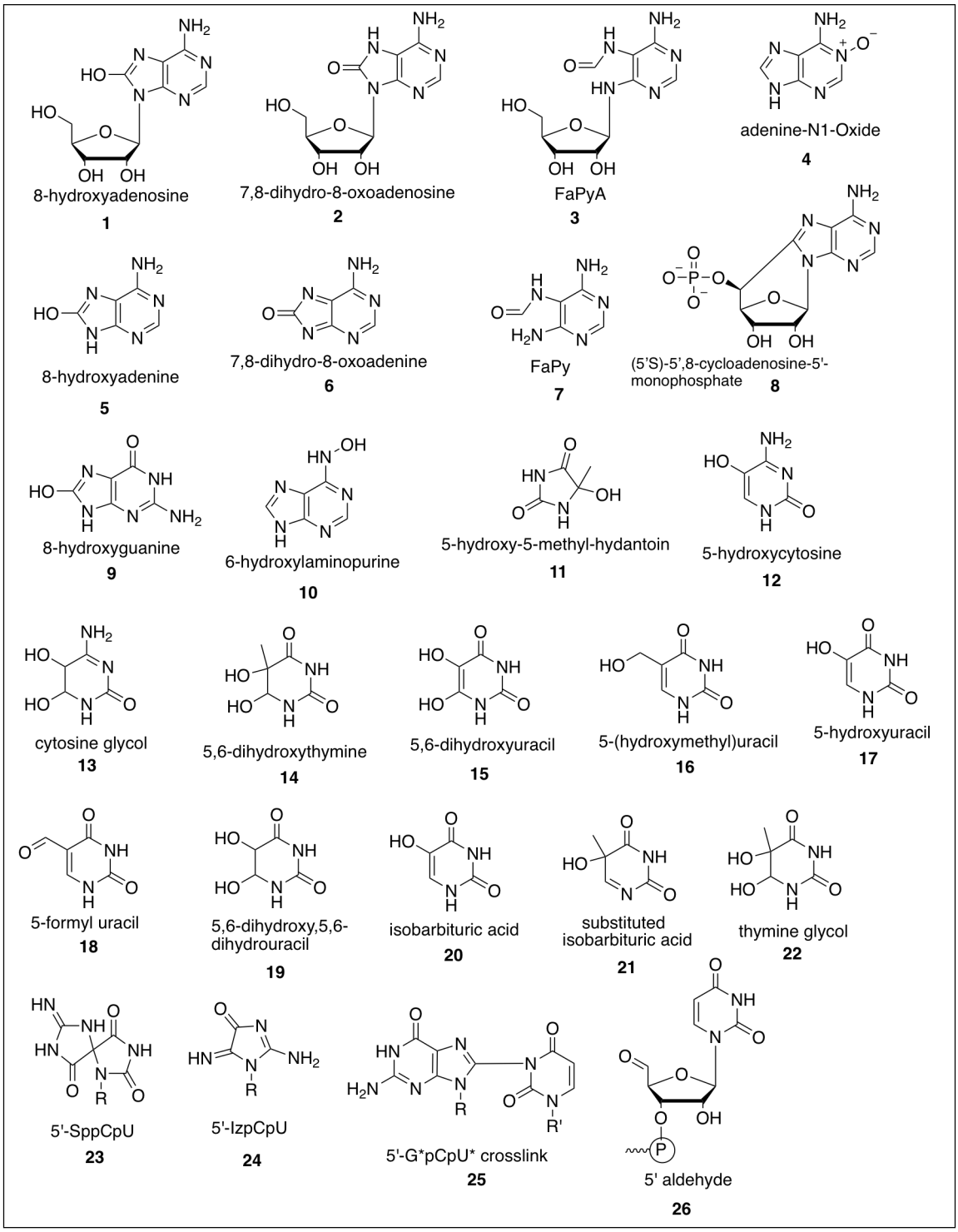


Figure 1-1. Hydroxyl Radical Lesions

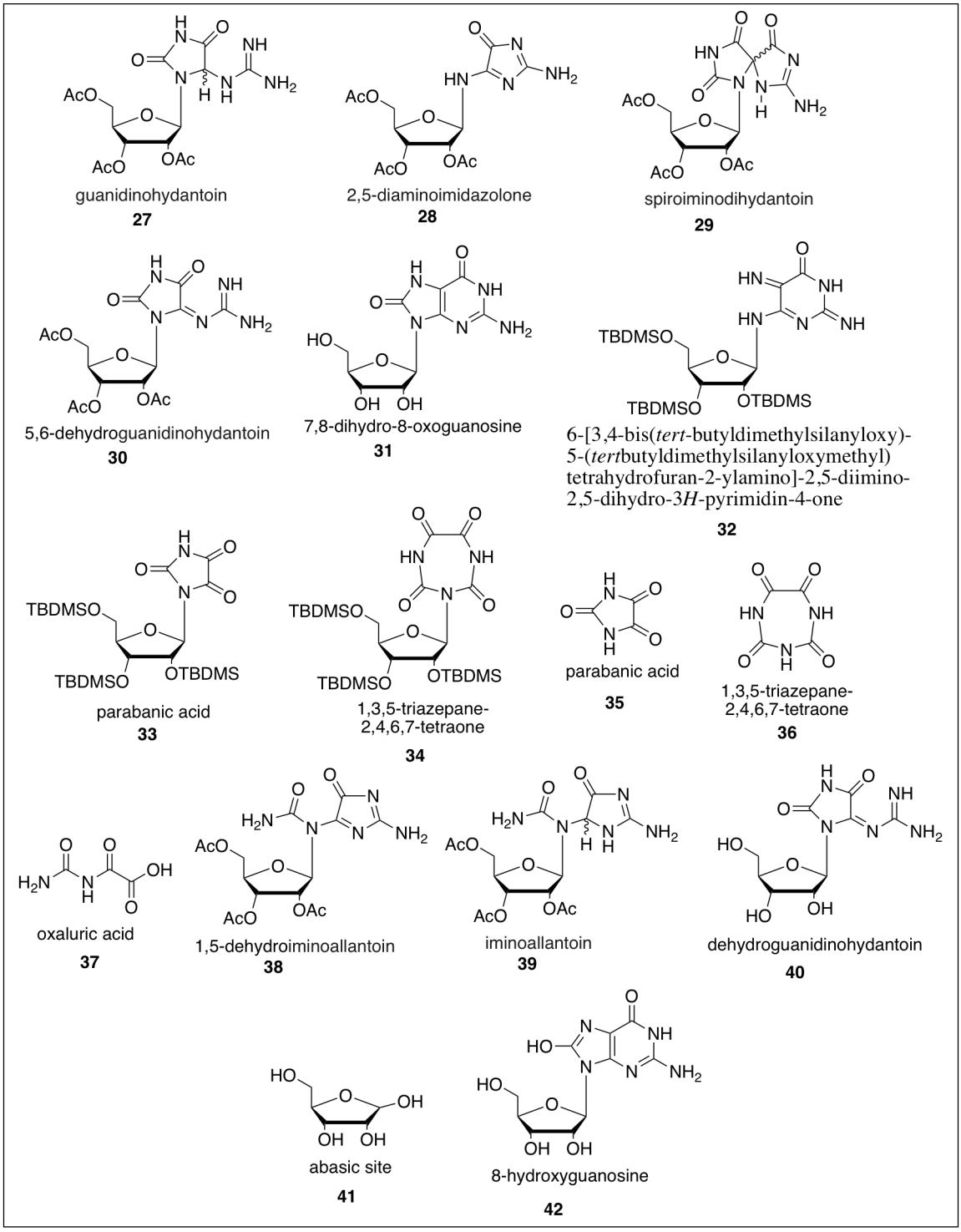


Figure 1-2. Singlet Oxygen Lesions

damaged, it can have deleterious ramifications. RNA lesions can lead to strand scission [3-5], slow down or stop translation [6-8], and change base pairing, making them mutagenic [9-15]. RNA lesions have been implicated in disease states, especially neurodegenerative diseases [16-29].

One of the most common damaging modifications that occurs in RNA is oxidation. The most common and promiscuous oxidative agent is the hydroxyl radical. The hydroxyl radical can abstract a hydrogen atom, undergo radical addition to the molecule, or perform a one-electron abstraction. Some lesions associated with this can be seen in **Figure 1-1**, **1-8** and **26** [30-32]. However, the hydroxyl radical isn't the only oxidizing agent found in the body. Peroxyl radicals can also damage RNA as seen with compounds **5** and **9-16** [33]. Lesions from the sulfoxyl radical are seen with compounds **17** and **18** [34]. Compounds **19-22** are formed *via* the *tert*-butoxy radical [35]. The phosphate radical anion also gives rise to **19** and **20** with substrates uracil and cytosine. [36]. The carbonate radical anions yield **23-25** with a trinucleotide substrate [37].

**Figure 1-2** shows lesions whose formation are associated with singlet oxygen, **27-36** [38-40]. Riboflavin as a one electron oxidant has been employed to study the product distribution of 8-oxoguanosine, wherein **27-30**, **35**, and **37-39** were the products [41]. Another method of investigating electron transfer-mediated damage involves the use of cationic manganese porphyrin associated with $KHSO_5$ as an oxidant [42]. The generated lesions were **29** and **40** when guanosine was in the anticodon of 17-mer tRNA (transfer RNA). This method of studying RNA oxidation also seems to be selective for G residues. $Na_2IrCl_6$, $K_3Fe(CN)_6$, and $CoCl_2$/ $KHSO_5$ are one electron oxidants used to study RNA

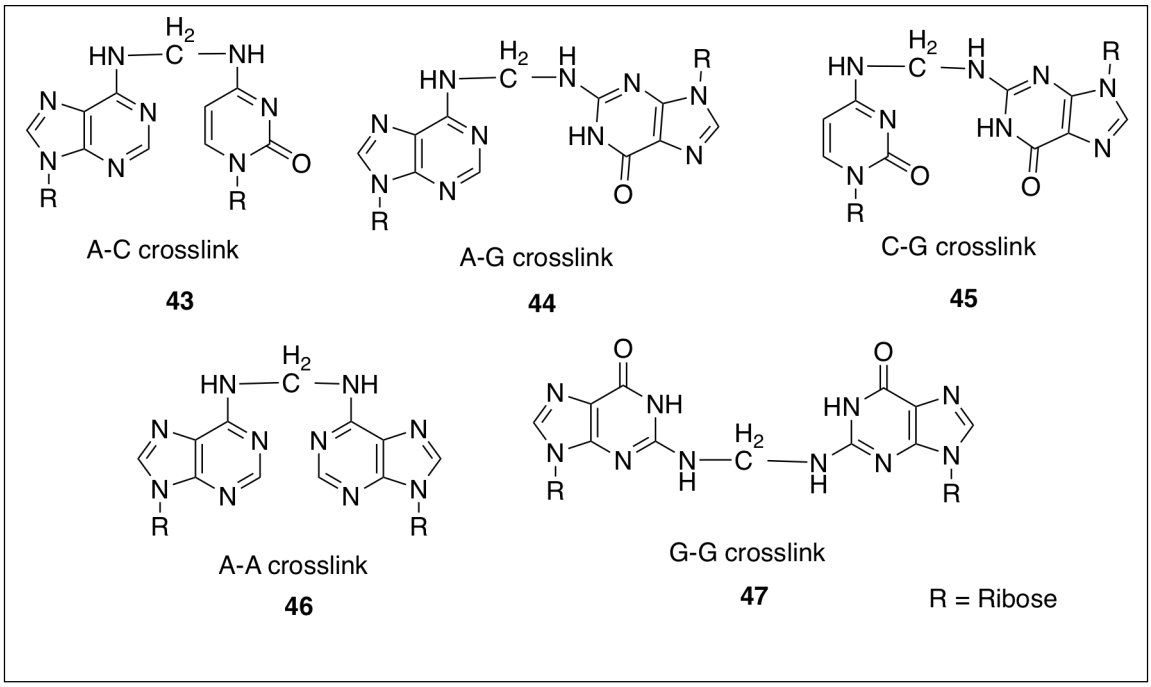


Figure 1-3. Formaldehyde Cross-Links

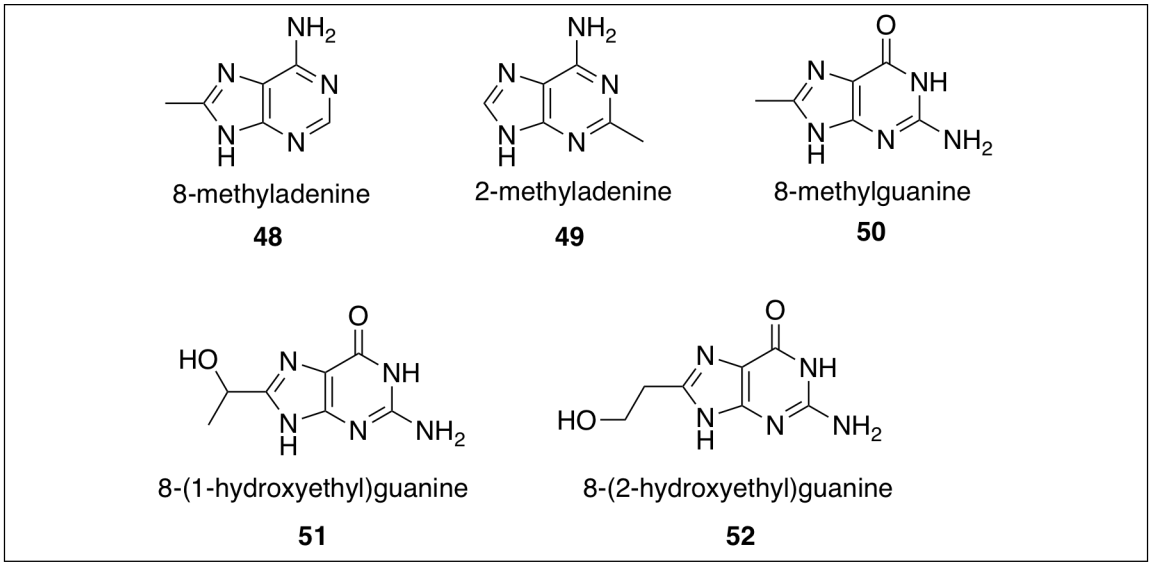


Figure 1-4. Alkylation Lesions

oxidation [43, 44]. Lesions formed in these systems are **27**, **32**, **38**, and **39**. Likewise, cytochrome c/$H_2O_2$ oxidizes guanosine in tRNA and leads to depurination to give **41** and **42** [45]. Cytochrome c, which has also been observed to form a crosslink with RNA, could go on to trigger cellular apoptosis. Formaldehyde can also form cross-links with RNA, as seen in **Figure 1-3** with **43-47** [46].

Oxidative damage to RNA can have a multitude of biological effects. 8-Oxo-7,8-dihydroguanosine is the most common RNA oxidation lesion and is mutagenic [9, 12, 47]. 8-Oxo-7,8-dihydroadenosine, 5-hydroxyuridine, and 5-hydroxycytosine have also been shown to be mutagenic, while 8-oxo-7,8-dihydroadenosine can destabilize RNA in a position-dependent manner [11, 13, 14, 48]. 5-Formyluridine may interfere with RNA metabolism and can base pair with guanine and cytosine, making it mutagenic as well [10]. Abasic sites in RNA templates follow the 'A Rule' as in DNA, where an adenosine is preferentially placed opposite the abasic site, however they are shown to be more stable and more promiscuous compared to their DNA counterpart [49, 50]. Some lesions have been studied for their effect on mRNA (messenger RNA) translation. Abasic sites are non-coding lesions that interrupt peptide synthesis. 8-Oxo-7,8-dihydroguanosine, 8-oxo-7,8-dihydroadenosine, 5-hydroxyuridine, and 5-hydroxycytidine lead to a mixture of full-length and truncated peptides [8].

Another form of RNA damage is alkylation. Normally, the body specifically methylates using SAM (S-Adenosyl Methionine). However, agents, such as the methyl radical, can methylate RNA as well. The methyl radicals usually add to the base, as seen in **Figure 1-4**, **48-50** thus disrupting base pairing [51]. Methylation of tRNAs has been

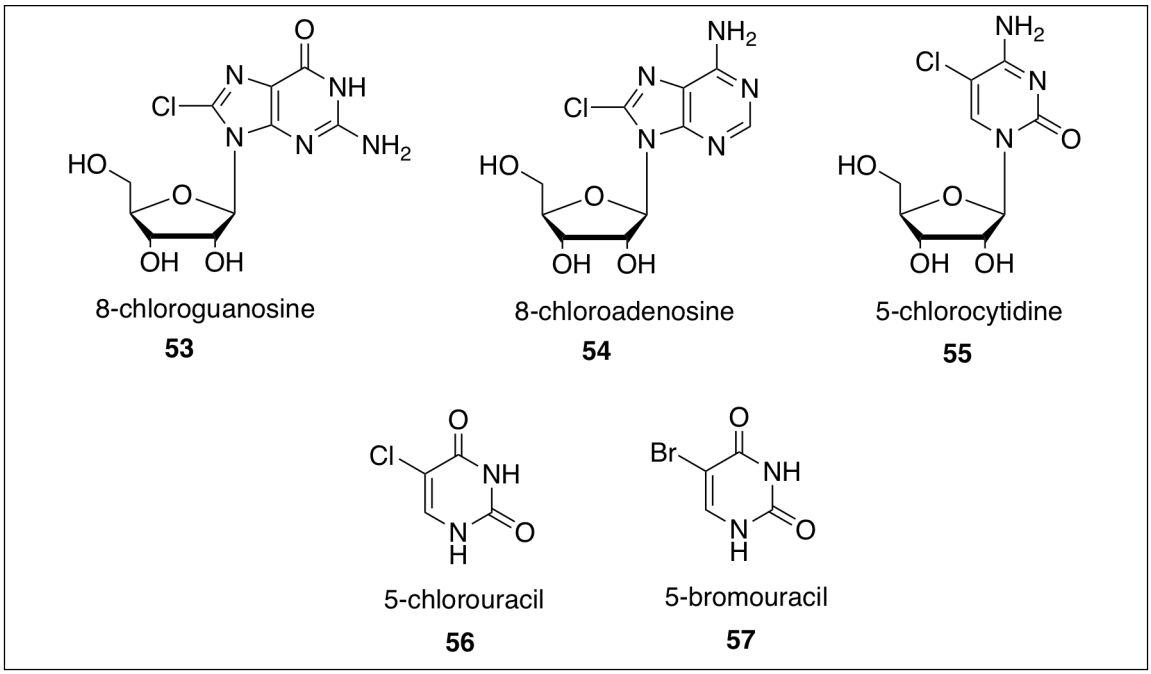


Figure 1-5. Halogenation Lesions

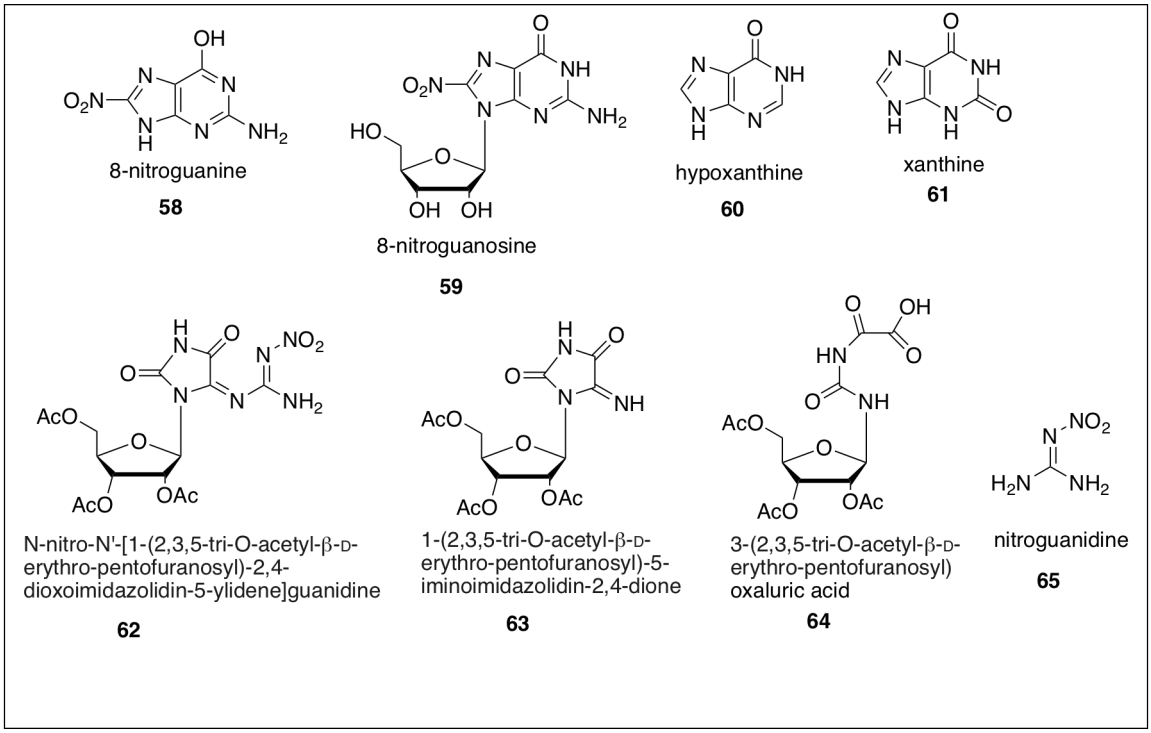


Figure 1-6. Nitration Lesions

shown to inhibit aminoacylation, while methylation of both tRNAs as well as mRNAs can inhibit translation [52]. Methylation can also interfere with tRNA – ribsome binding at the A site [53]. In a Fenton system, ethanol oxidation can lead to oxidation/alkylation lesions **51** and **52** [54, 55]. 8-Methylguanosine, as well as 8-oxo-7,8-dihydroguanosine, have been shown to induce cell proliferation in certain cells, but more work has to be done to investigate the potential of these lesions in free radical-mediated carcinogenesis [56].

RNA can also be halogenated as seen in **Figure 1-5**, and has been shown to be more susceptible to chlorination than DNA [57]. Lesions associated with this can be seen with hypochlorous acid (HOCl), **53-56** [58-60]. In an eosinophil peroxidase system, uracil was brominated to **57** by HOBr [61]. In pre-mRNA, 5-chloro and 5-bromouridine were unable to be recognized for splicing [62]. 8-Chloroadenosine is currently in phase I clinical trials for the treatment of chronic lymphocytic leukemia and has also been looked at for the treatment of breast cancer [63, 64]. The mechanisms by which it acts are inhibition of global transcription and reduction of intracellular ATP (adenosine triphosphate) concentrations.

**Figure 1-6** shows lesions associated with nitration, another important type of damage that effects RNA. Peroxynitrite can react with guanine to form 8-nitroguanine, **58** [65]. In an *H. pylori* infection study, it was shown that there was an increase in 8-nitroguanine due to inflammation [66]. This was also correlated to an increase in gastric cancer in patients. 8-Nitroguanosine, **59**, has been shown to be involved in the pathogenesis of murine pneumotropic virus infections [67]. Unlike DNA, 8-

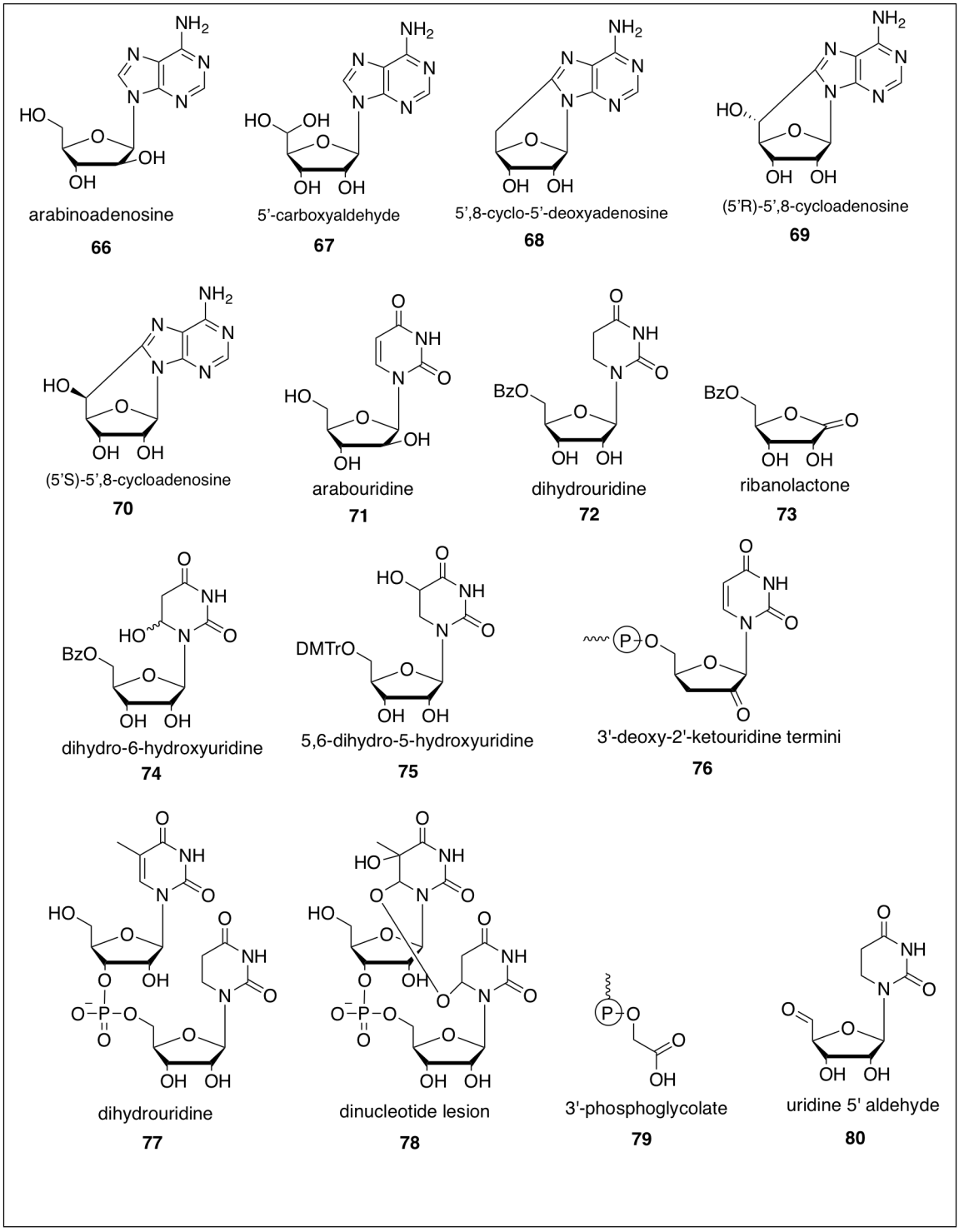


Figure 1-7. Chemical Elucidation Lesions

nitroguanosine is very stable in RNA [68]. Nitric oxide can cause the formation of **60** and **61** from deamination of guanine and adenine in calf thymus RNA. In rat kidneys, hypoxanthine was shown to induce lipid peroxidation [69, 70]. When ribose-protected 8-oxo-7,8-dihydroguanosine was exposed to peroxynitrite, **62-65** were formed [71].

The endogenous exposome has also been investigated using organic chemistry. Not only has the automated synthesis of oligonucleotides been invaluable, but so has the use of radical precursors. There have been a few groups to utilize this method, including our own, to identify **66-80** in **Figure 1-7** [3-5, 72-77]. Dihydrouridine is the most common post-transcriptional modification in tRNA and has the opposite effect of a pseudouridine or ribose methylation modification [78]. Dihydrouridine stabilizes the C2'-endo sugar conformation, giving the RNA more flexibility. This may have an undesired destabilizing effect when present.

## 1.2 Organic Chemistry as a Tool in the Study of RNA Damage

### 1.2.1 Radical Precursors

Radical precursors have been a useful tool for the selective generation of a radical at a site of interest to mimic oxidative damage. This is accomplished by employing a photolabile group, such as a pivaloyl moiety. This functionality when subjected to UV wavelengths ≥ 240 nm causes a Norrish Type I cleavage as seen in **Figure 1-8** [79].

Giese et al. were the first to employ these radical precursors to study RNA when they looked at the 4' position of the sugar in adenosine [77]. A radical precursor with a

photolabile acetyl group was incorporated into a strand of RNA then irradiated to generate the 4' radical. Comparison with the corresponding radical in DNA revealed that the cleavage of the latter was 3 times faster than that of the RNA. Under aerobic conditions it was also found that the presence of the 2' hydroxyl influenced product composition by slowing a ß-elimination of **84** allowing for the attack of water leading to the formation of the 3'-phosphoglycolate **79** as seen in **Scheme 1-1**. The 2' radical in the adenosine monomer was also generated and found to result in the release of adenine [72].

Greenberg et al. group has also worked with radical precursors in RNA. First, their group focused on the C5 and C6 positions of the base in uridine, looking at both monomer and oligomer reactive intermediates. When generating the 5,6-dihydrouridin-6-yl radical in the monomer, dihydro-6-hydroxyuridine **74** was the major product found under aerobic conditions and under anaerobic conditions the reduced dihydrouridine **72** was the major product [3]. It was also reported that the reactivity was similar to the corresponding radical in DNA. The same radical in an oligomer led to strand scission through the formation of a C2' radical intermediate, as did the C5 dihydrouridine radical, which was faster [4, 5, 75]. The proposed mechanism is shown in **Scheme 1-2** leading to the formation of the 3'-deoxy-2'-ketouridine termini **76**. They also generated the C2' radical in uridine and found that it underwent base release to give uracil in monomer studies [74]. Oxygen and β-mercaptoethanol were unable to compete with base loss while thiol was able to compete in less polar solvents. Greenberg's group then incorporated their C2' radical precursor into strands of RNA and investigated it's reactivity [73, 80]. They found that C2′-hydrogen atom abstraction was the rate-determining step, and, like before,

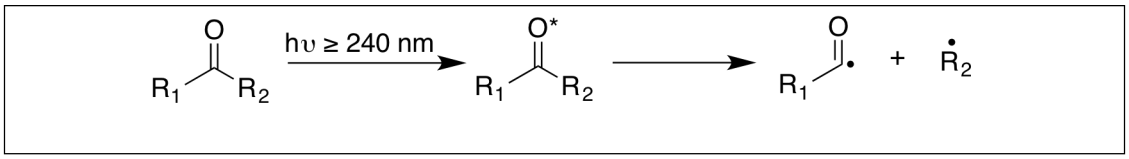


Figure 1-8. Norrish Type I Cleavage

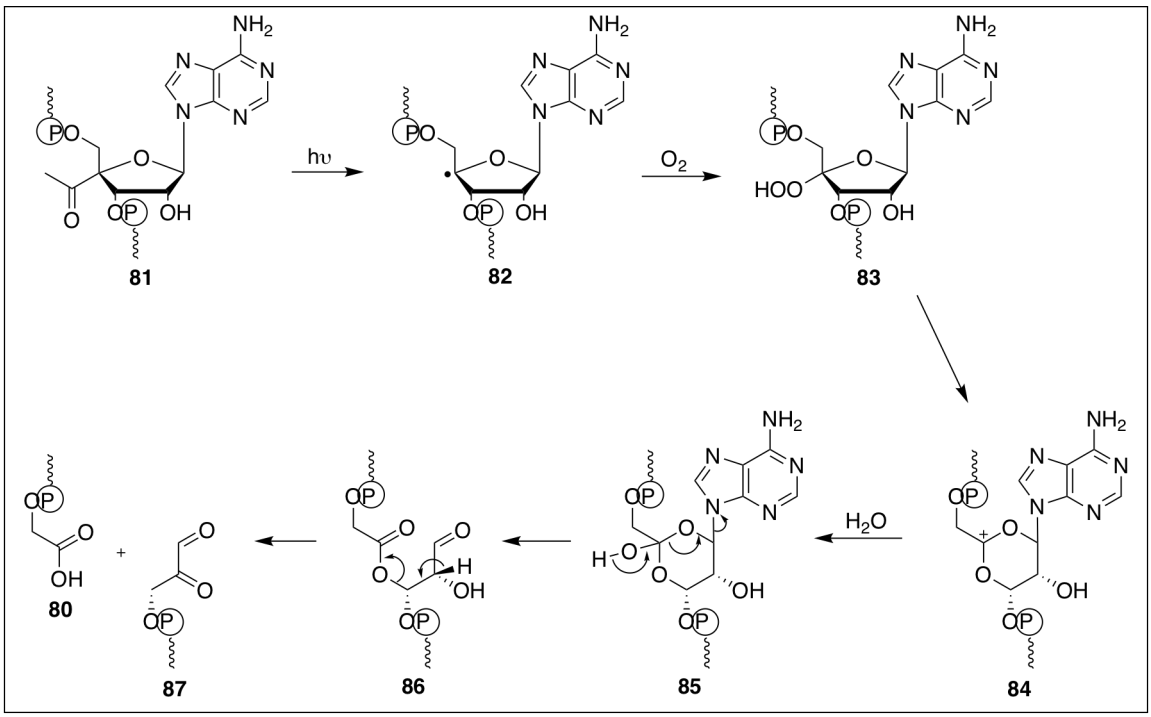


Scheme 1-1. Adenosyl 4' Radical Mechanism

the major product was the 3'-deoxy-2'-ketouridine termini **76**, as well as a 3'-phosphate derived from the site where strand scission occurred. This happened with or without oxygen in the presence of β-mercaptoethanol. Uracil loss still occurred in modified strands, however its formation was unable to compete with the elimination of the 3'-phosphate leading to strand scission. Due to the major group of reactive intermediates formed on pyrimidines, the hydroxyl radical adducts, and the role the C2′-hydroxyl plays in the rate limiting step, it can be suggested that RNA appears to be more susceptible to strand scission than DNA.

### 1.2.2 Oligoribonucleotide Synthesis

Automated oligonucleotide synthesis is widely used to synthesize strands of DNA and RNA for various uses. The basis for which this works is the coupling of the phosphorous moiety of the added nucleotide with the free hydroxyl group of the extending strand of nucleotides. This process includes coupling, oxidation, and deprotection steps, which are repeated until the desired length is achieved. Automated RNA synthesis can be accomplished using a variety of building blocks, however the most commonly used are the phosphoramidites and H-phosphonates. Both utilize the same base protecting groups such as benzoyl and isobutyryl and both use similar sugar protecting groups such as dimethoxytrityl for 5' protection and a *tert*-butyldimethylsilyl for 2' protection. The difference is in the phosphorus moiety at the 3' position, which both utilize P(III). Many phosphoramidites contain a bulky diisopropyl-amino group and require a cyanoethyl protecting group while the H-phosphonate contains a phosphoryl

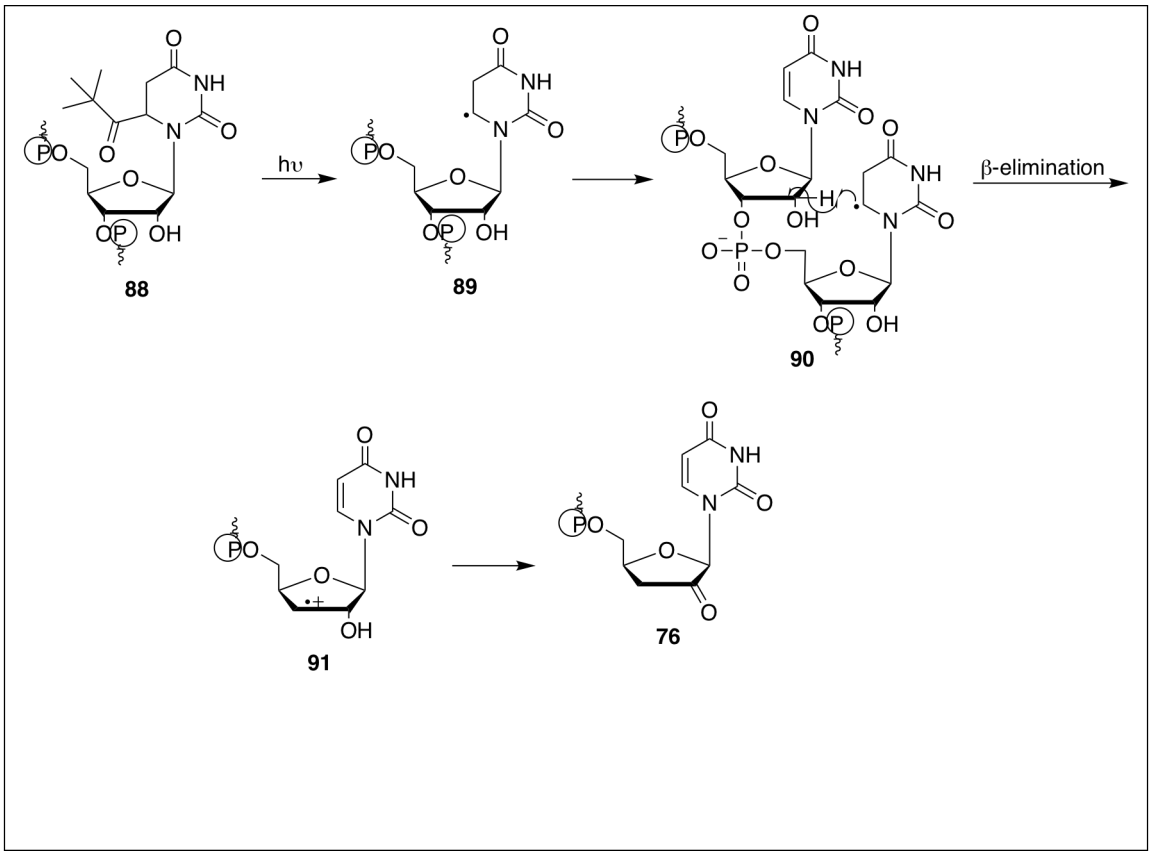


Scheme 1-2. 5,6-Dihydrouridin-6-yl Radical Mechanism

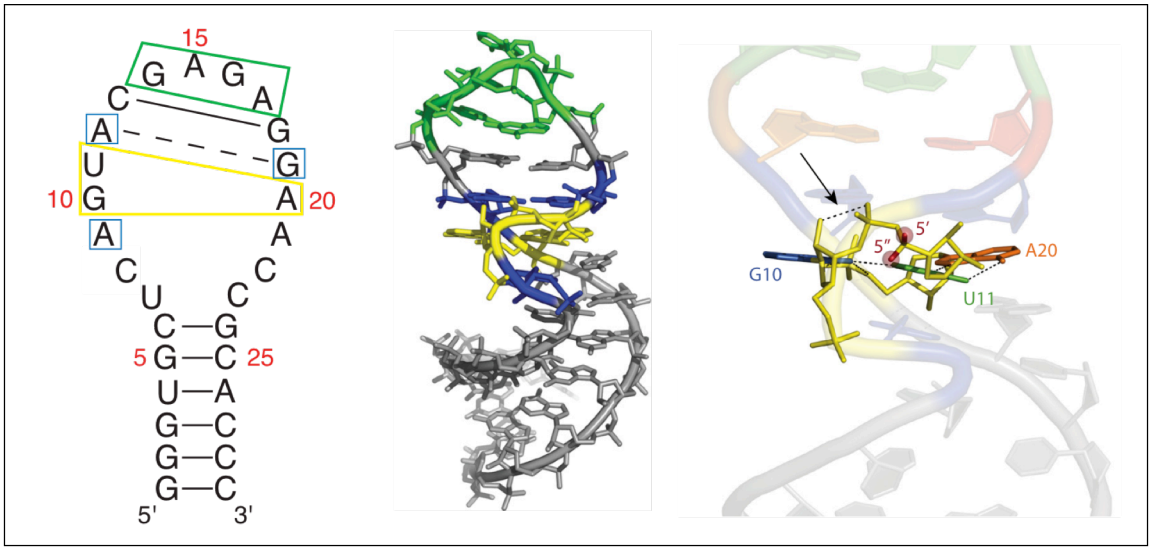


Figure 1-9. Sarcin/Ricin Loop RNA [32]

functionality as well as a hydrogen atom attached to the phosphorous. Due to this difference, the automated synthesis using these methods must be altered slightly. H-Phosphonates have a tetrahedral geometry like P(V) compounds and lack a pair of electrons, making them electrophilic [81]. This makes them much more stable to oxidation compared to phosphoramidites, which require an oxidation step after each coupling cycle. Aside from this, the steps for the two are very similar. First, the dimethoxytrityl group is removed giving a free 5' hydroxyl to couple with the added monomer, which is facilitated by an activator. After the condensation, there is a capping step to ensure no further reactivity. Finally, in the case of the phosphoramidite, there is the oxidation step. This is repeated until the oligomer is of the desired length, then the final base and 2' deprotections, as well as the removal of the solid support, are performed.

*In vitro* transcription has also been useful for the investigation of RNA damage. This method utilizes an RNA polymerase and a template strand of DNA, which transcribes to the complementary strand of RNA. This method was utilized by Tullius et al. to obtain the sarcin/ricin loop RNA as shown in **Figure 1-9**. It was determined that the structural environment that occurs within a GUA triplet in RNA leads to unusual reactivity of a hydroxyl radical with the C5' hydrogen of the uridine [32]. They showed that the hydroxyl radical abstracted the C5' hydrogen on U11 in the sarcin/ricin loop and gave rise to the 5' aldehyde terminus **26** at the cleavage site as shown in **Figure 1-10**.

All of the work reported in this chapter was done with RNA substrates. However, much of the work in the field of nucleic acid damage has been conducted on DNA. Though the presence of the 2' hydroxyl group changes its reactivity, many of the lesions found in DNA may also be present in RNA. More work must be completed in this field in

order to further elucidate the diversity of RNA damage and to be able to better compare the damage that occurs in nucleic acids.

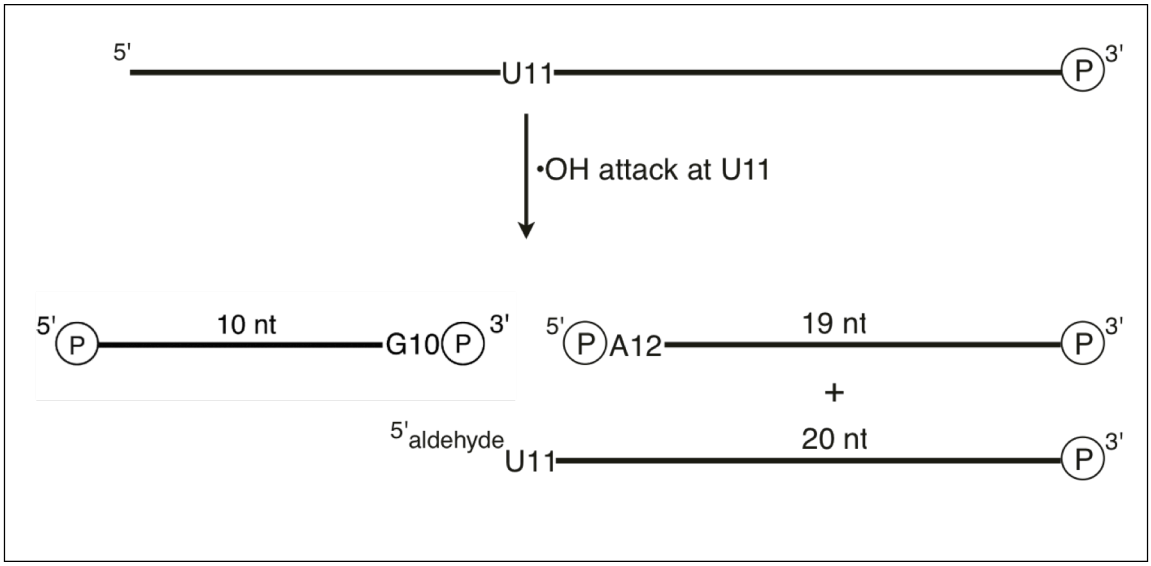

Figure 1-10. Formation of 5' aldehyde [32]

# Chapter 2

# Results and Discussion

## 2.1 5' Uridinyl Radical Precursor Synthesis

As shown in Chapter 1, RNA damage can take many forms and have a multitude of adverse effects in the body. Both the base and sugar portion of RNA are susceptible, and there are many different causative agents. Of these, oxidation is the most prevalent, and the most promiscuous oxidizing agent is the hydroxyl radical. To study oxidative damage, it is helpful to look at the reactivity of specific nucleic acid radicals. Just as Giese's group investigated the 4' position of adenosine and Greenberg's group the 2' position of uridine, so has our group studied the 5' position of uridine, which Tullius' group has shown to generate the radical of interest under certain RNA structural motifs in the presence of the hydroxyl radical [32, 72-74, 76, 77, 80].

To site-specifically generate the 5' radical, a *tert*-butyl ketone, or pivaloyl group, was installed on the 5' position of the sugar in uridine. This was previously accomplished by our group and the first part of this project was to validate and optimize the synthesis shown in **Scheme 2-1** [76]. Conditions explored for the optimization can be shown in **Table 2-1**.

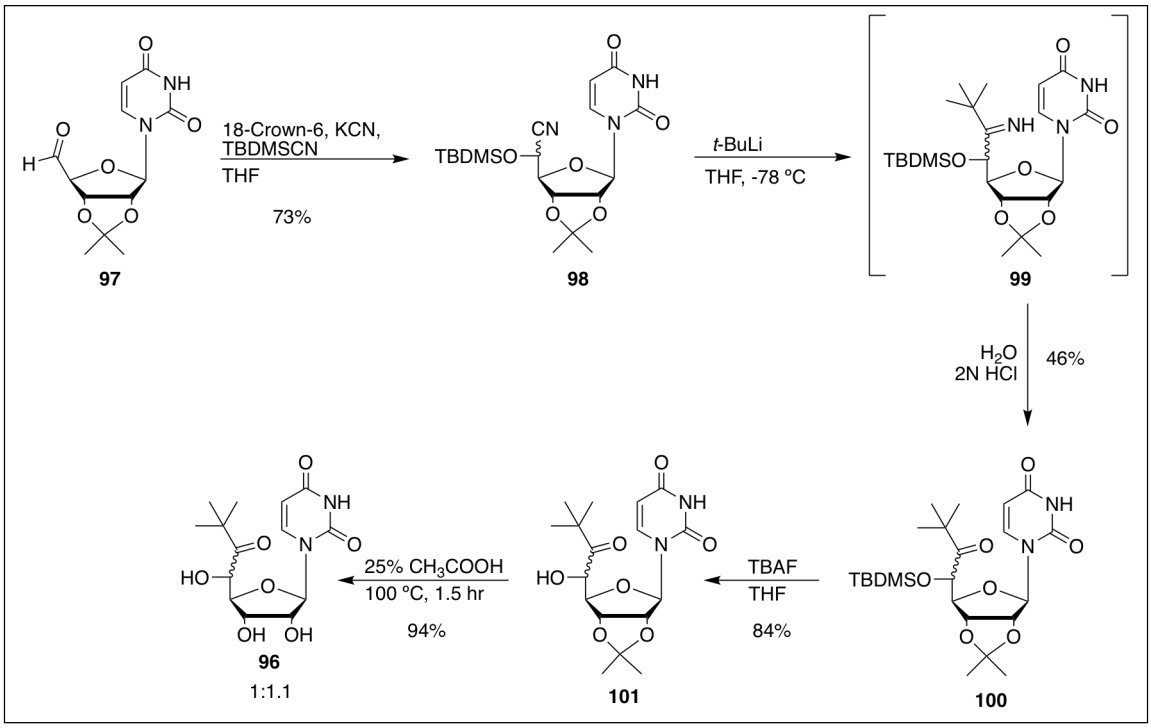


Scheme 2-1. Synthesis of 5' Uridinyl Radical Precursor

| *t*-BuLi Reaction Conditions | Crude % Yield of **99** | Hydrolysis Conditions | % Yield of **100** |
|---|---|---|---|
| 15 min | - | THF, pH 7 | 15 |
| 2 min | 43 | - | - |
| 4 min | 71 | - | - |
| 8 min | 63 | - | - |
| 4 min | - | THF, pH 6 | 30 |
| 4 min | - | pH 6, added ACN, 30 ºC | 18 |
| 4 min | - | ACN, pH 4, 60 ºC | 46 |

Table 2-1. 5' Uridinyl Radical Precursor Synthetic Optimization

Compound **97** was made from uridine following standard literature protocols, with the entire synthesis itself being based on work by Chatgilialoglu [82-84]. Compound **97** was treated with *tert*-butyldimethylsilyl cyanide (TBDMSCN) in the presence of catalytic amounts of 18-Crown-6 and potassium cyanide (KCN) in THF (tetrahydrofuran) to give compound **98** as a mixture of diastereomers [76]. Cyanohydrin **98** was then converted to the imine using *t*-BuLi (*tert*-butyllithium) at – 78 ºC followed by hydrolysis to give protected ketone **100** [76]. This was followed by the use of TBAF (tetrabutylammonium fluoride) to remove the 5' silyl group and then acid hydrolysis to give radical precursor **96** [76].

**Table 2-1** shows the conditions used in the optimization of the reaction conditions leading from cyanohydrin **98** to ketone **100**. The first step was to find the best reaction time for the *t*-BuLi reaction. Initially, 15 min was used, however it should not take so long for the completion of this reaction and prolonging the exposure to *t*-BuLi may lower the yield. *t*-BuLi is an extremely reactive reagent, so much so that it will combust upon exposure to the air. It will even react with the solvent, THF [85]. Using 4 equivalents of *t*-BuLi means that there is extra reagent present able to participate in side reactions after it has reacted with the nucleoside at the nitrile. Starting from 2 min, the time was increased to 4 min then 8 min, which showed that 4 min had the highest crude yield for the reaction. Next, the hydrolysis conditions were tested. Initially THF was used with water and 2 N HCl (hydrochloric acid), however when the pH was tested, it was still too close to 7. In order to facilitate the acid hydrolysis without the removal of any of the acid labile protecting groups, the pH was maintained between 5-6. Simply reducing the *t*-BuLi reaction time to 4 min and the pH to 6 doubled the percent yield, but the reaction still

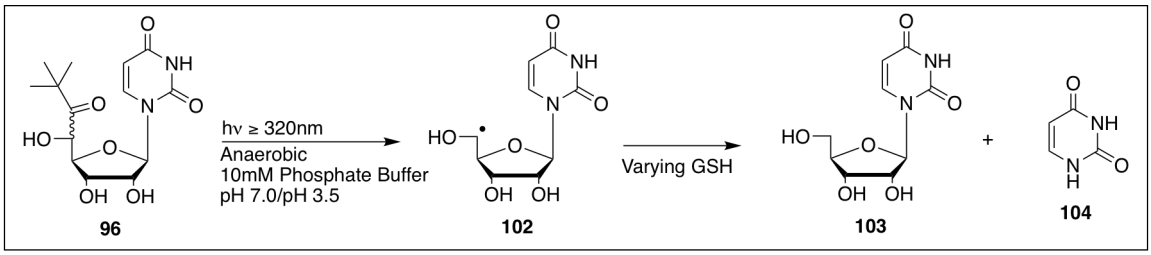


Scheme 2-2. Preliminary Anaerobic 5' Uridinyl Radical Formation

| pH | GSH (mM) | Uridine **103** (%) | Uracil **104** (%) |
|---|---|---|---|
| 7.0 | 0 | n.d. | 33.9 ± 0.83 |
| | 2 | 7.12 ± 0.12 | 43.7 ± 4.98 |
| | 4 | 9.44 ± 0.02 | 44.3 ± 3.26 |
| | 8 | 7.30 ± 1.45 | 47.8 ± 2.86 |
| | 16 | 7.79 ± 2.96 | 43.1 ± 3.75 |
| | 24 | 10.5 ± 0.87 | 42.3 ± 5.51 |
| | 32 | 15.4 ± 0.55 | 43.3 ± 3.21 |
| 3.5 | 0 | n.d. | 13.6 ± 1.15 |
| | 2 | 30.3 ± 0.75 | 10.4 ± 0.45 |
| | 4 | 45.7 ± 2.10 | 11.2 ± 1.09 |
| | 8 | 54.6 ± 0.45 | 11.2 ± 0.17 |
| | 16 | 66.9 ± 2.39 | 10.7 ± 0.17 |
| | 24 | 70.0 ± 0.72 | 8.38 ± 1.52 |
| | 32 | 75.9 ± 1.82 | 8.55 ± 1.26 |

Table 2-2. Preliminary Anaerobic 5' Uridinyl Radical Product Distribution

took 91 hours. On the second attempt, just water and acid were used while adjusting the temperature to 30 ºC after 23 hours. There were solubility issues with the nucleoside, and, after 43 hours, ACN was added. The initial, and continued heating, as well as the addition of acetonitrile both appeared to drive the reaction forward. However, the total reaction time was 94 hours. Acetonitrile (ACN) is a more polar aprotic solvent than THF and can aid in the solubility of the compound, which was seen. Going forward, ACN and heat were added from the beginning, heating up to 60 ºC. The pH was also adjusted more acidic, to pH 4. This reaction only took 90 min to complete with much higher yield.

### 2.2 5' Uridinyl Radical Precursor Photolysis

To investigate the reactivity of the 5' uridinyl radical, precursor **96** was photolyzed under a variety of conditions. Our lab previously ran a study showing the differences in product distribution when photolyses were performed at either pH 7.0 or pH 3.5 under anaerobic conditions with varying amounts of GSH for one hour, which is shown in **Scheme 2-2** and **Table 2-2** [76]. This showed that uracil formation was not GSH dependent like uridine formation. It also showed that reduction by GSH was much more efficient at lower pH, which confirms what has been reported in the literature [86].

The 5' uridinyl radical reactivity was further investigated in my project under anaerobic conditions using a physiologically relevant amount of GSH (8 mM) in phosphate buffer at pH 7.0 with varying photolysis times (1, 2, 4, 8, 15, 30, and 60 min). This was done to ascertain whether any reactive intermediates were forming within that 60 min window.

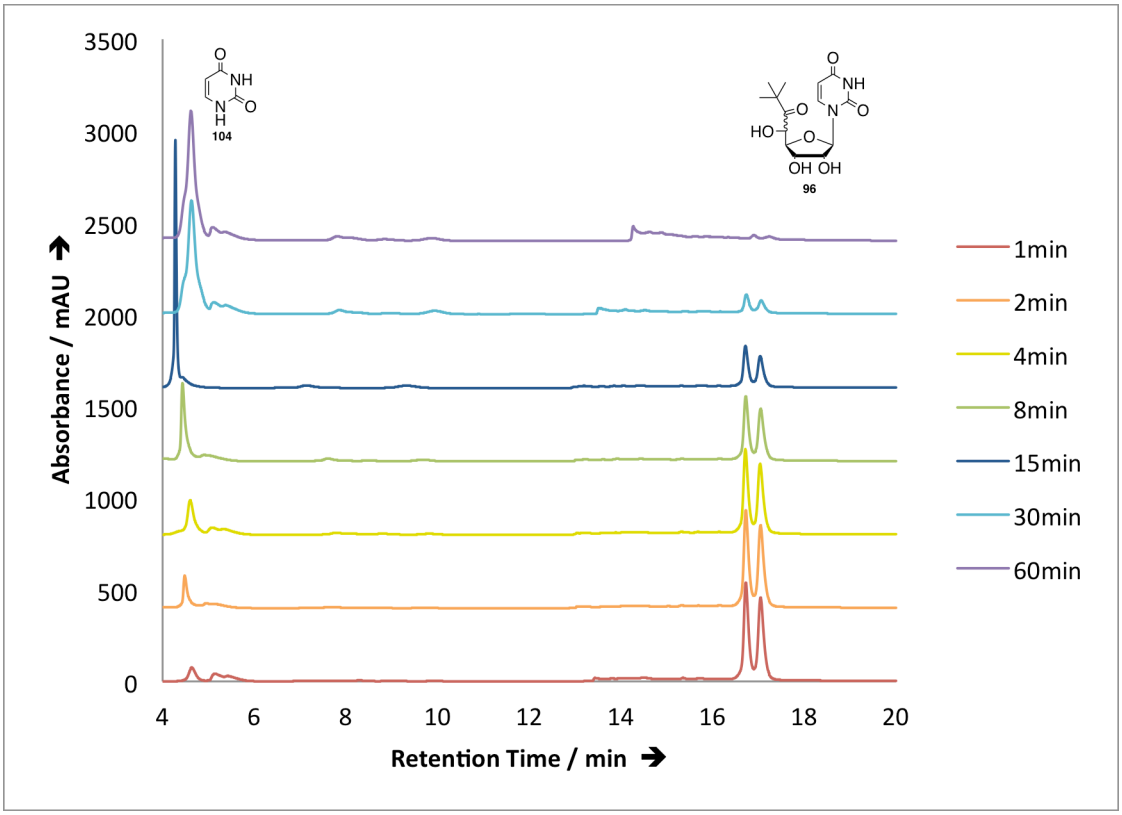


Figure 2-1. RP-HPLC Results for Anaerobic Photolysis of 5' Uridinyl Radical Precursor

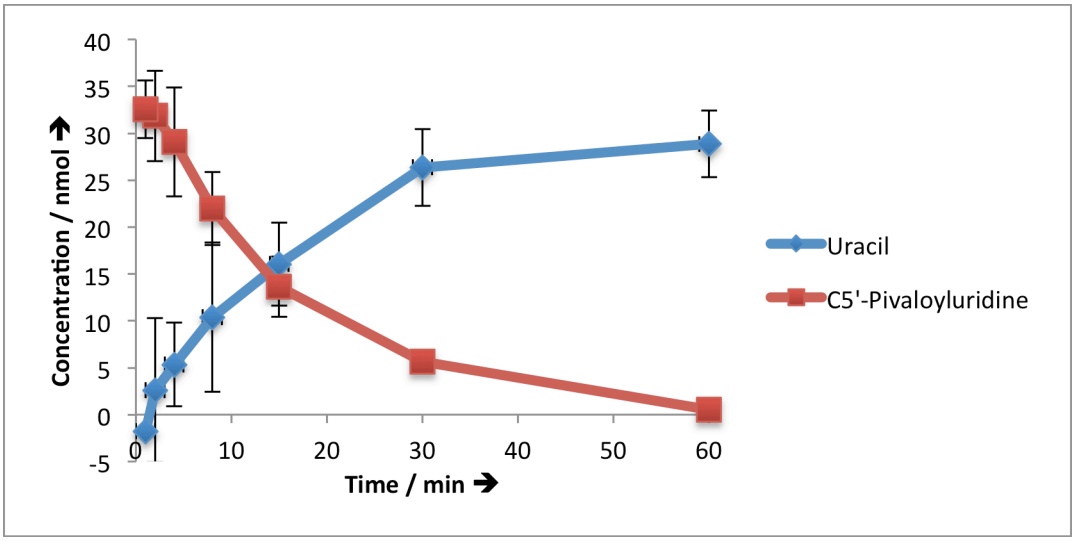


Figure 2-2. Conversion of 5' Uridinyl Radical Precursor to Uracil under Anaerobic Conditions

The RP-HPLC results were overlaid in **Figure 2-1**. Here, there were no UV active intermediates found and uridine was below the limit of detection. The mass recovery in this study was 80 – 93% and it was shown that after 60 min there was a 78% conversion of radical precursor **96** to uracil, as seen in **Figure 2-2**.

This project was continued to photochemically generate the 5' uridinyl radical under aerobic conditions using 8 mM GSH and 10 mM ammonium acetate at pH 7.0 and 3.5 for 30 min. The results can be seen in **Figure 2-3**. It was found that the 5' aldehyde (11.8 min), or its corresponding hydrate, as well as the base elimination product uracil (12.9 min) were the major products formed. Small amounts of uridine (18.8 min) were also observed, as well as some peaks that we were unable to identify at both pH 7 and 3.5. The peak at 24 min was seen when GSH was injected alone, and the masses observed are 613.5 and 307.4 in positive ion mode and 611.4 in negative ion mode. This points towards oxidized GSH (GSSG) at 612.63. The peaks at 39.2 min and 43.9 min are in the blank for the column. The percent conversion of the precursor to radical related products was 56.2% at pH 7 and 58.0% at pH 3.5. Of the amount of radical generated, there was 1.7% conversion to uridine at pH 7 and pH 3.5. For uracil, there was 14.4% conversion at pH 7 and 15.1% at pH 3.5. Based on calculations for the 5' aldehyde, it is 108.7% and 110.0% for pH 7 and 3.5 respectively. For the 5' aldehyde, the calculations are slightly skewed due to what must be another UV active compound with a very similar retention time. Accounting for uracil and uridine formation, as well as a small amount of unknown product, the conversion to the 5' aldehyde is close to 80%. This is also confirmed with what is seen on MS.

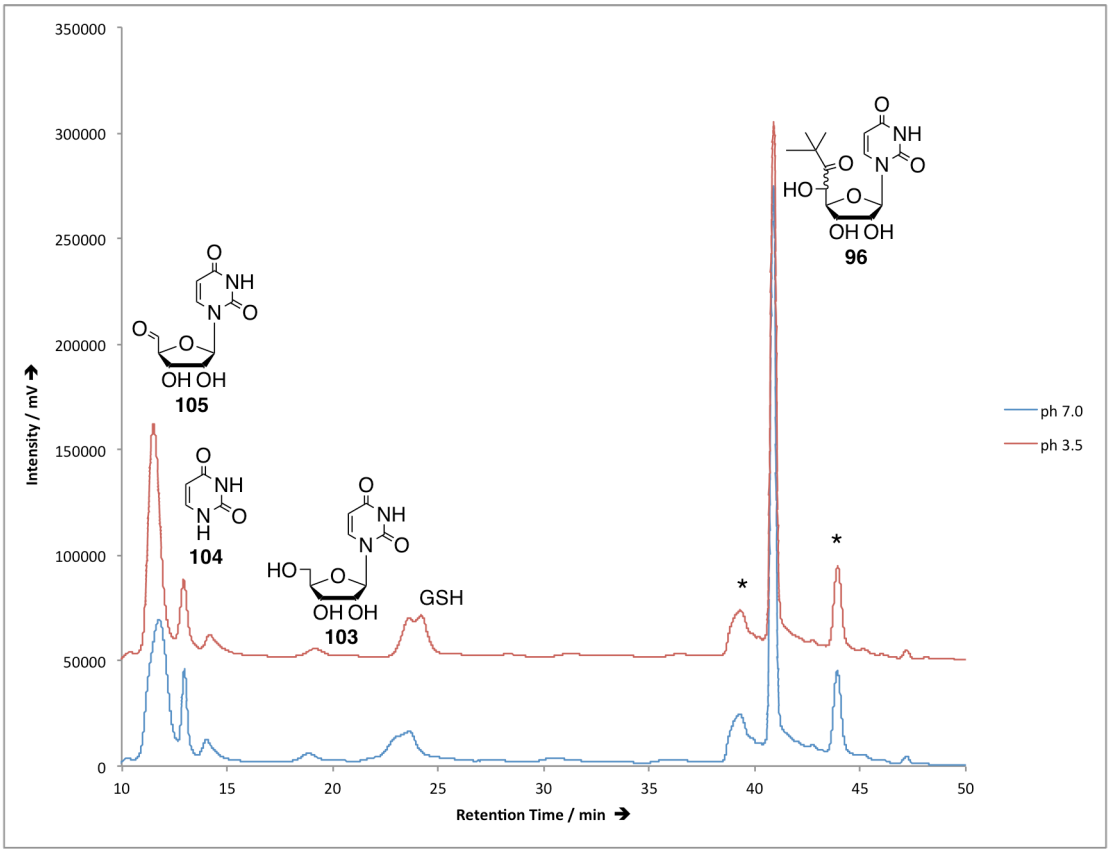


Figure 2-3. RP-HPLC Results for Aerobic Photolysis of 5' Uridinyl Radical Precursor
* Column Contaminants

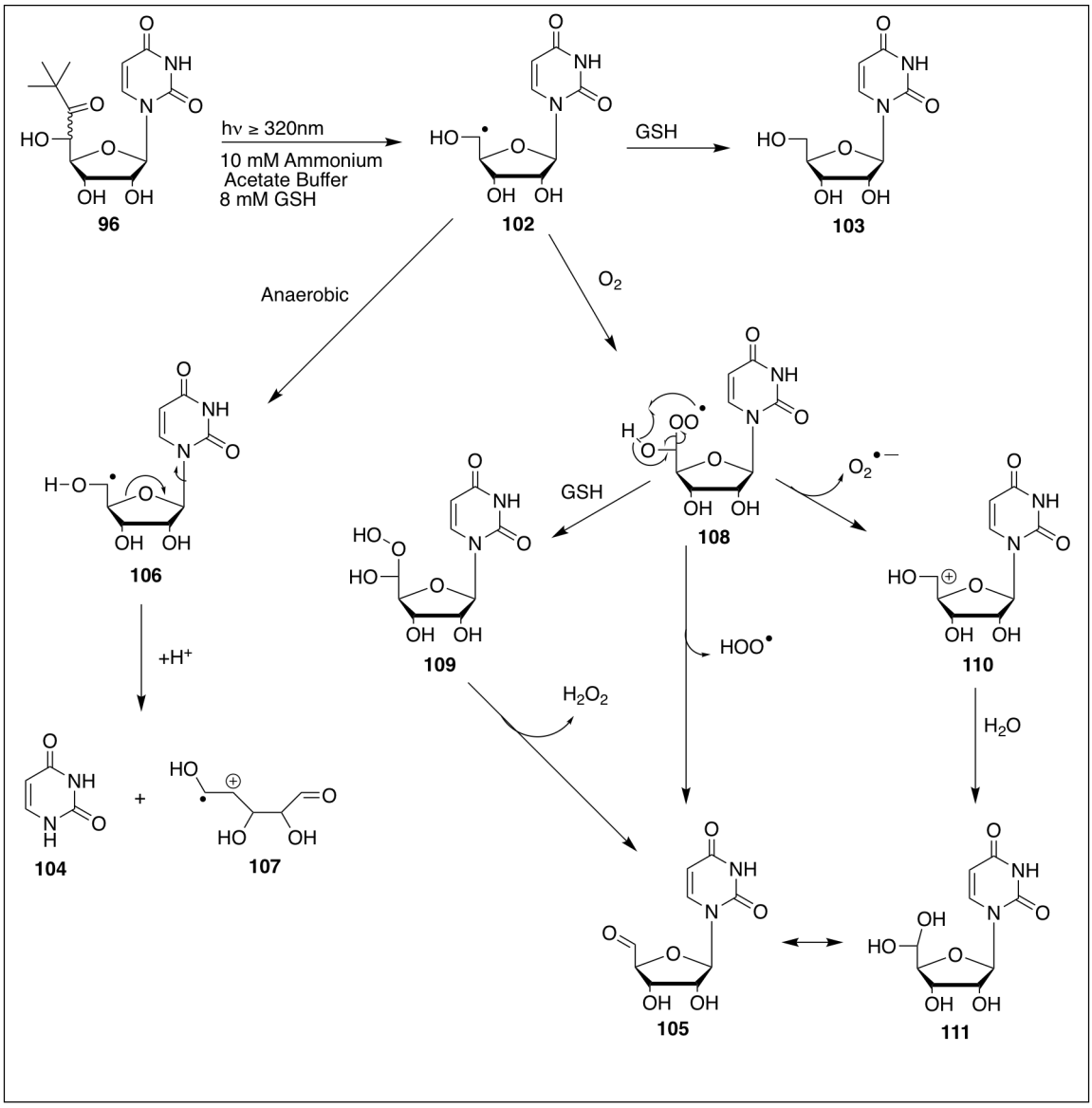


Scheme 2-3. Proposed Mechanism of 5' Uridinyl Radical

## 2.3 5' Uridinyl Radical Mechanism

The formation of uridine suggests that radical **102** is indeed generated and involved in the degradation of the molecule. Uracil formation was found to be independent of glutathione concentration under anaerobic conditions, and there were no other compounds identified. This suggests a competition, under anaerobic conditions, of base release and reduction by GSH, the former of which appears to be much faster under physiological conditions. **Scheme 2-3** shows the proposed mechanism under both anaerobic and aerobic conditions [76]. It is suggested that the C4'-O bond breaks in a ß-elimination reaction to release uracil, facilitating ring opening. ß-Elimination reactions are common when dealing with radicals, and uracil is an excellent leaving group [87, 88]. This mechanism appears to be in competition with the fate of the radical under aerobic conditions. Oxygen can react at a rate to of $10^9$, while GSH reacts at a rate of $10^6$ in nucleic acid radicals, which explains why so little uridine is seen [89].

Once intermediate **108** is formed, there are three possible outcomes. First, reduction by GSH can to lead to the hydroperoxide **109**, which would have a similar reaction rate as before. Second is the loss of $O_2$•-, superoxide radical anion, leaving a positive charge on the 5' position, which would lead to the nucleophilic addition of water and hydrate formation. This process can occur at a rate of $10^4$ making it unable to compete with GSH [90]. The third possibility is the loss of HOO•, hydroperoxy radical. This loss has been shown to occur via the mechanism shown in **Scheme 2-3** [91-96]. It is also a much more favorable outcome compared to the loss of $O_2$•- or the H atom abstraction event that could occur [91, 93]. A study of α–amino-peroxyl radicals showed that

in a vacuum, the H atom abstraction event was on the order of $10^8$ while the loss of the HOO• was $10^{12}$. They also found that α–hydroxy-peroxyl radicals were more likely to undergo loss of the HOO• and that a polar solvent system made it even more favorable [91]. MS and RP-HPLC confirmed formation of **105** as the major lesion, and, to our knowledge, this is the first time this lesion has been identified in a monomeric ribonucleoside.

### 2.4 5' Uridinyl Radical Precursor H-Phosphonate Synthesis

In order to further study the reactivity of the 5' uridinyl radical and the effect of RNA damage, the 5' uridinyl radical precursor **96** needs to be incorporated into strands of RNA. To accomplish this, **96** was derivatized to contain a 5' H-phosphonate with the appropriate protecting groups for RNA synthesis. The synthesis is shown in **Scheme 2-4**. First, **96** was protected with a dimethoxytrityl group on the 3' hydroxyl using DMTrCl and DMAP in pyridine. Compound **93** was then acylated at the 2' hydroxyl using $Ac_2O$ (acetic anhydride) $NEt_3$ and a catalytic amount of DMAP in DCM [97, 98]. This was then subjected to H-phosphonate addition conditions using $PCl_3$ and $NEt_3$, then TEAB. Compound **113** was confirmed by HRMS, however the $^{31}P$ NMR clearly shows that it was oxidized to monophosphate **94**. Though H-phosphonates are more stable to oxidation than their phosphoramidite counterparts, it can still occur [99]. Likely, the purification of compound **113** left it too exposed. In the future, this should be used without further purification, as are many H-phosphonates, to prevent this issue.

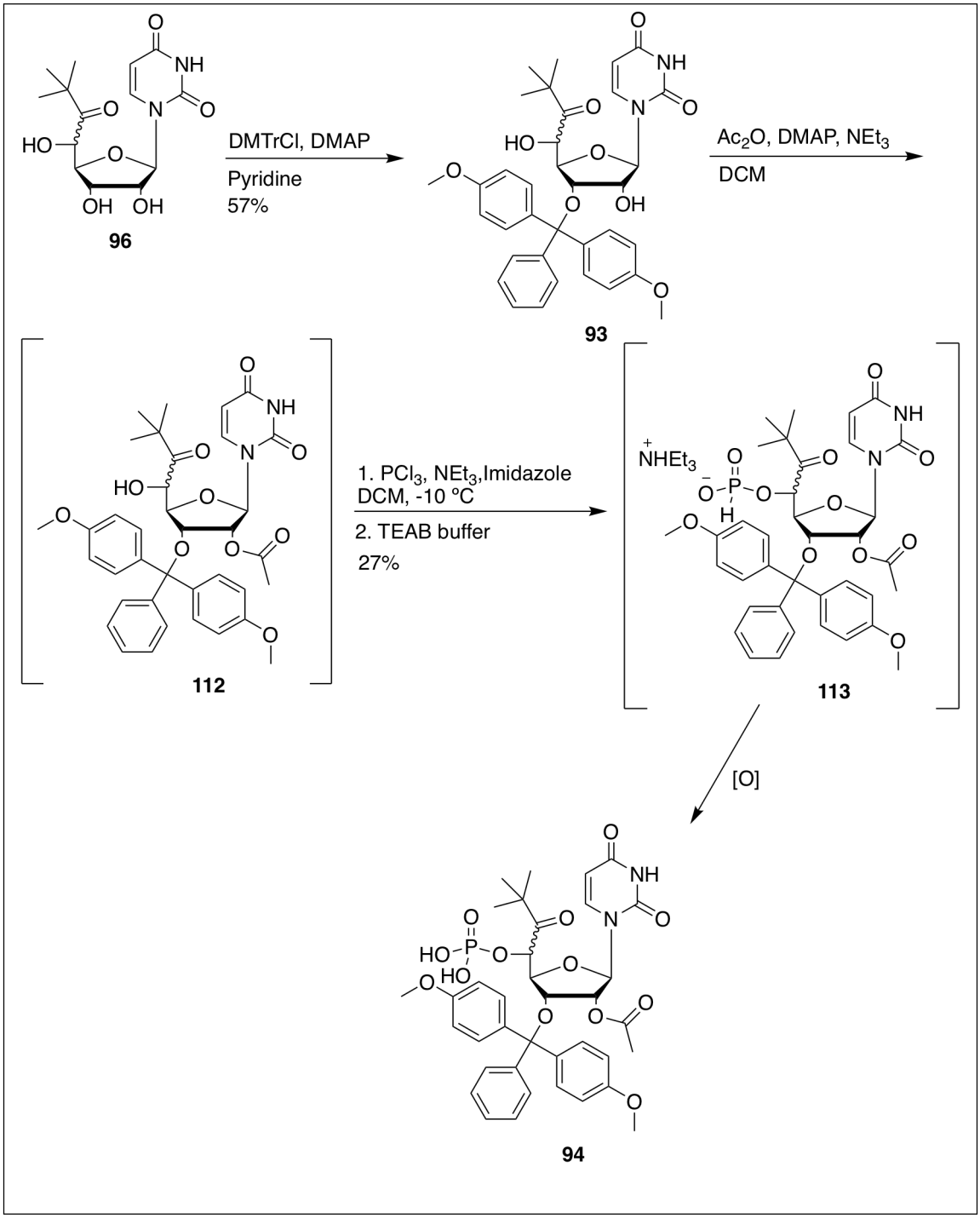


Scheme 2-4. Synthesis of Uridine 5' H-Phosphonate Radical Precursor

## 2.5 H-Phosphonate Monomer Syntheses

### 2.5.1 Overview of 5' H-Phosphonate Synthesis

In order to incorporate our radical precursor into strands of RNA, we endeavored to design a new automated RNA synthesis technique based on the assembly of the oligomer in the 5′ to 3′ direction using 5′ H-phosphonates. This included the synthesis of the four RNA building blocks, uridine, cytidine, adenosine, and guanosine 5′ H-phosphonates. Recently, there has been work to develop RNA synthetic methods in the reverse direction, from 5′ to 3′, using 5′ phosphoramidites [100-103]. These methods still utilize a 2′ O-silyl protecting group with a dimethoxytrityl protecting group at the 3′ position. This work was foundational for our studies.

Synthesis in the 5′ to 3′ direction would allow for the introduction of a variety of 3′ modifications such as ligands and chromophores to aid research in multiple fields. For example, this could be applicable for RNA therapeutics by providing easy access to 3′ modifications on the sense strand of siRNA, which should not interfere with recognition since antisense siRNA strands guide target recognition [100]. Synthesis in the 5′ to 3′ direction also allows for more steric modifications on the sugar moiety, especially the 5′ position when using an H-phosphonate, suiting our purposes well.

There are also advantages to using H-phosphonate chemistries over that of phosphoramidites. Phosphoramidites require an oxidation step after each coupling cycle,

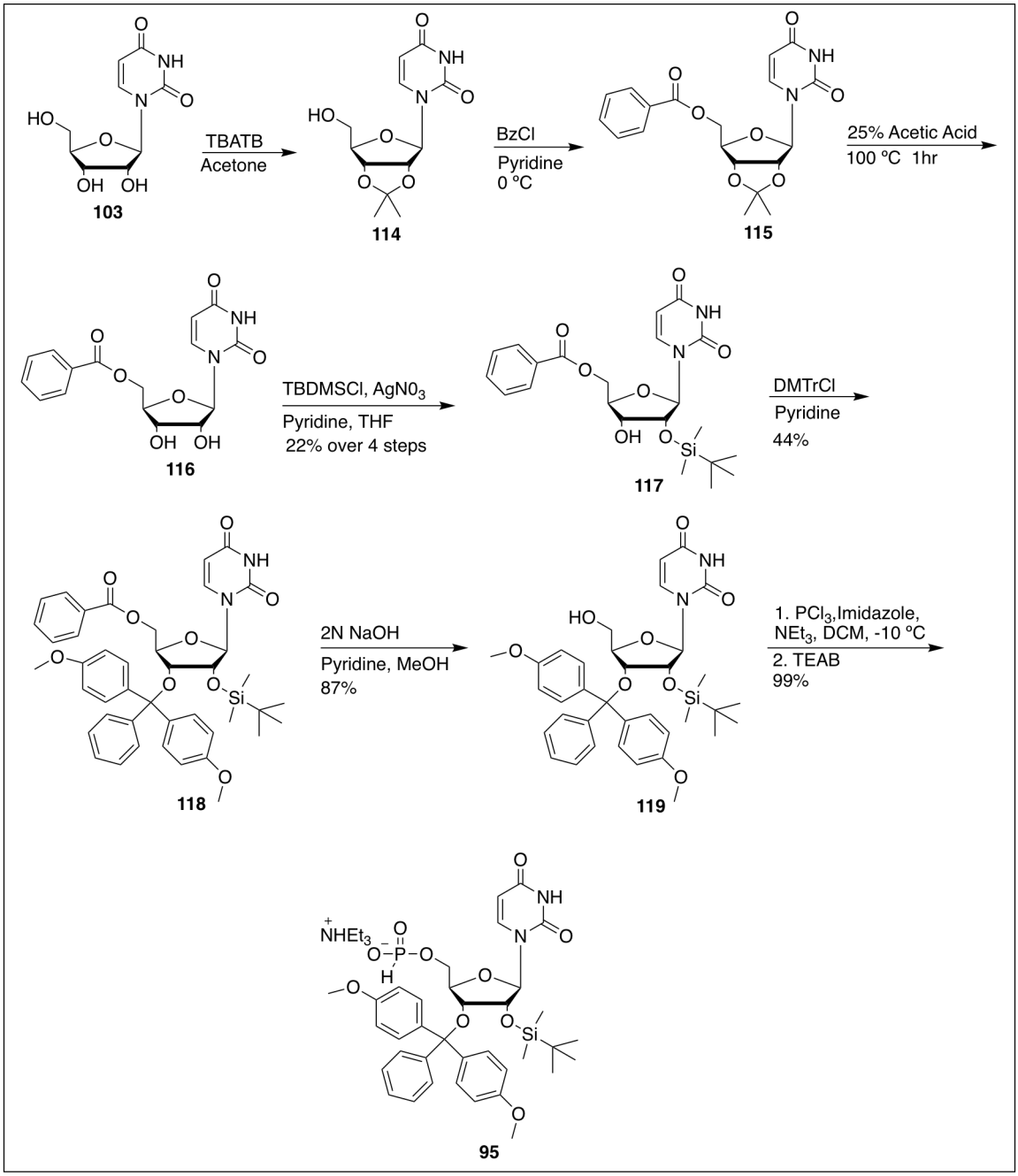


Scheme 2-5. Synthesis of Uridine 5' H-Phosphonate

whereas in H-phosphonate chemistry only one oxidation step is required at the end of oligomer assembly. This cuts down the number of steps required in each cycle, as well as the cycle time. H-phosphonates are also more stable than phosphoramidites and have the potential to be recovered after coupling [99, 104]. H-phosphonate chemistry also uses some of the same readily available reagents used in the phosphoramidite approach.

### 2.5.2 Uridine 5' H-Phosphonate Synthesis

The synthesis of **95** can be seen in **Scheme 2-5**. First, uridine was protected using a catalytic amount of tetrabutylammonium tribromide (TBATB) in acetone to give **114** [83]. This was benzoylated at the 5' position using benzoyl chloride (BzCl) in pyridine to afford **115** [105]. Fully protected **115** then underwent acidic hydrolysis using 25% acetic acid and heat to give **116** [76]. Compound **116** was selectively silylated at the 2' position using *tert*-butyldimethylsilyl chloride and silver nitrate ($AgNO_3$) in a mixture of pyridine and tetrahydrofuran [106]. Compound **117** was then protected using dimethoxytrityl chloride in pyridine to give **118**, which was finally selectively deprotected using 2N sodium hydroxide (NaOH) in pyridine and methanol to give 5' hydroxyl **119** [102]. The addition of the H-phosphonate was completed using phosphorous trichloride, imidazole, and triethylamine in dichloromethane using protocols developed in our lab [107].

### 2.5.2 Cytidine 5' H-Phosphonate Synthesis

The attempted synthesis of **127** can be seen in **Scheme 2-6**. First, cytidine was protected using a catalytic amount of perchloric acid in acetone to give **121** [108]. This was benzoylated at the 5' position, as well as on the exocyclic amine, using benzoyl chloride

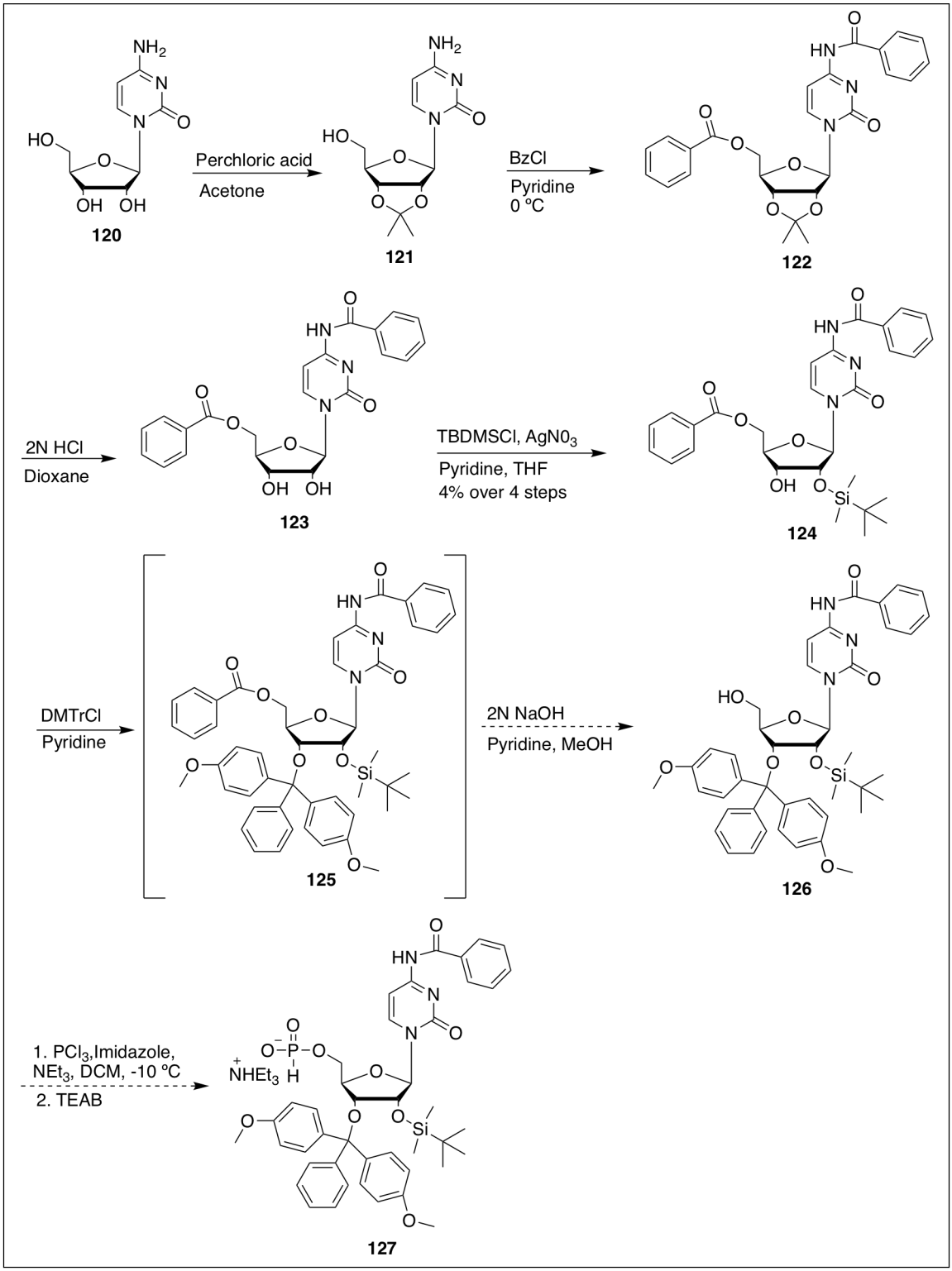


Scheme 2-6. Attempted Synthesis of Cytidine 5' H-Phosphonate

(BzCl) in pyridine to afford **122** [105]. These first two steps had high crude yields and likely are not part of the problem of the low combined yield. Fully protected **122** then underwent acidic hydrolysis using dilute hydrochloric acid (HCl) in dioxane to give **123** [102]. This gave a crude yield of approximately 50%. In the workup, the crude product is redissolved in EA and THF, but there are solubility issues. Even when DCM and MeOH are added to help this, it is possible that in the aqueous washes some product is lost. This acid hydrolysis has also been shown to be problematic with the guanosine and adenosine nucleosides, perhaps causing more compound degradation than initially thought. To further investigate this, **122** should be purified before the acid hydrolysis. Compound **123** was selectively silylated at the 2' position using *tert*-butyldimethylsilyl chloride and silver nitrate ($AgNO_3$) in a mixture of pyridine and tetrahydrofuran [106]. The selective protection gives preference to the formation of the desired 2' hydroxyl, however it also gives rise to the protected 3' hydroxyl and bis-protected compounds. Combined, these steps delivered **124** in a very low yield. In part, this was due to the lack of purification in between any of these reactions. In the future, compound **122** should be purified before moving forward, and, most importantly, compound **123** should be very carefully purified so as to give one pure compound going into the selective protection. Another possibility is to deploy a scheme similar to what was adopted with guanosine where there is a transient protection of the three hydroxyl groups to start with a base protected nucleoside, removing the need to perform the isopropylidene removal. Compound **124** was then protected using dimethoxytrityl chloride in pyridine to give **125** in a crude yield of 84%, after which an attempt to selectively deprotect by using 2N sodium hydroxide (NaOH) in pyridine and methanol failed [102]. In the future, **125** should be purified before moving forward to ensure

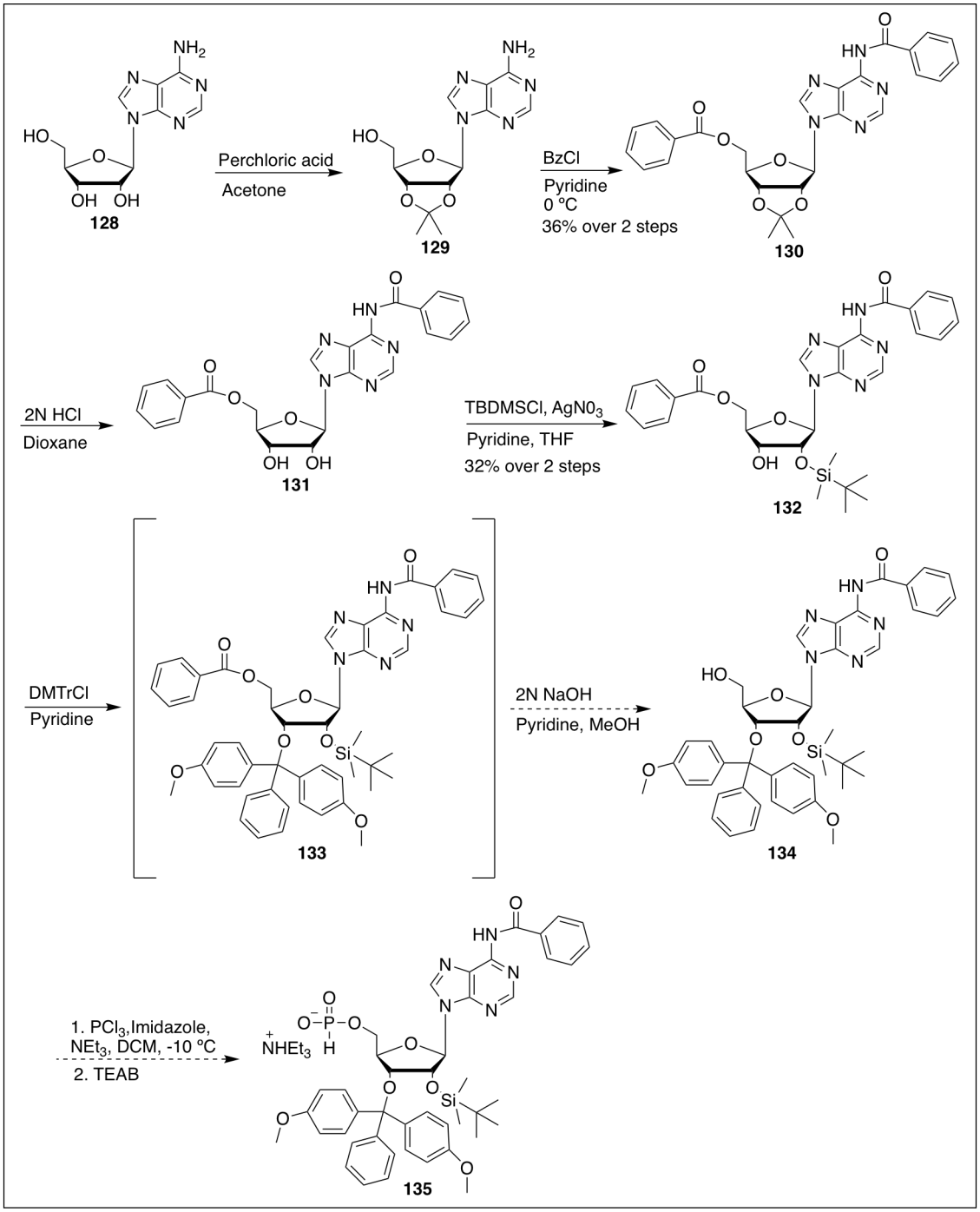


Scheme 2-7. Attempted Synthesis of Adenosine 5' H-Phosphonate

there is one pure product to test the reaction with.

### 2.6.2 Adenosine 5' H-Phosphonate Synthesis

The attempted synthesis of **135** can be seen in **Scheme 2-7**. First, adenosine was protected using a catalytic amount of perchloric acid in acetone to give **129** [108]. This was benzoylated at the 5' position, as well as on the exocyclic amine, using benzoyl chloride (BzCl) in pyridine to afford **130** [105]. Here, it is also possible to form a compound with two Bz protecting groups on the exocyclic amine. It was observed that this had started to form before the starting material was fully consumed, so the reaction was stopped. In the future, varying conditions should be tested to optimize this procedure, with the possibility of moving forward with an adenosine compound obtaining three Bz protecting groups. Fully protected **130** then underwent acidic hydrolysis using dilute hydrochloric acid in dioxane to give **131** [102]. Again, this saw low crude yields. Compound **131** was selectively silylated at the 2' position using *tert*-butyldimethylsilyl chloride and silver nitrate ($AgNO_3$) in a mixture of pyridine and tetrahydrofuran [106]. Compound **132** was then protected using dimethoxytrityl chloride in pyridine to give **133** with a crude yield of 88%, which was pushed forward to attempt the selective deprotection using 2N sodium hydroxide (NaOH) in pyridine and methanol which failed [102]. In the future, **133** should be purified before going forward to ensure a single, pure product to test the reaction with. As stated before, the scheme could be modified as in the case of guanosine to remove the need to use an isopropylidene protecting group on the 2' and 3' hydroxyls, which should reduce the number of steps used and potentially increase the overall yields.

2.7.2 Guanosine 5' H-Phosphonate Synthesis

An appropriately protected guanosine is required for RNA synthesis and multiple candidates were investigated in an attempt to achieve this (**Figure 2-4**). The protecting groups could vary for the base, however the isobutyryl (Ibu) group is the most commonly used for guanosine, likely due to it's easier removal during automated synthesis. For the 5' protecting group, the benzoyl (Bz) group aided greatly in compound solubility.

First, the same approach as used in the other nucleosides was attempted, seen in **Scheme 2-8**. Guanosine was protected using a catalytic amount of perchloric acid in acetone to give **137** [108]. This was benzoylated at the 5' position, as well as on the exocyclic amine, using benzoyl chloride (BzCl) in pyridine to afford **138** [105]. Fully protected **138** then underwent acidic hydrolysis using dilute hydrochloric acid in dioxane to give **139** [102]. This reaction was performed multiple times, and the product would sometimes degrade during the reaction. However, more success was observed during faster acidic hydrolysis prompted by heat. Compound **139** was selectively silylated at the 2' position using *tert*-butyldimethylsilylchloride and silver nitrate in a mixture of pyridine and tetrahydrofuran [106]. This reaction was more successful when the previous reaction was purified or the product was washed with a saturated sodium bicarbonate solution and brine, however **139** does have some solubility issues. Under these reaction conditions, the compound was also prone to decompose via base release. Compound **140** was then protected using dimethoxytrityl chloride in pyridine to give **141** [102]. The selective

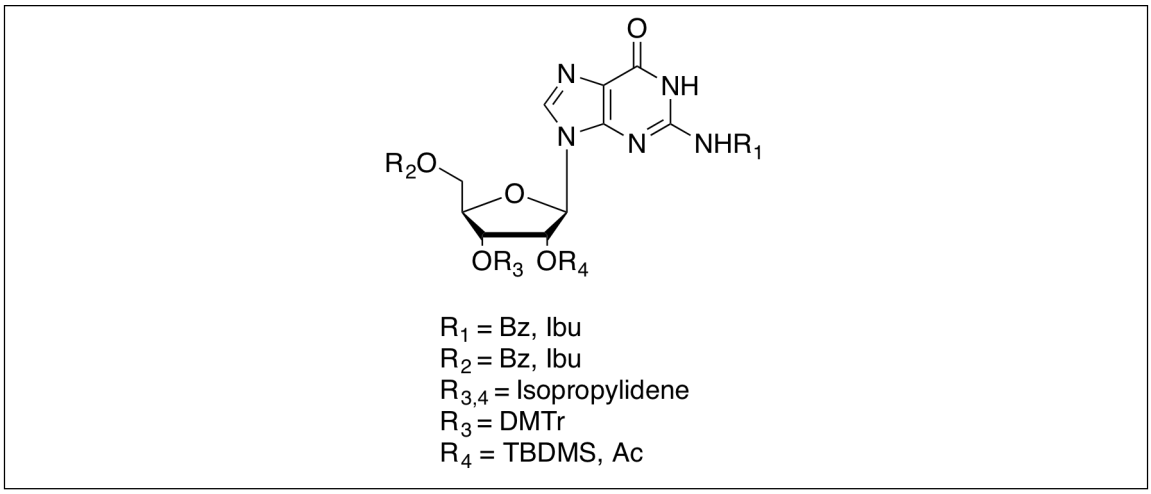


Figure 2-4. Guanosine Protecting Groups

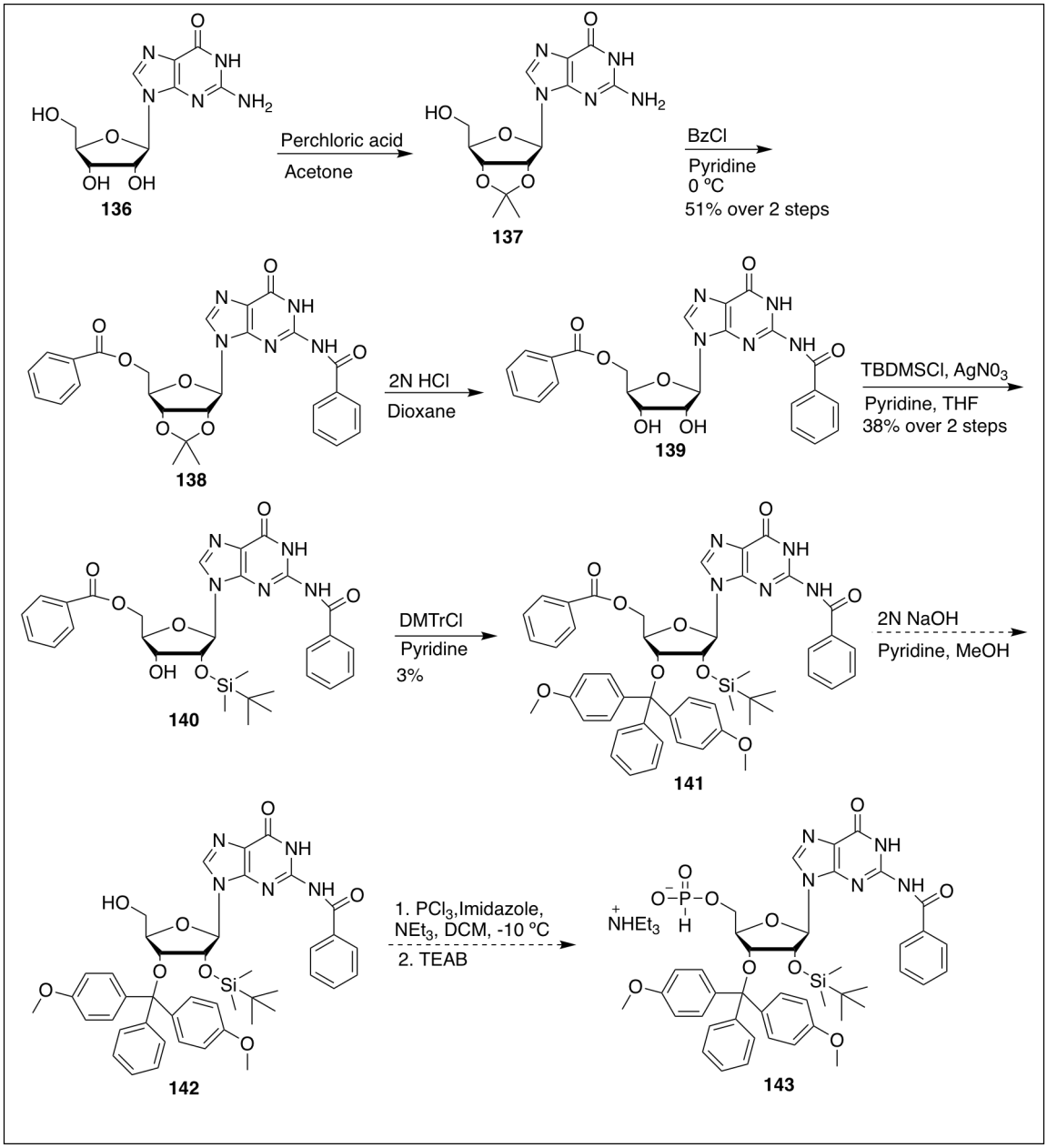


Scheme 2-8. Attempted Synthesis of Guanosine 5' H-Phosphonate Using Benzoyl Protecting Groups

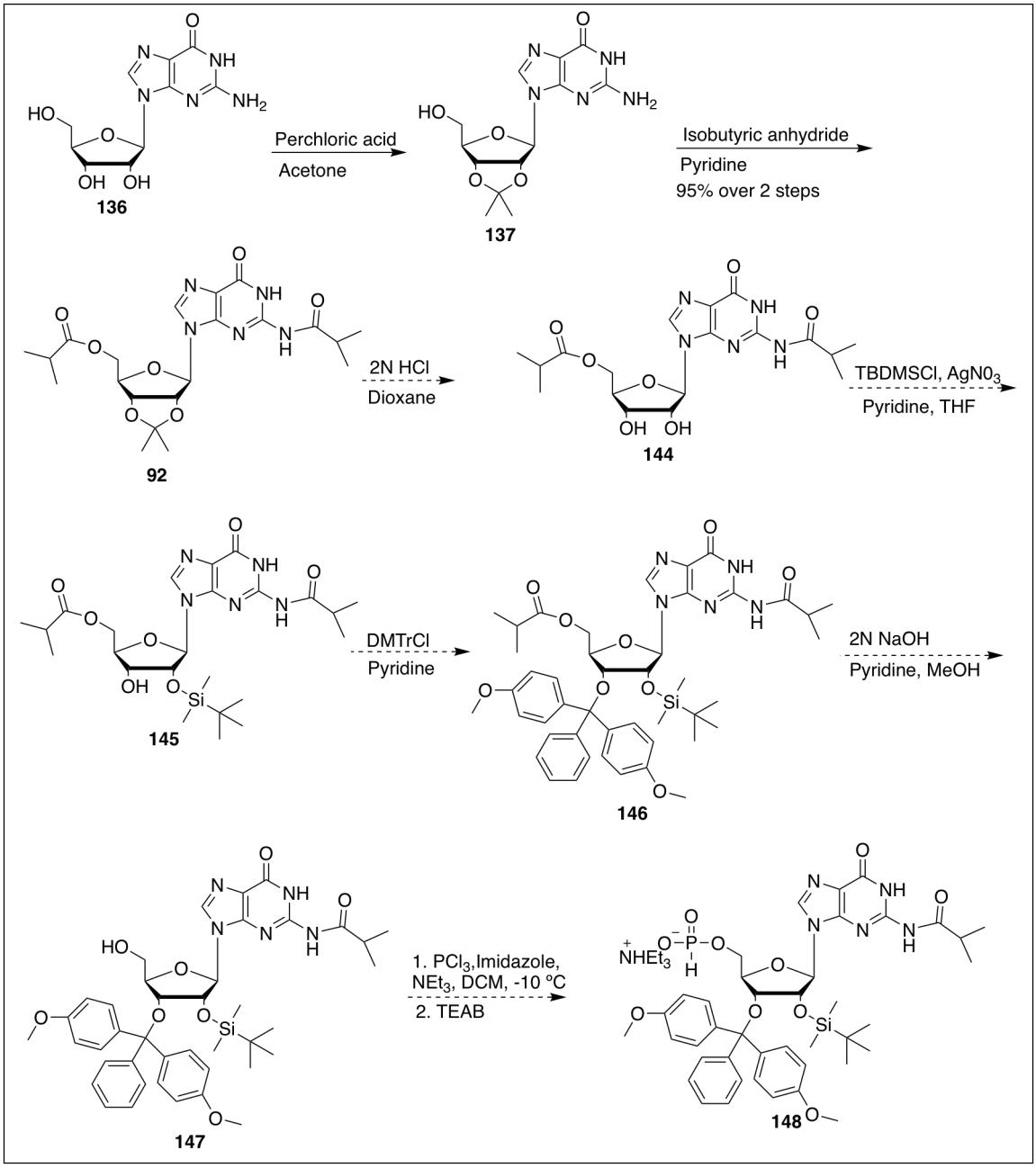


Scheme 2-9. Attempted Synthesis of Guanosine 5' H-Phosphonate Using Isobutyryl Protecting Groups

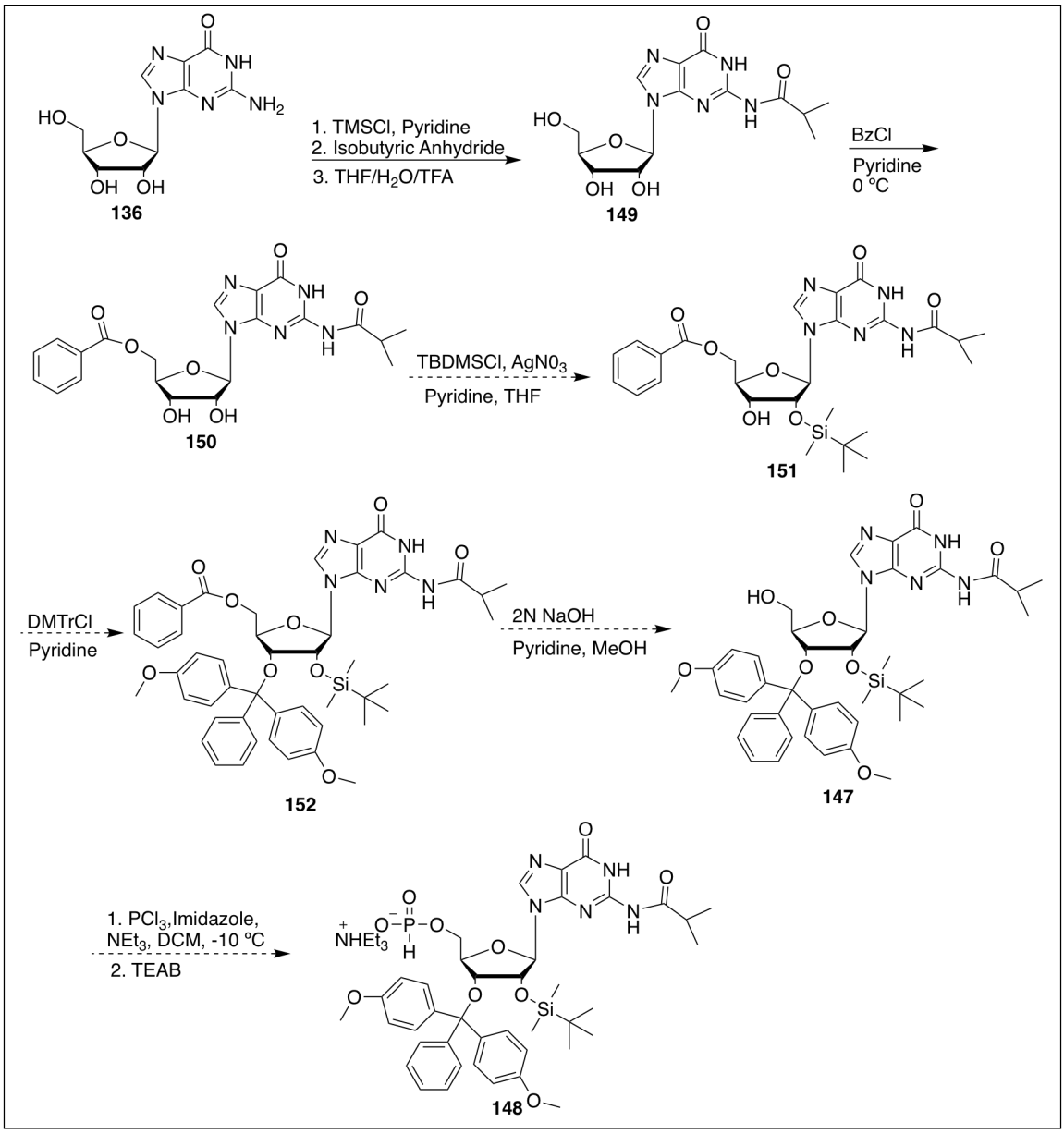


Scheme 2-10. Attempted Synthesis of Guanosine 5' H-Phosphonate Using a Combination of Isobutyryl and Benzoyl Protecting Groups

debenzoylation was attempted and appeared to work, however the compound degraded shortly after the purification.

Second, a similar approach as was used in the other nucleosides was attempted using the isobutyryl protecting groups, a more commonly used base protecting group for guanosine, seen in **Scheme 2-9**. Guanosine was protected using a catalytic amount of perchloric acid in acetone to give **137** [108]. This was protected at the 5' position, as well as on the exocyclic amine, with Ibu using isobutyric anhydride in pyridine to afford **92** [109]. Fully protected **92** underwent acidic hydrolysis using dilute hydrochloric acid in dioxane with the attempt of forming **139** [102]. However, under these conditions, the 5' isobutyryl group was consistently lost as well.

Finally, the approach outlined in **Scheme 2-10** was adopted. This removed the need to use the isopropylidene altogether, as well as utilized the more common Ibu protecting group on the base and the Bz group beneficial for solubility on the 5' position. The hydroxyl groups of guanosine were exposed to transient protection using TMSCl (trimethlysilyl chloride) in pyridine, followed by the addition of isobutyric anhydride to protect the base and then the addition of water and THF with TFA (triflouroacetic acid) to secure the removal of the TMS groups to afford **149** [105, 109]. In the future, adding methanol may be more beneficial than water yielding more methyl isobutyrate, which has a lower boiling point than isobutyric acid and may be easier to remove. This also may allow for the purification of this compound in the future, though it will certainly have solubility issues.

# Chapter 3

# Conclusions

The goal of this work was to study the reactivity of the C5'-uridinyl radical and the lesions formed from its generation. Herein, the synthesis of the C5'-uridinyl radical precursor **96** was greatly improved, increasing the yield of multiple reactions for the continued study of this compound. Using instrumentation such as HPLC and MS, the outcomes of the C5'-uridinyl radical were studied. Under anaerobic conditions it was shown that no UV-active reactive intermediates formed under physiological conditions and that the base release product uracil was the major product. Using aerobic conditions, it was found that the 5' aldehyde **105** was the predominant lesion formed, with some uracil and uridine, as well as a product we were unable to identify. Though pH played a role in the product distribution in the anaerobic studies, it did not appear to have an effect on the outcomes under aerobic conditions. A mechanism for the formation of **105** was proposed using a combination of the data from this work and other literature sources. The H-phosphonate C5'-uridinyl radical precursor was synthesized for incorporation into strands of RNA, however much of it degraded to form phosphate **94**. This work also began the journey towards a new automated RNA synthesis in the 5' to 3' direction with

the synthesis of uridine 5' H-phosphonate, as well as laying the groundwork for the future synthesis of cytidine, adenosine, and guanosine 5' H-phosphonates **127**, **135**, and **148**.

# Chapter 4

# Future Work

In order to further this work, the synthesis of cytidine, adenosine, and guanosine 5' H-phosphonates **127**, **135**, and **148** must be completed as described in Chapter 3. When all 4 H-phosphonates are in hand, a DNA synthesizer can be used to develop the automated RNA synthesis shown in **Scheme 4-1**. While the synthesis of these compounds are underway, the new automated RNA synthesis can begin development using the uridine 5' H-phosphonate that is in hand.

While the development of this automated synthesis is underway, more of H-phosphonate radical precursor **113** can be synthesized to incorporate into oligoribonucleotides, specifically, the Sarcin/Ricin Loop RNA. This RNA has already been used to study RNA oxidation and found that the 5' H atom was abstracted to form the C5' radical in U11 [32]. Once obtained, hand-coupling techniques can be used to incorporate **113** into position 11 of a portion of the Sarcin/Ricin Loop. After purification, this can then be ligated with the remainder of the Sarcin/Ricin Loop RNA as seen in **Scheme 4-2**. Once isolated, the modified Sarcin/Ricin Loop RNA **168** can be subjected to photolysis conditions with excess GSH to prove that the radical is generated (**Scheme 4-3**). With excess GSH under anaerobic conditions, the radical should be reduced to give

the unmodified Sarcin/Ricin Loop RNA. Once the method is tested, aerobic conditions can be used to compare results to Tullius' study[32]. When this proof of concept has been completed, **113** could be used in a number of strands of RNA to study the effect of RNA oxidation.

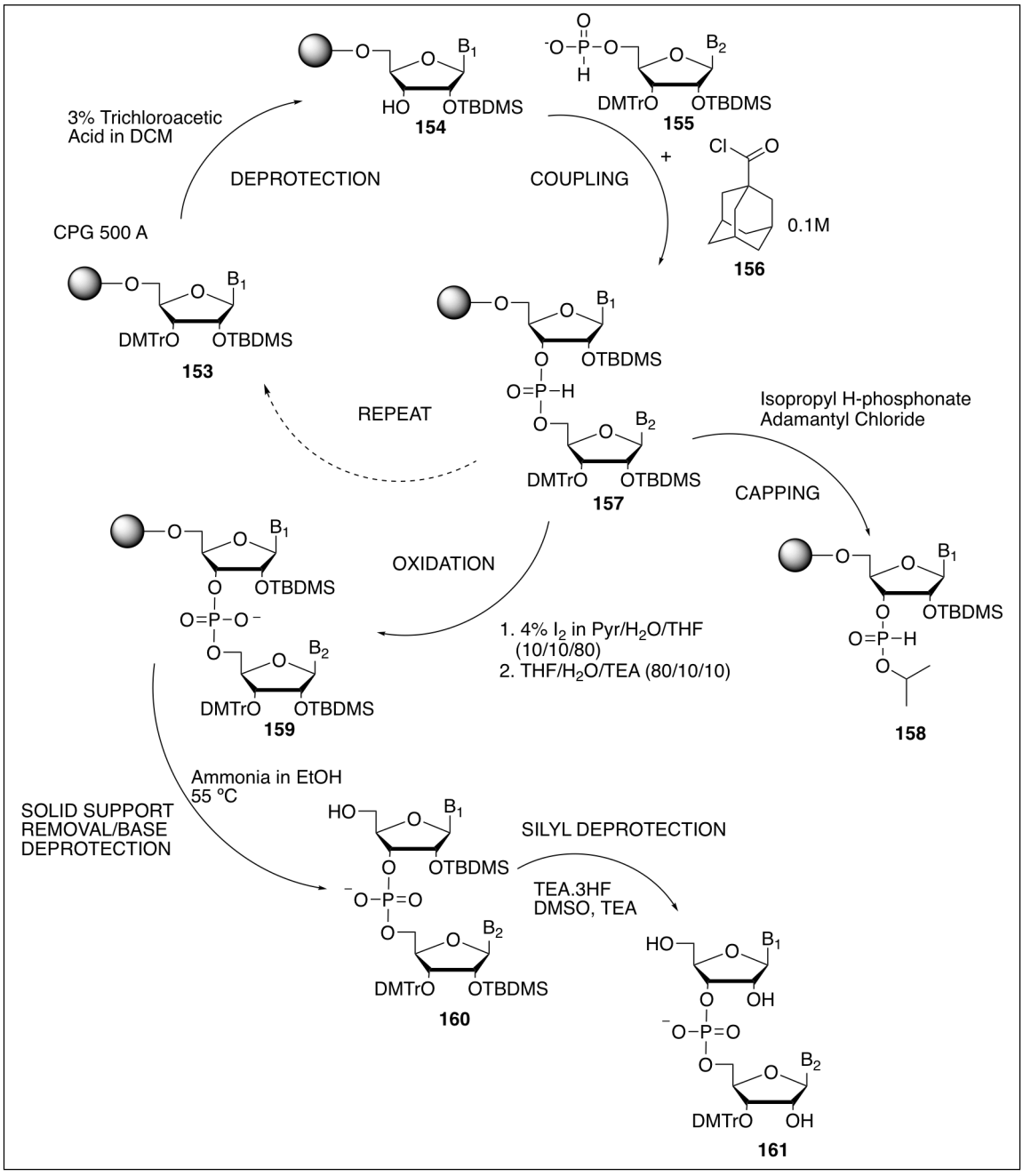


Scheme 4-1. Proposed Automated RNA Synthesis Approach

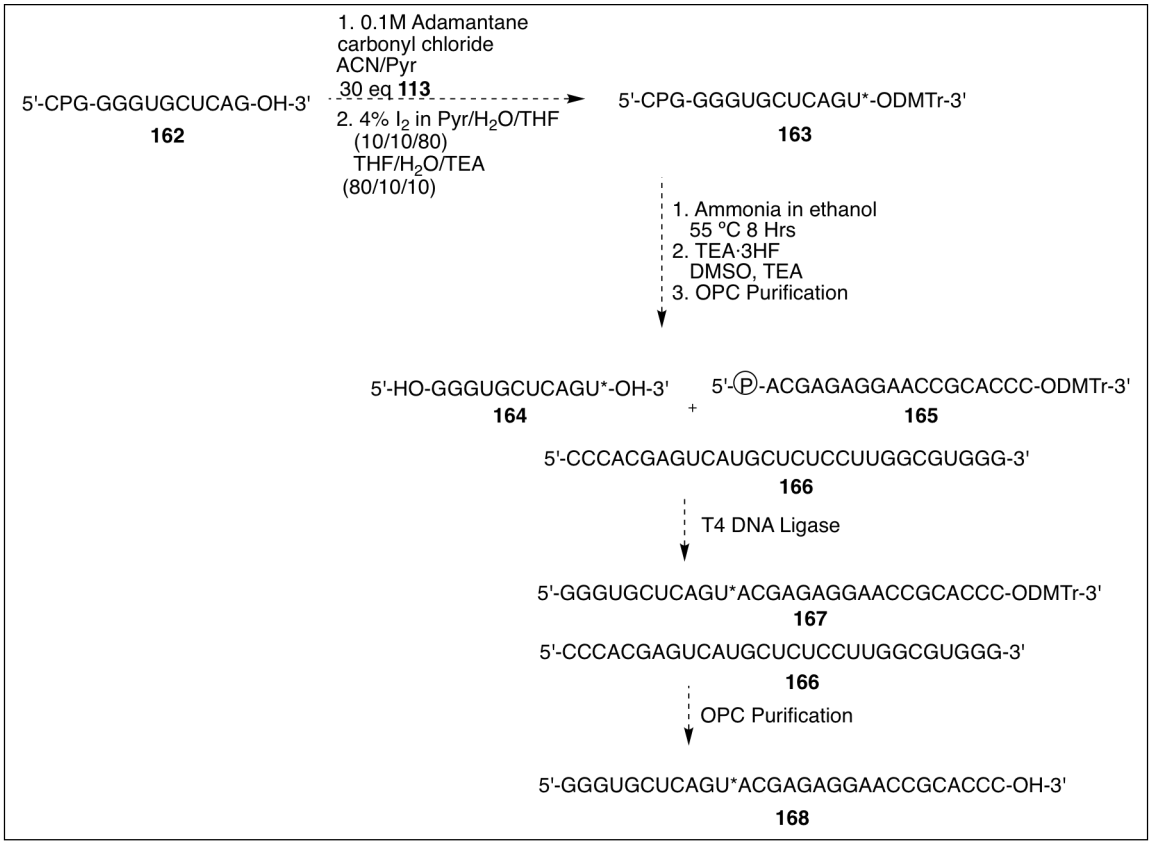


Scheme 4-2. Synthesis of Modified Sarcin/Ricin Loop RNA

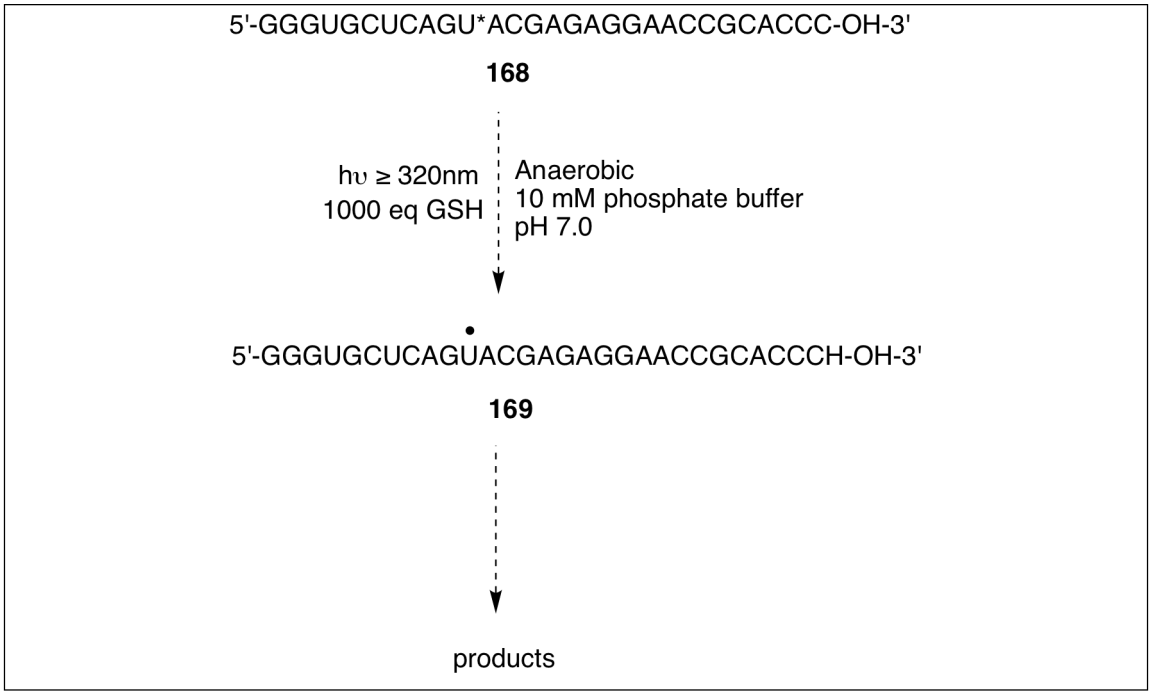


Scheme 4-3. Photolysis of Modified Sarcin/Ricin Loop RNA

# Chapter 5

# Experimental Procedures

## 5.1 Materials, Methods, and Equipment

All reactions were carried out under laboratory conditions using argon or nitrogen in clean, oven-dried flask unless stated otherwise. All chemicals and reagents were obtained commercially and used without further purification unless otherwise stated. New compounds were characterized using Nuclear Magnetic Resonance (NMR) and High Resolution Mass Spectrometry (HRMS). $^{1}$H NMR were obtained on a VXR 400, Inova 600, or Avance 600 NMR using $CDCl_3$ or MeOH-$d_4$. $^{13}$C NMR were obtained on an Avance 600 NMR using $CDCl_3$ or MeOH-$d_4$. $^{31}$P NMR were obtained on a VXR 400 using $CDCl_3$. HRMS were obtained from Dr. Dragan Isalovic's laboratory using an electrospray ionization (ESI)-quadrupole time-of-flight (Q-TOF) mass spectrometer. Low Resolution Mass Spectrometry were obtained using either an Esquire-electrospray ionization mass spectrometer or a Shimadzu LCMS 2020. High-Performance Liquid Chromatography (HPLC) was completed using either a Dionex Ultimate 3000 equipped with a variable wavelength detector or a Shimadzu LC 20-AT with a UV detector. High-Performance Liquid Chromatography-Mass Spectrometry (LCMS) was accomplished

using a Shimadzu LC 20-AT connected to a Shimadzu LCMS 2020. Purification of compounds was done using either a manual column with silica or alumina or a Biotage SP4 automated chromatography system using Biotage SNAP pre-packaged silica columns. Thin Layer Chromatography (TLC) was carried out using silica gel 60 F254 aluminum backed plates and visualized by UV light at 254 nm followed by staining and burning using anisaldehyde dip. Photolysis reactions were carried out using a Thermo Oriel with a 500 W mercury lamp and cut-off filter for wavelengths greater or equal to 320 nm, a Thermo Haake K20 cooling system and a Varian SPV Cary single cell peltier accessories. Other equipment used include a solvent purification system (Innovative Technology PS-MD-2 Pure Solvent System), rotary evaporators (Heidolph Collegiate Brinkmann rotovap), high vacuum pump (Edwards RV3), speed vacuum (Thermo electron savant DNA120), micro centrifuge (Thermo Sorvall Legend Micro 21), vortex mixer (Fisher Scientific), Milli-Q water purification system, pH meter (Fisher Accumet Basic AB15), and pipettes (Eppendorf Series 2100).

## 5.2 Synthesis of Novel Compounds

5.2.1 ((3a*R*,4*R*,6*R*,6a*R*)-6-(2-isobutyramido-6-oxo-1,6-dihydro-9*H*-purin-9-yl)-2,2-dimethyltetrahydrofuro[3,4-*d*][1,3]dioxol-4-yl)methyl isobutyrate **92**

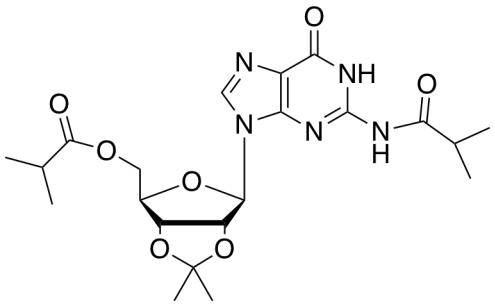

**92**

5.10 g (18.0 mmol) guanosine was dissolved in 245 mL of acetone and then 3.5 mL of perchloric acid was added dropwise while stirring. After 24 hours, the mixture was submerged in an ice bath and 3.0 mL of ammonium hydroxide was added dropwise. The media was filtered and the collected precipitate was washed with cold acetone to afford a white solid. The compound was coevaporated with toluene then dissolved in 210 mL of pyridine and then 25 mL of isobutyric anhydride were added slowly while stirring. After 25 hours, the reaction was quenched with 25 mL of water and concentrated. The compound was purified on a silica column using an eluent of 1% to 10% methanol (MeOH) in dichloromethane (DCM). 95% yield. $^{1}$H NMR (600 Mz, $CDCl_3$) δ 12.12 (1H, s), 7.69 (1H, s), 5.99 (1H, d, J = 1.3), 5.30 (1H, dd, J = 11.1, 9.5), 5.07 (1H, dd, J = 6.2, 1.3), 4.96 (1H, dd, J = 6.5, 3.3), 4.44 (1H, m), 3.83, (1H, dd, J = 11.2, 5.8), 2.77 (1H, sep, J = 7.1), 2.65 (1H, sep, J = 7.1), 1.91 (1H, s), 1.57 (3H, s), 1.32 (3H, s), 1.29 (3H, d, J = 6.9), 1.26 (3H, d, J = 6.9), 1.21 (3H, d, J = 7.1), 1.19 (3H, d, J = 7.0). $^{13}$C NMR (600 Mz,

$CDCl_3$) δ 179.37, 178.62, 155.64, 148.14, 147.25, 138.43, 122.54, 114.47, 91.49, 86.21, 85.70, 82.27, 62.85, 36.56, 34.28, 27.28, 25.53, 19.36, 19.18, 19.05, 19.02. HRMS $[M + H]^+$ calculated for $C_{21}H_{29}N_5O_7$ 464.2145. Found 464.2142.

5.2.2 1-((2*R*,3*R*,4*S*,5*R*)-4-(bis(4-methoxyphenyl)(phenyl)methoxy)-3-hydroxy-5-(1-hydroxy-3,3-dimethyl-2-oxobutyl)tetrahydrofuran-2-yl)pyrimidine-2,4(1*H*,3*H*)-dione **93**

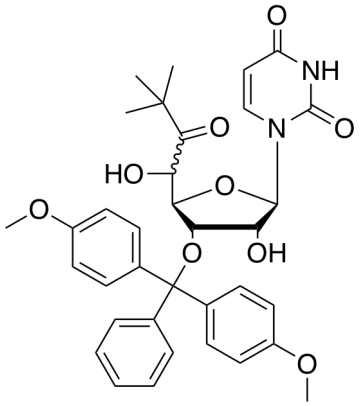


**93**

0.54 g (1.64 mmol) **96** was dissolved in 8 mL of pyridine then 0.65 g (1.92 mmol) dimethoxytrityl chloride (DMTrCl) was added. The reaction was stirred at room temperature. After 74 hours, an additional 0.10 g (0.30 mmol) dimethoxytrityl chloride and 0.02 g (0.16 mmol) DMAP (4-dimethylaminopyridine) were added to the solution. The reaction was chilled in an ice bath and quenched with 0.2 mL of methanol after 115 hours then concentrated. The compound was purified on a silica column using an eluent of 50% to 60% ethyl acetate (EA) in hexane with 5% triethylamine ($NEt_3$). 57% yield. $^1H$ NMR (600 Mz, MeOH-$d_4$) δ 7.65 (1H, d, J = 8.0), 7.63 (1H, d, J = 8.0), 7.47 (2H, d, J = 8.0), 7.47 (2H, d, J = 8.0), 7.37 (2H, d, J = 8.9), 7.37 (2H, d, J = 8.5), 7.33 (2H, d, J =

8.9), 7.32 (2H, d, J = 8.9), 7.21 (3H, t, J = 7.5), 7.20 (3H, t, J = 8.5), 6.82 (2H, d, J = 9.1), 6.80 (2H, d, J = 8.8), 6.77 (2H, d, J = 8.1), 6.76 (2H, d, J = 8.8), 6.31 (1H, d, J = 7.8), 6.27 (1H, d, J = 7.8), 5.49 (1H, d, J = 8.2), 5.48 (1H, d, J = 8.2), 4.59 (1H, d, J = 2.9), 4.52 (1H, d, J = 2.2), 4.46 (1H, dd, J = 7.9, 4.6), 4.45 (1H, d, J = 2.1), 4.34 (1H, dd, J = 7.5, 4.7), 4.27 (1H, d, J = 2.5), 3.77 (3H, s), 3.74 (3H, s), 3.74 (3H, s), 3.72 (3H, s), 3.23 (1H, d, J = 4.7), 2.86 (1H, d, J = 4.7), 1.12 (9H, s), 1.11 (9H, s). $^{13}$C NMR (600 Mz, MeOH-$d_4$) δ 214.98, 214.75, 166.37, 160.59, 160.53, 160.48, 160.42, 152.97, 152.84, 146.77, 146.72, 142.97, 142.78, 137.05, 136.05, 136.84, 136.79, 131.94, 131.82, 131.64, 131.60, 129.39, 129.34, 129.02, 128.95, 128.09, 126.43, 114.51, 114.48, 114.33, 103.68, 103.52, 88.80, 88.77, 88.26, 88.04, 87.50, 87.40, 77.90, 77.33, 75.15, 74.87, 72.99, 70.54, 55.80, 44.50, 44.10, 27.34, 26.81. HRMS $[M + Na]^+$ calculated for $C_{35}H_{38}N_2O_9$ 653.2475. Found 653.2484.

5.2.3 (2*R*,3*R*,4*R*,5*S*)-4-(bis(4-methoxyphenyl)(phenyl)methoxy)-5-(3,3-dimethyl-2-oxo-1-(phosphonooxy)butyl)-2-(2,4-dioxo-3,4-dihydropyrimidin-1(2*H*)-yl)tetrahydrofuran-3-yl acetate **94**

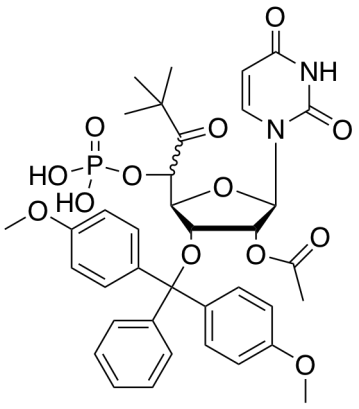

**94**

0.06 g (0.095 mmol) **93** and 2.50 mg (0.02 mmol) DMAP were dissolved in 8.0 mL of DCM. 10 µL of acetic anhydride and 20 µL of triethylamine were added and the reaction was stirred for 126 hr until quenched with methanol and concentrated. The reaction mixture was run through a silica column using an eluent of 30% to 40% ethyl acetate in hexane with 5% triethylamine then 1% to 3% methanol in 40/60 ethyl acetate/hexane with 5% triethylamine. After concentrating, the crude product was used directly in the next step. 0.07 g (1.03 mmol) imidazole was coevaporated with acetonitrile twice then dissolved in 3.0 mL of DCM and submerged in an ice salt bath. 0.03 mL of phosphorous trichloride ($PCl_3$) was added slowly followed by 0.15 mL of triethylamine in 0.15 mL of DCM. This solution was allowed to stir for 30 min. Then 0.06 g (0.089 mmol) of the nucleoside was coevaporated separately in toluene twice and dissolved in 2.0 mL of DCM. This was added dropwise to the stirring solution. After 1 hour, the flask was removed from the ice bath and 6.0 mL of triethylammonium bicarbonate buffer (TEAB)

was added. The organic layer was separated and washed with an equal volume of triethylammonium bicarbonate buffer again then concentrated. The H-phosphonate compound was purified on a silica column using an eluent of 0% to 8% methanol in dichloromethane with 5% triethylamine, leading to its oxidation. 27% yield. $^{1}$H NMR (600 Mz, $CDCl_3$) δ 7.40 (1H, d, J = 1.9), 7.39 (1H, d, J = 1.4), 7.35 (1H, d, J = 8.3), 7.30 (2H, d, J = 9.1), 7.29 (2H, d, J = 8.6), 7.24 (3H, t, J = 5.7), 6.77 (2H, d, J = 3.5), 6.75 (2H, d, J = 3.5), 6.46 (1H, d, J = 8.3), 6.27 (1H, d, J = 8.4), 5.66 (1H, d, J = 8.3), 5.59 (1H, d, J = 8.3), 5.46 (1H, d, J = 3.8), 5.43 (1H, d, J = 2.4), 4.38 (1H, d, J = 5.6), 4.36 (1H, d, J = 2.2), 4.23 (1H, dd, J = 8.2, 5.2), 3.77 (3H, s), 3.76 (3H, s), 3.63 (6H, q, J = 7.5), 3.59 (1H, d, J = 5.5), 2.17 (3H, s), 2.10 (3H, s), 2.04 (3H, s), 1.99 (3H, s), 1.47 (9H, t, J = 7.0), 1.13 (9H, s), 1.12 (9H, s). $^{13}$C NMR (600 Mz, $CDCl_3$) δ 207.21, 206.66, 170.63, 168.51, 162.37, 159.12, 158.75, 150.46, 144.11, 139.57, 139.10, 135.15, 135.06, 130.10, 130.07, 129.26, 128.13, 128.12, 127.99, 127.89, 127.63, 127.22, 113.41, 113.39, 113.29, 103.62, 87.38, 86.03, 81.51, 74.73, 74.41, 72.93, 55.44, 55.40, 53.13, 45.97, 43.53, 26.83, 26.48, 21.11, 20.65, 8.28. $^{31}$P NMR (400 Mz, $CDCl_3$) δ 47.9, 9.3. HRMS $[M + H]^+$ calculated for $C_{37}H_{41}N_2O_{12}P$ 737.2475. Found 737.1410.

5.2.4 ((2*R*,3*R*,4*R*,5*R*)-3-(bis(4-methoxyphenyl)(phenyl)methoxy)-4-((*tert*-butyldimethylsilyl)oxy)-5-(2,4-dioxo-3,4-dihydropyrimidin-1(2*H*)-yl)tetrahydrofuran-2-yl)methyl phosphonate triethylammonium salt **95**

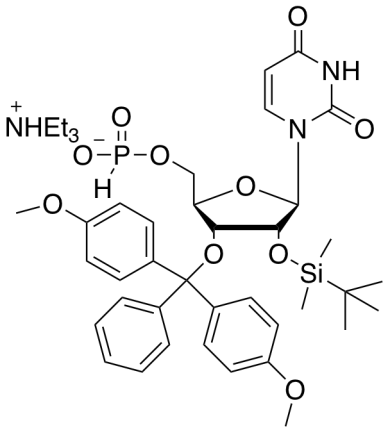

**95**

0.28 g (5.88 mmol) imidazole was coevaporated in toluene three times then dissolved in 10.0 mL of DCM and submerged in an ice salt bath. 0.15 mL of phosphorous trichloride was added dropwise followed by 0.85 mL of triethylamine. The reaction was left to stir for 30 min then 0.21 g (0.50 mmol) 2′-*O*-TBDMS-3′-*O*-DMTr-Uridine was coevaporated separately three times in toluene and dissolved in 7.0 mL of DCM before adding to the solution dropwise. Reaction was left stirring for 85 min and then brought to room temperature and quenched with 25 mL of TEAB. The DCM layer was separated and washed with an equal volume of TEAB again then concentrated. Compound was purified on a silica column using an eluent of 0 – 8% methanol in dichloromethane with 3% triethylamine. 99% yield. $^{1}$H NMR (400 Mz, $CDCl_3$) δ 8.01 (1H, d, J = 8.1), 7.54 (2H, d, J = 7.5), 7.41 (4H, d, J = 8.8), 7.25 (3H, t, J = 8.1), 6.79 (4H, d, J = 8.1), 6.29 (1H, d, J =

8.1), 5.69 (1H, d, J = 8.1), 4.15 (1H, dd, J = 6.4, 5.0), 4.04 (1H, d, J = 5.0), 3.76 (6H, s), 3.74 (1H, d, J = 4.9), 3.56 (1H, d, J = 7.1), 3.38 (1H, unresolved d), 2.90 (6H, q, J = 14.1, 7.1), 1.23 (9H, t, J = 7.3), 0.92 (9H, s), 0.05 (3H, s), -0.06 (3H, s). $^{13}$C NMR (600 Mz, $CDCl_3$) δ 163.29, 158.83, 150.75, 145.67, 141.50, 136.98, 136.56, 113.40, 102.62, 87.85, 86.72, 81.97, 74.90, 74.31, 63.15, 55.43, 45.76, 29.89, 26.05, 9.48, -4.17, -4.38. $^{31}$P NMR (400 Mz, $CDCl_3$) δ 5.6. HRMS $[M + H]^+$ calculated for $C_{42}H_{60}N_3O_{10}Psi$ 826.3858. Found 826.3860.

## 5.3 Photolysis of 96

### 5.3.1 Anaerobic Photolysis

Photolyses were carried out in plastic cuvettes (1 cm path length) with a 500 W mercury lamp with IR and cut-off filters and a focusing lens (≥ 320 nm) under argon. Reaction mixtures of 200 µL contained 37 nmol of **96** in 10 mM phosphate buffer at pH 7.0 and 8 mM GSH (glutathione) and were photolyzed at room temperature for varying amounts of time (1, 2, 4, 8, 15, 30, and 60 min) after first bubbling argon through the mixture for 15 min. After photolysis, mixtures were injected directly into a Dionex Ultimate 3000 HPLC system using a Hypersil BDS C18 RP column (5 µm, 4.6 x 250 cm). Solvent A was 50 mM TEAA (triethylammonium acetate) buffer at pH 7.0 and solvent B was acetonitrile. The program used was as follows: 0.2% B for 7 min, 0.2–22% B over 5 min, 22–0.2% B over 8 min. The flow rate was 1.0 mL/min and the temperature was 35 ºC. Wavelength detection was at 254 and 260 nm. Compound identity was

confirmed using independent standards, as were the RP-HPLC (reverse phase-HPLC) calibration curves.

### 5.3.2 Aerobic Photolysis

Experiments were performed in plastic cuvettes (1 cm path length) on 50 nmol **96** in 10 mM ammonium acetate buffer at pH 7.0 or 3.5 and 8 mM GSH using a 500 W mercury lamp (≥ 320 nm) with IR and cut-off filters and a focusing lens under oxygen. All samples were subjected to photolysis for 30 min after bubbling oxygen through the solution for 15 min. Samples were analyzed on a Shimadzu LCMS 2020 using RP-HPLC and ESI MS. A Hypersil BDS C18 column (5 µm, 4.6 x 250 mm) was used. Solvent A was water with 1% acetic acid and solvent B was acetonitrile with 0.1% acetic acid. The program used was as follows: 0-4% B over 25 mins, 4-98% B over 10 mins, 98% B for 10 mins, 98-0% B over 5 mins, 0% B for 10 mins. The flow rate was 0.3 mL/min, the column oven temperature was 30 ºC, and the wavelength detector was at 254 nm. For the ESI MS, the heat block was 400 ºC and drying gas was at 15 L/min. Data was collected in both positive and negative ion modes between 50 and 2000 m/z. Compound identification was determined using independent standards, as were the RP-HPLC calibration curves.

# Appendix

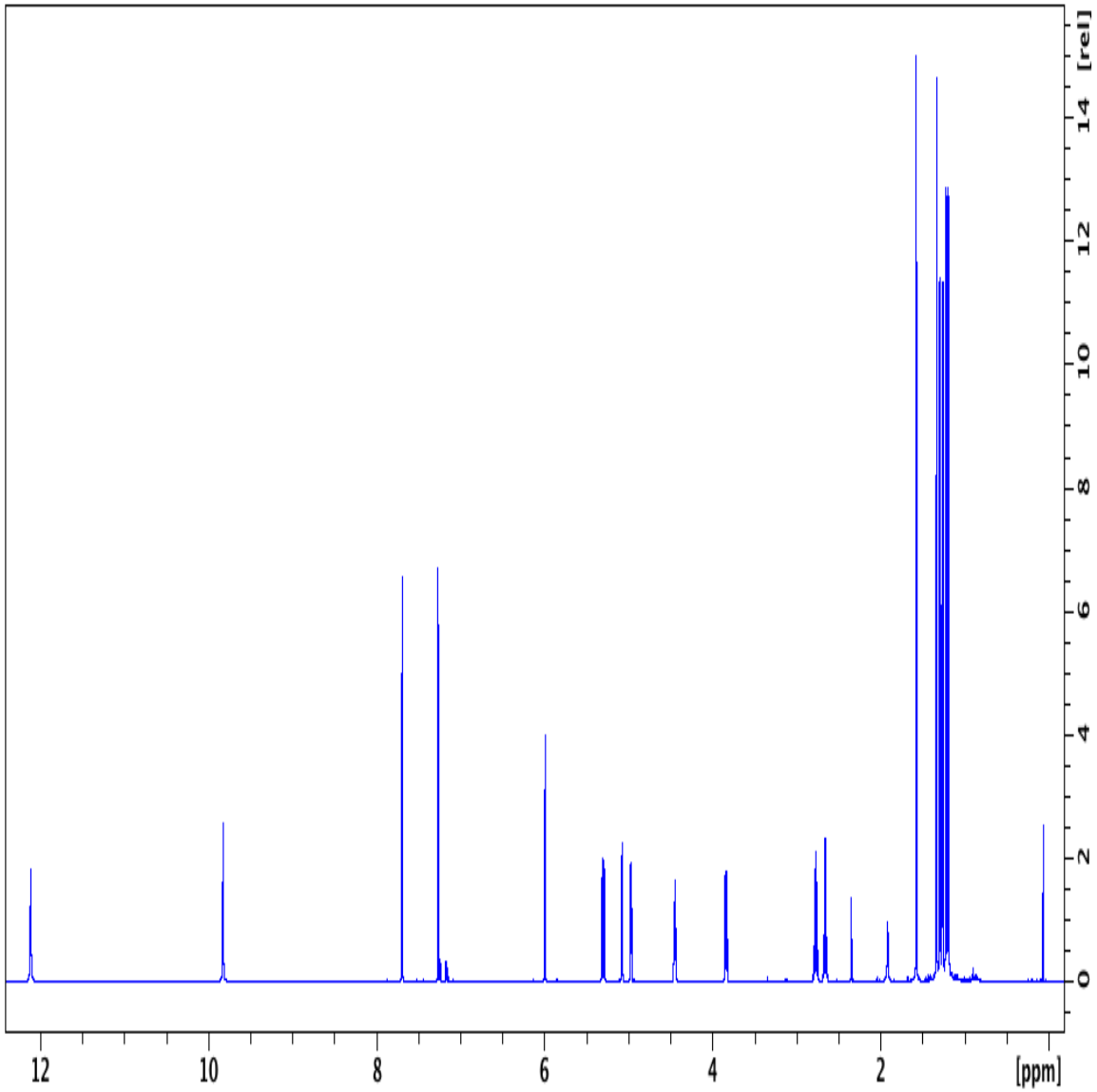


Figure A-1. $^{1}$H NMR for **92**

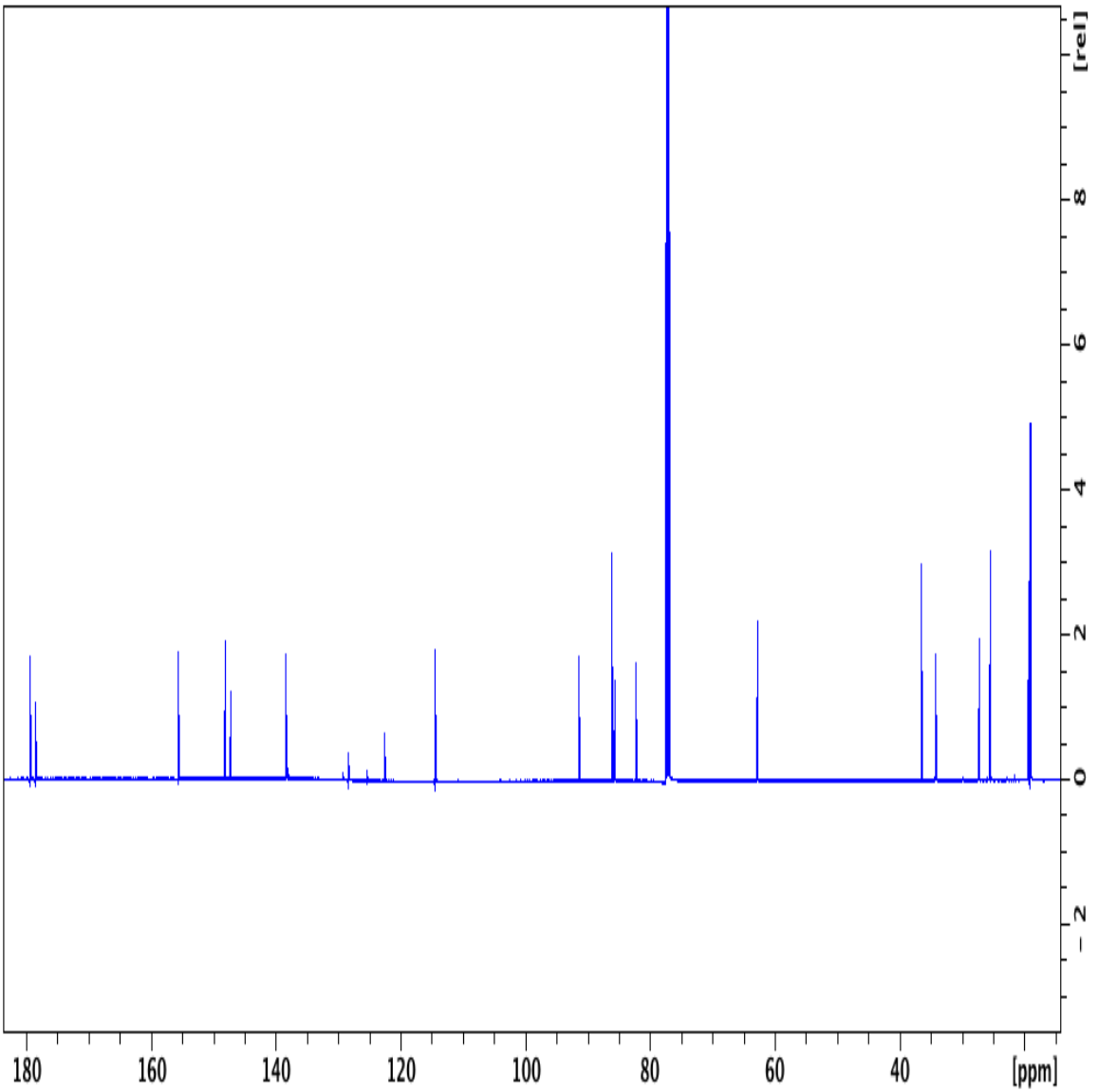


Figure A-2. $^{13}$C NMR for **92**

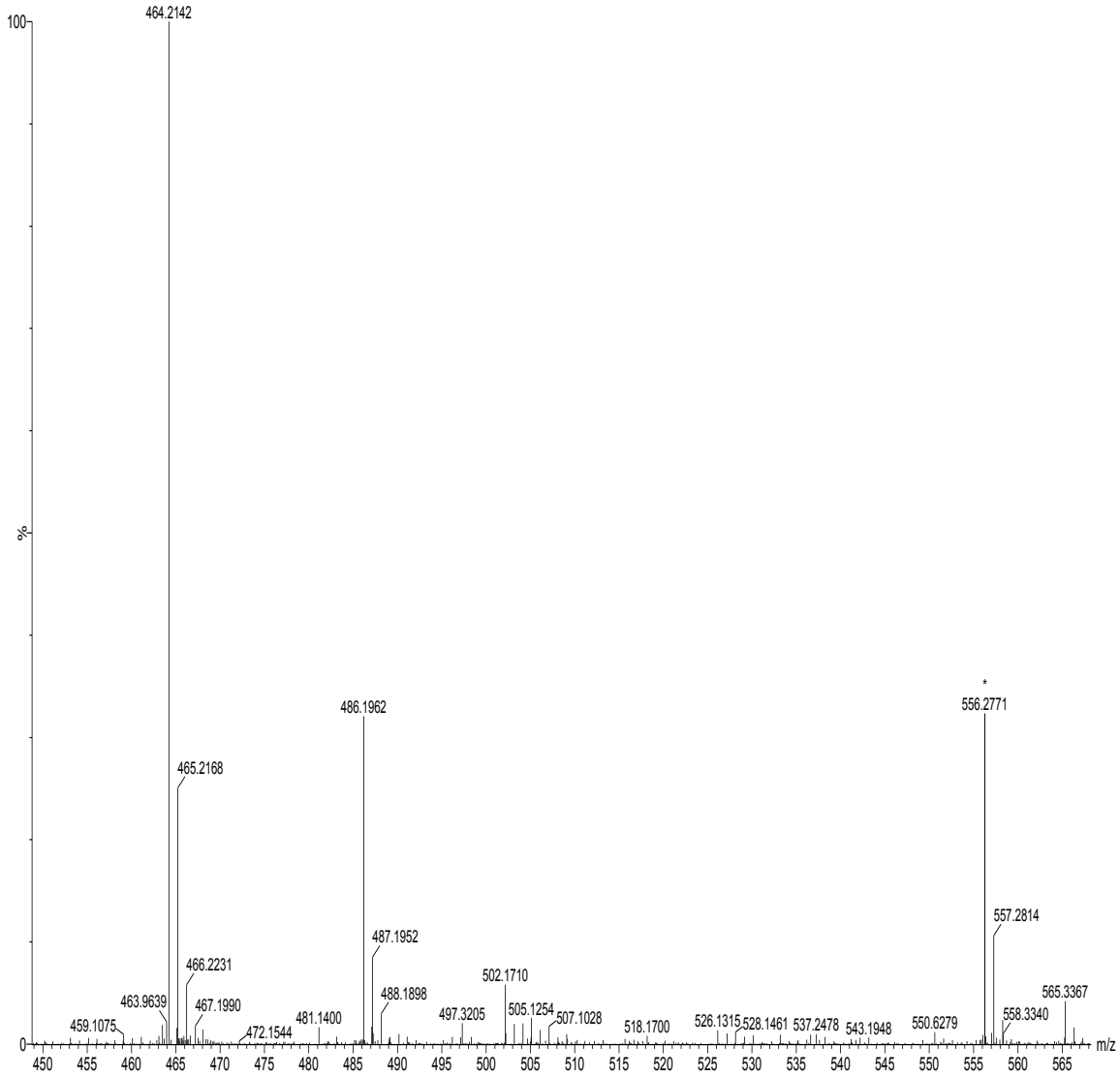


Figure A-3. HRMS for **92**

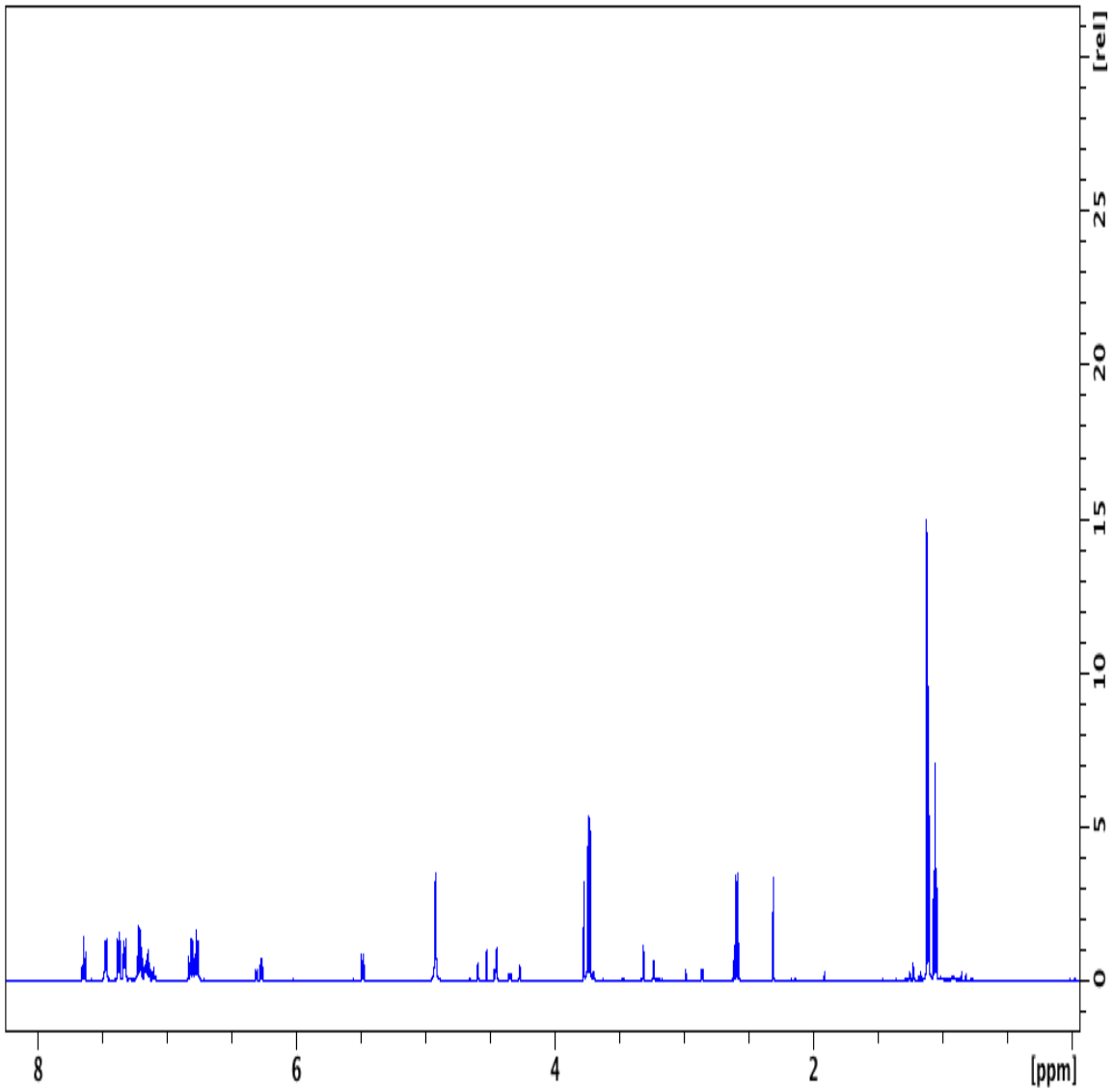


Figure A-4. $^{1}$H NMR for **93**

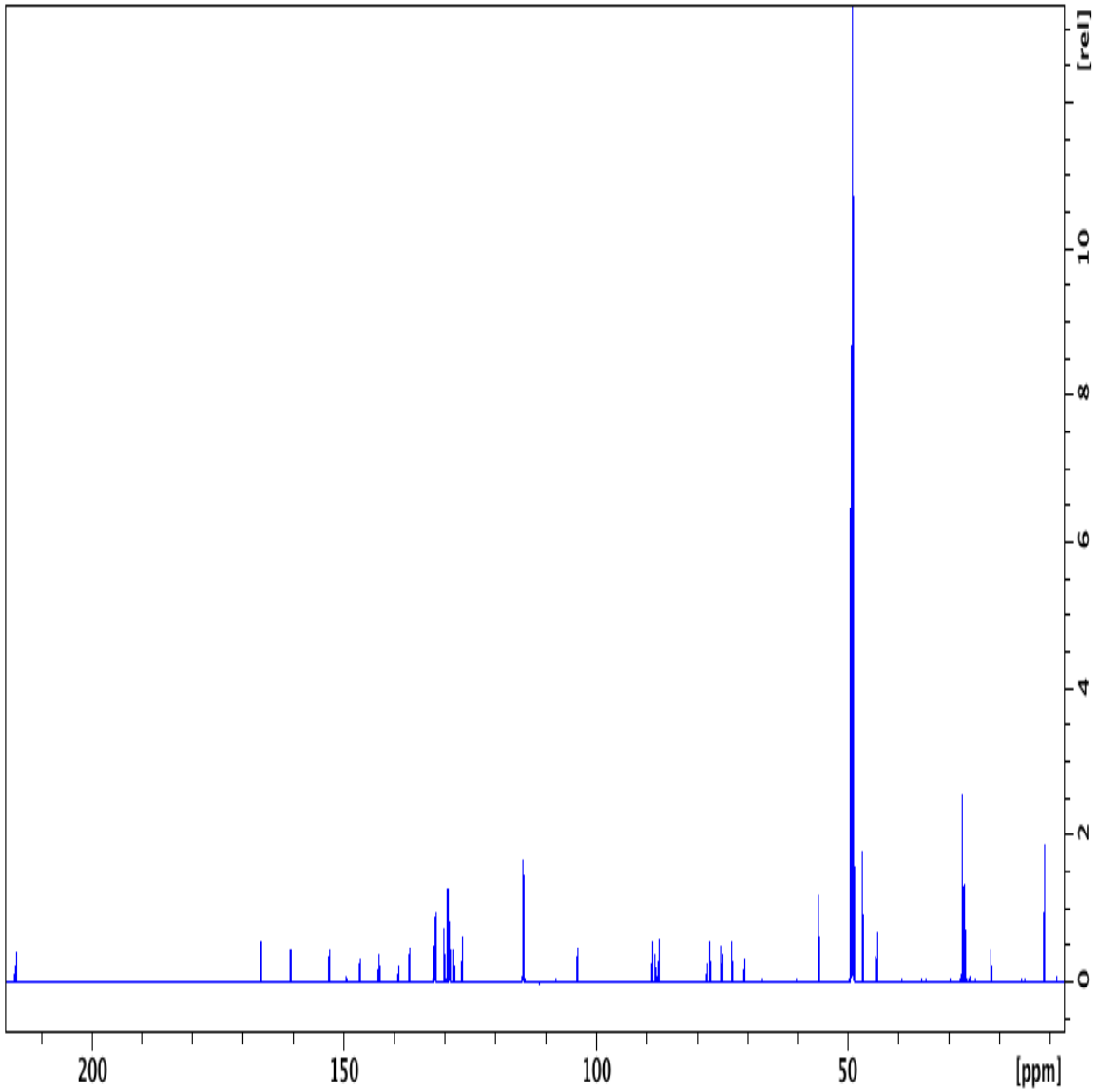


Figure A-5. $^{13}C$ NMR for **93**

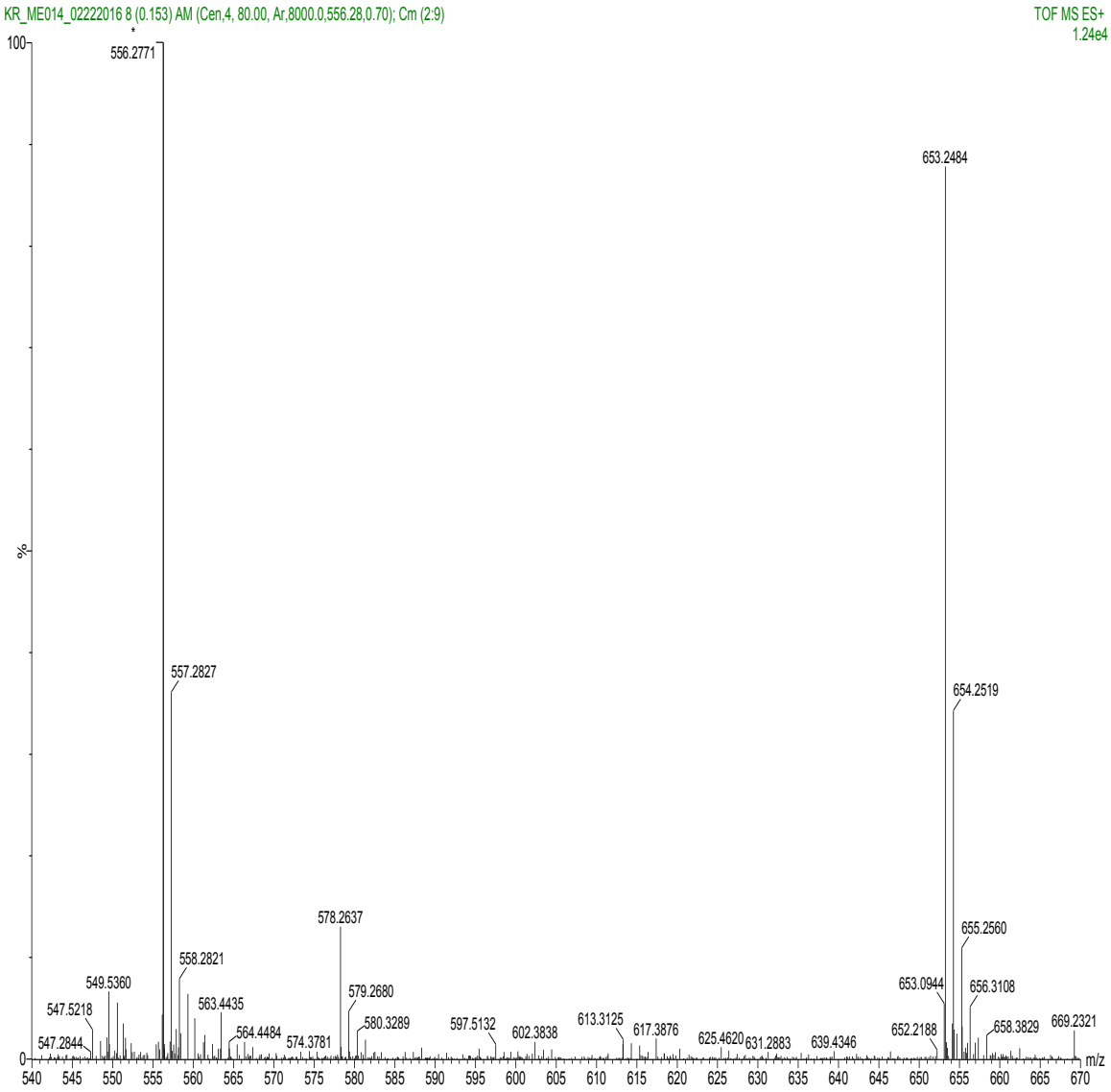


Figure A-6. HRMS for **93**

ME017 precursor phosphate

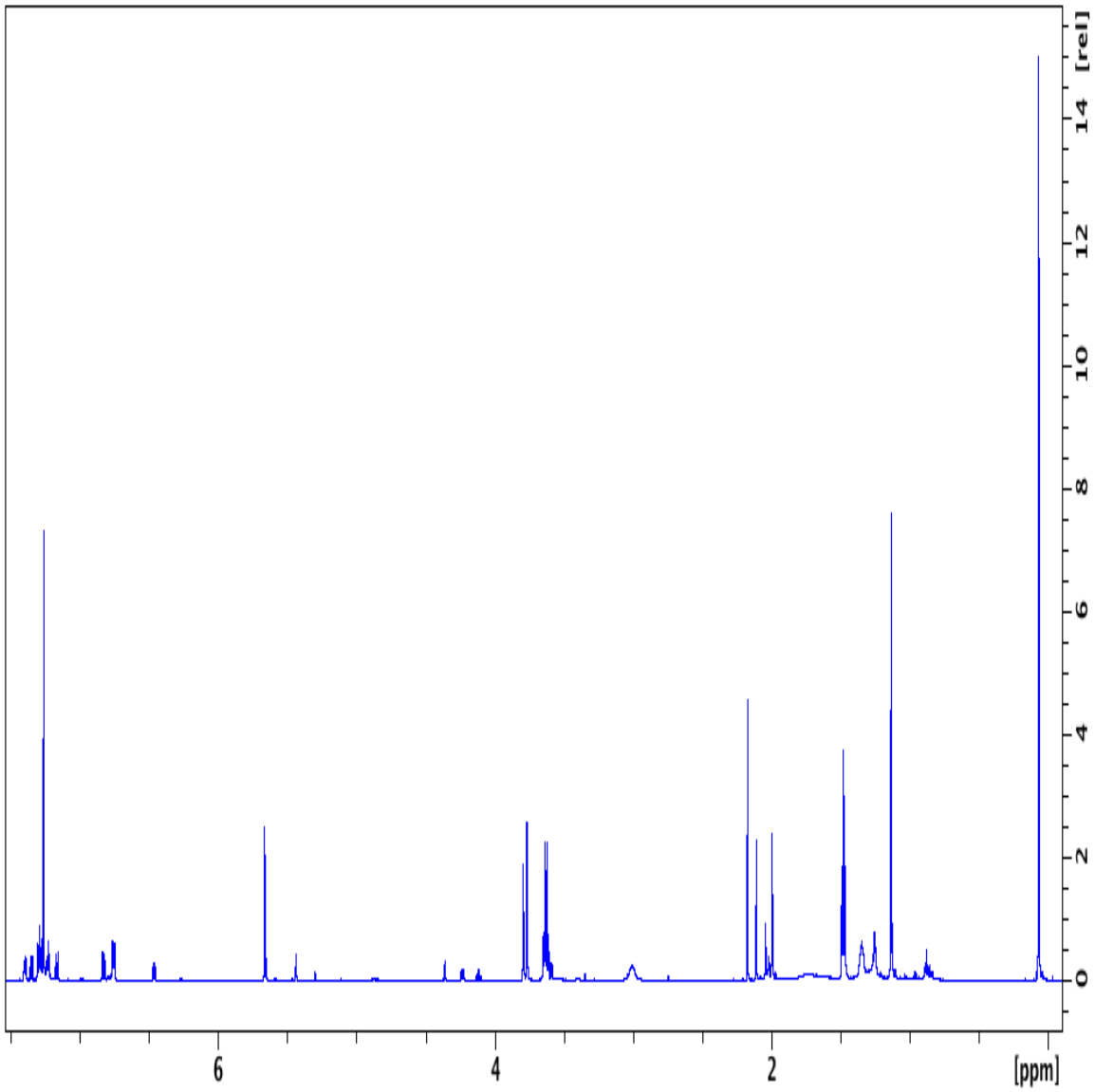


Figure A-7. $^{1}$H NMR for **94**

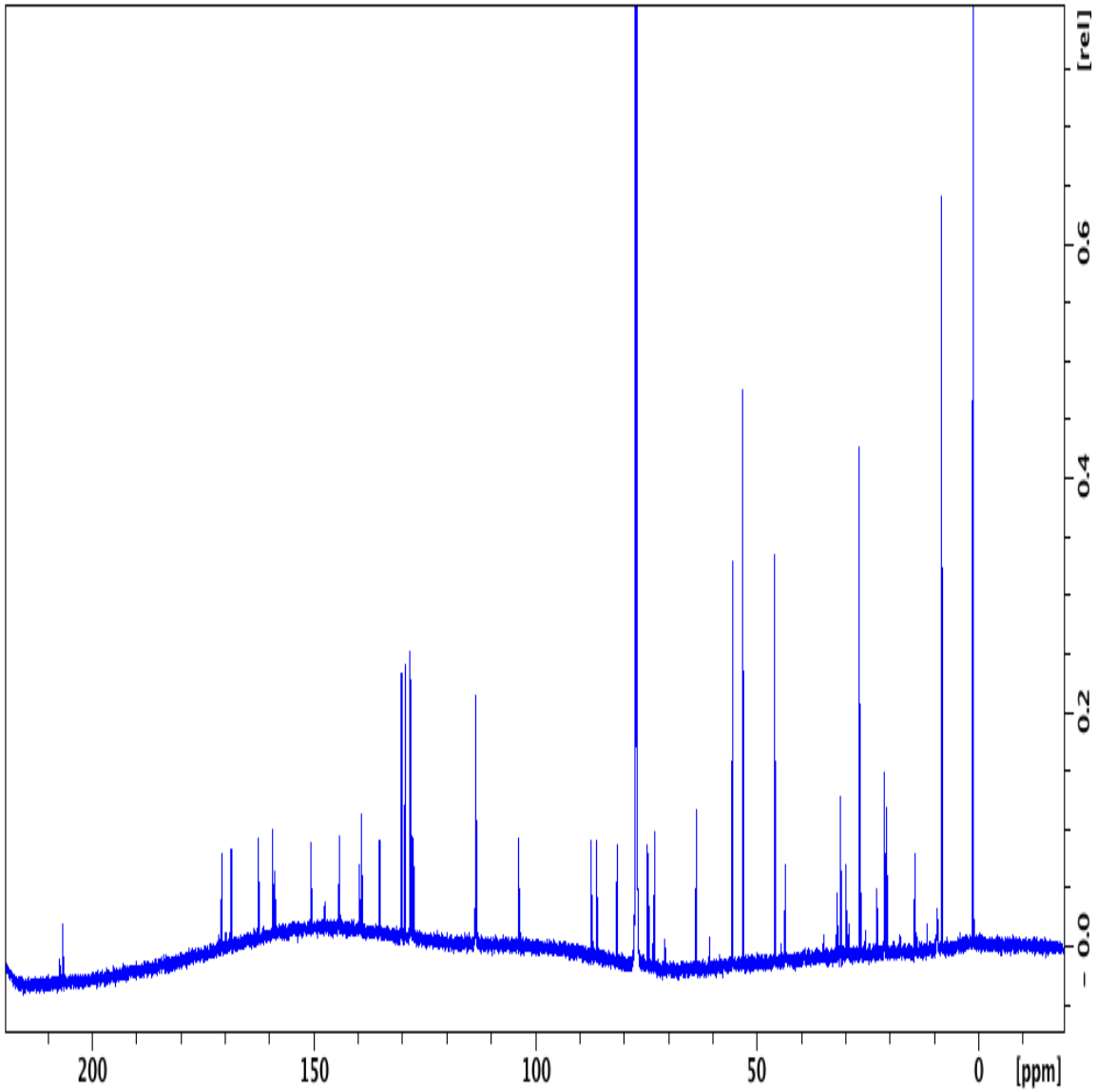


Figure A-8. $^{13}C$ NMR for **94**

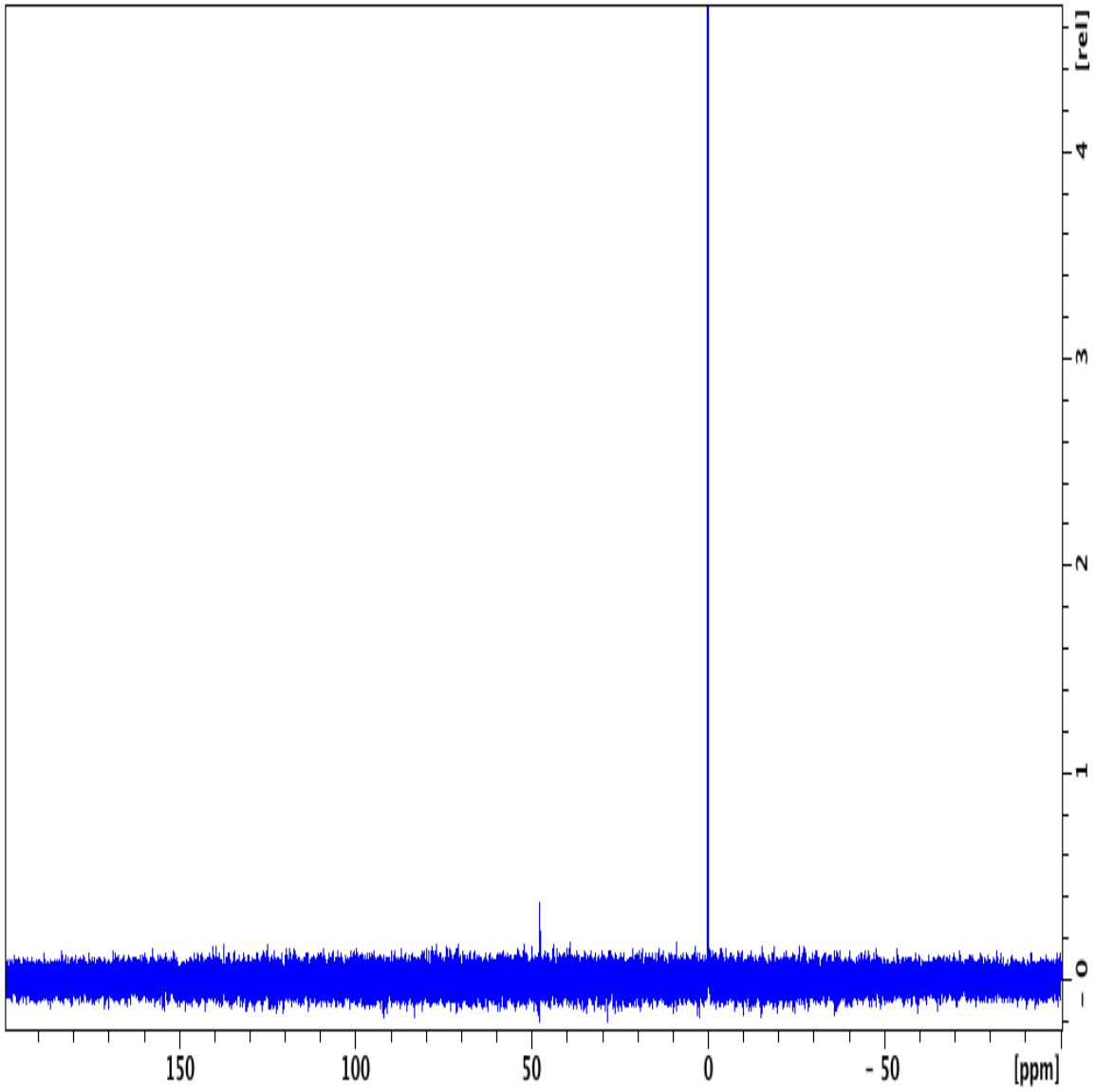


Figure A-9. $^{31}$P NMR for **94**

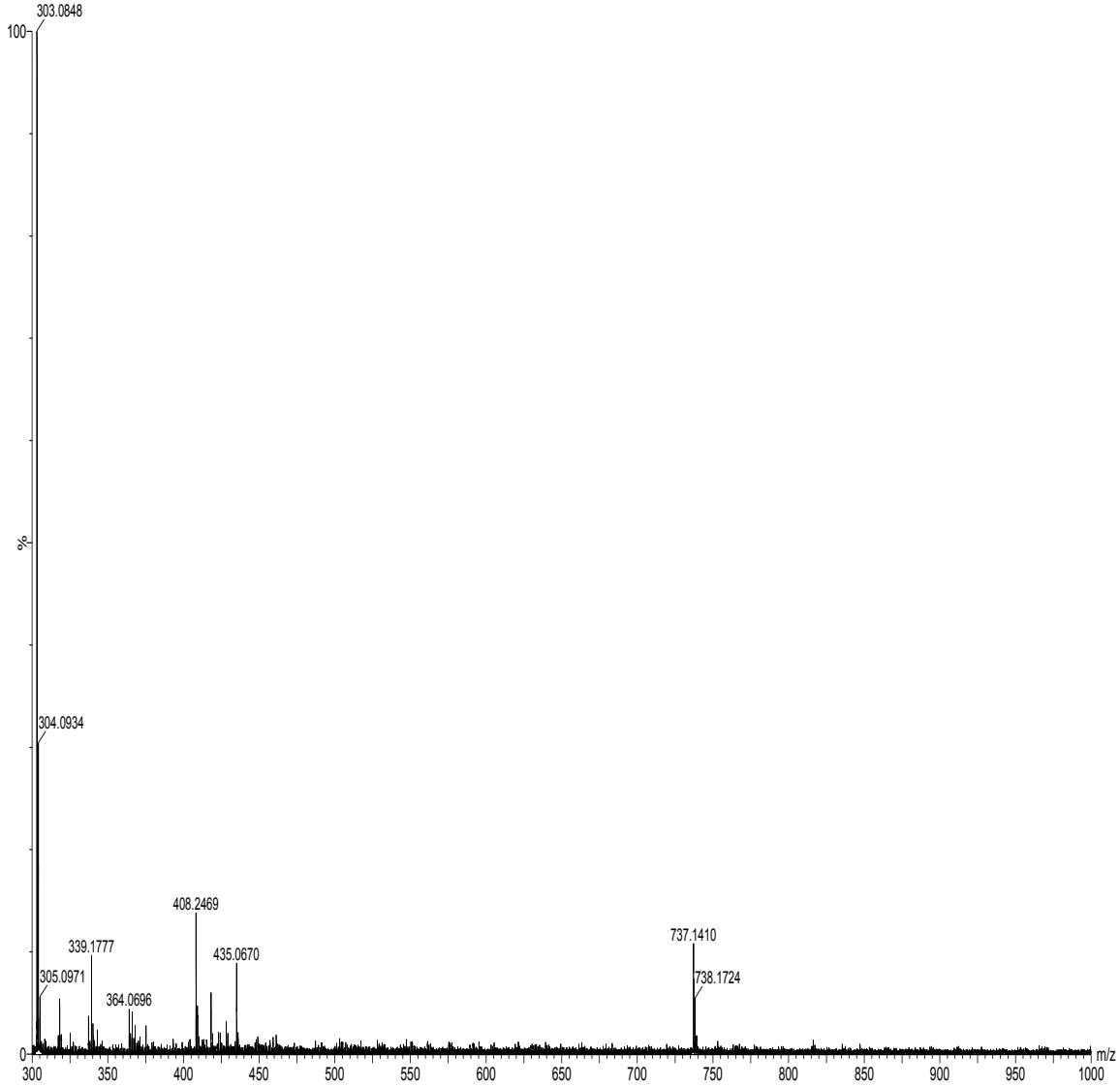


Figure A-10. HRMS for **94**

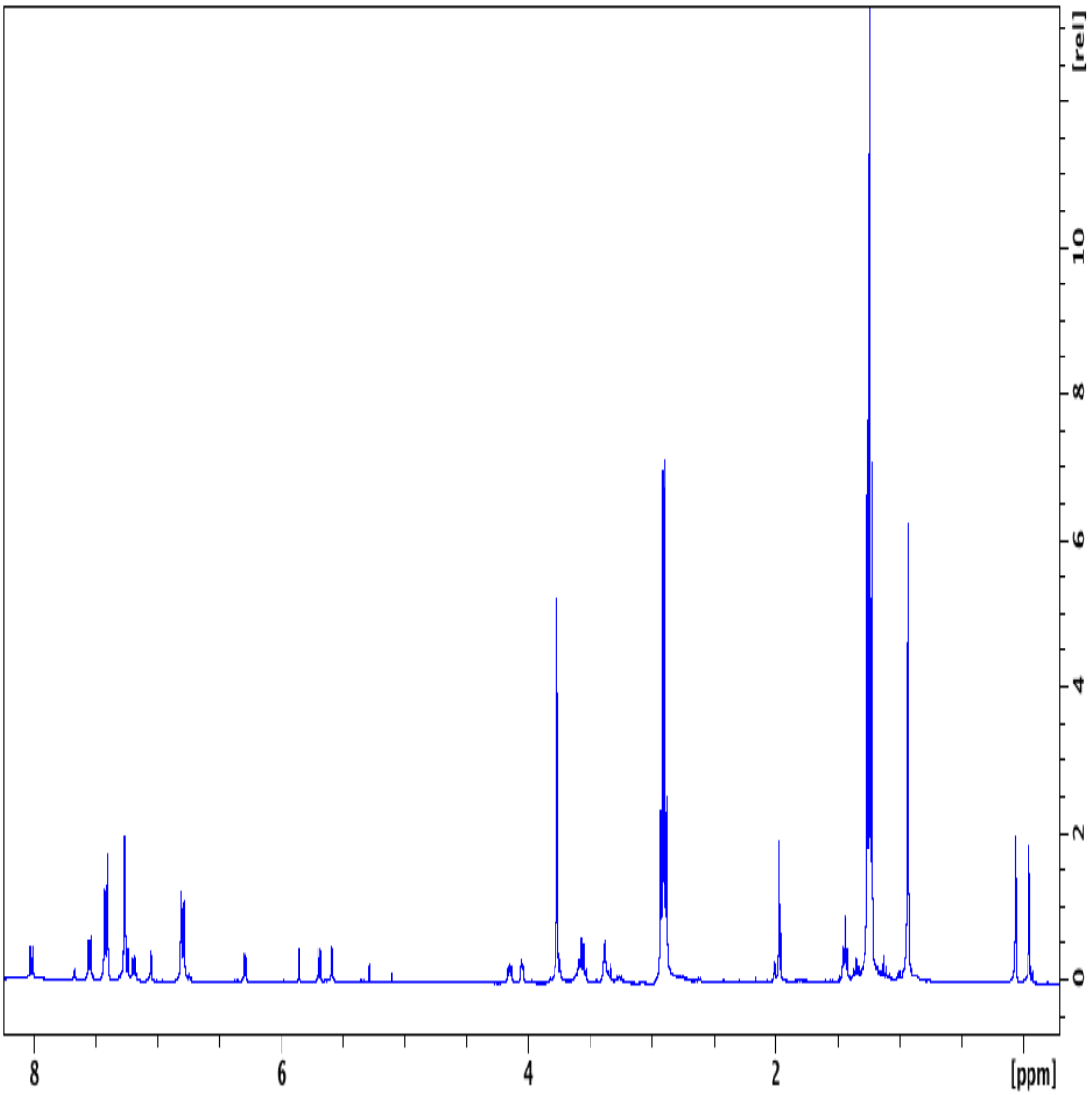


Figure A-11. $^{1}$H NMR for **95**

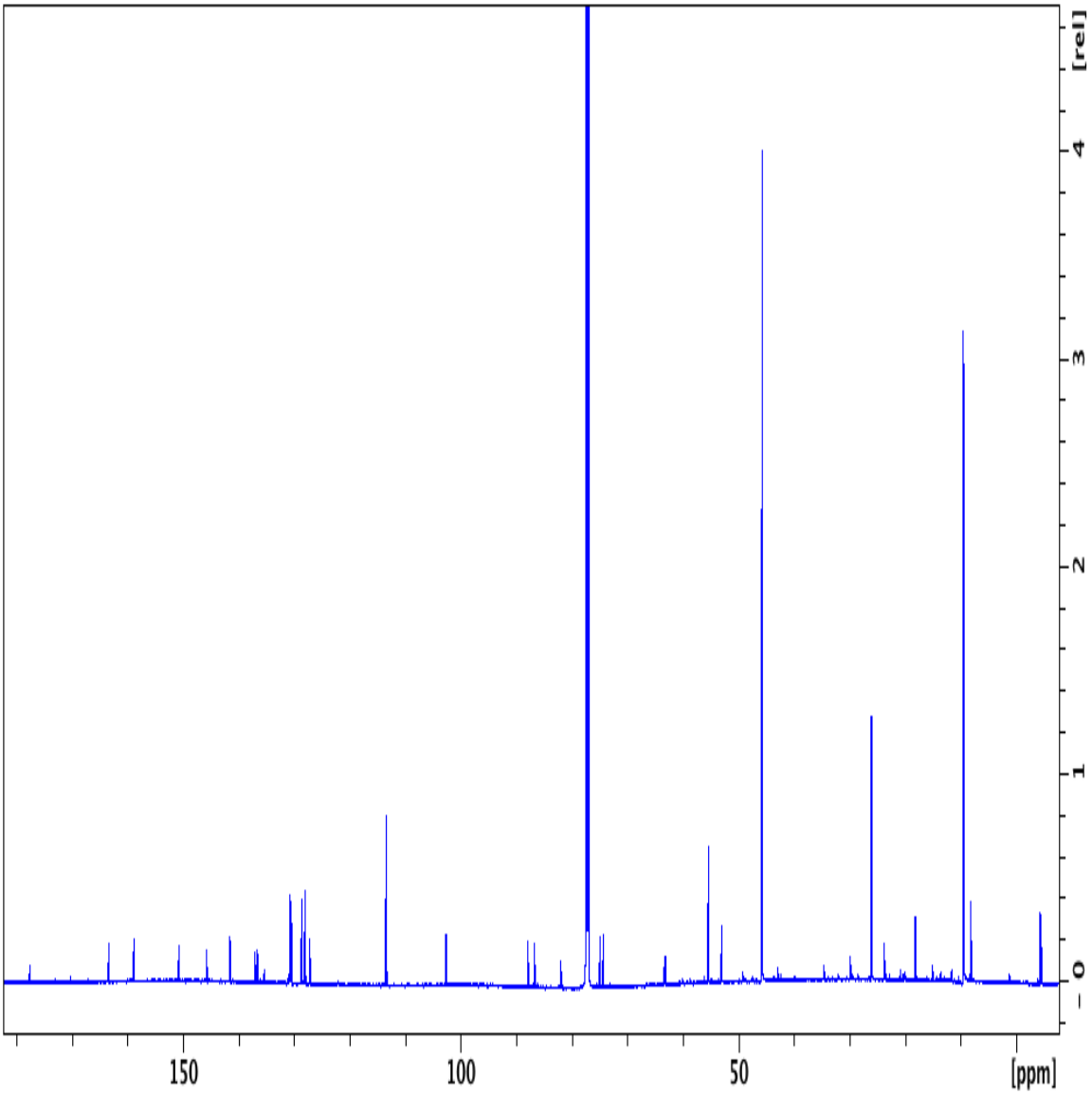


Figure A-12. $^{13}C$ NMR for **95**

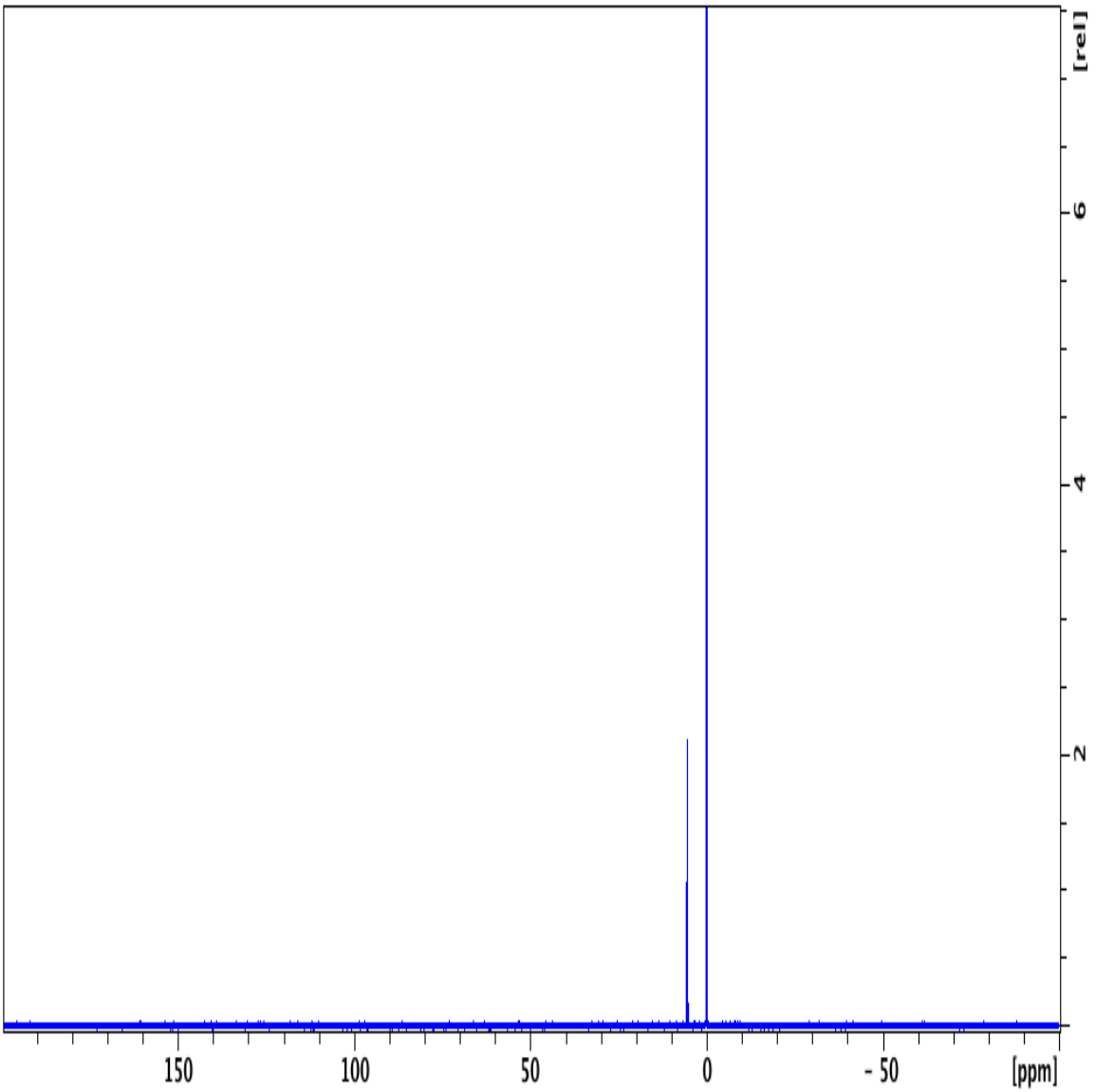


Figure A-13. $^{31}$P NMR for **95**

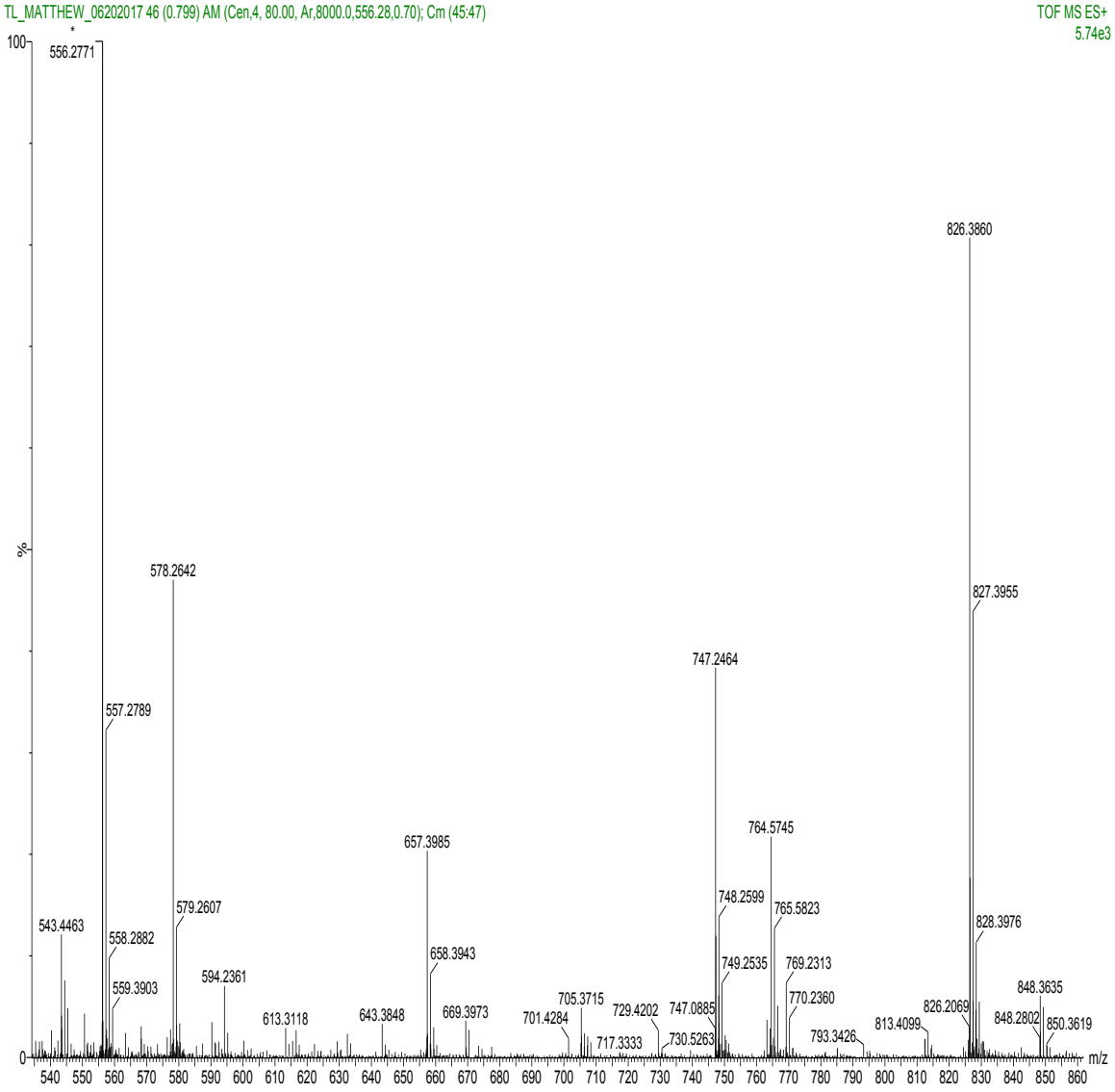


Figure A-14. HRMS for **95**

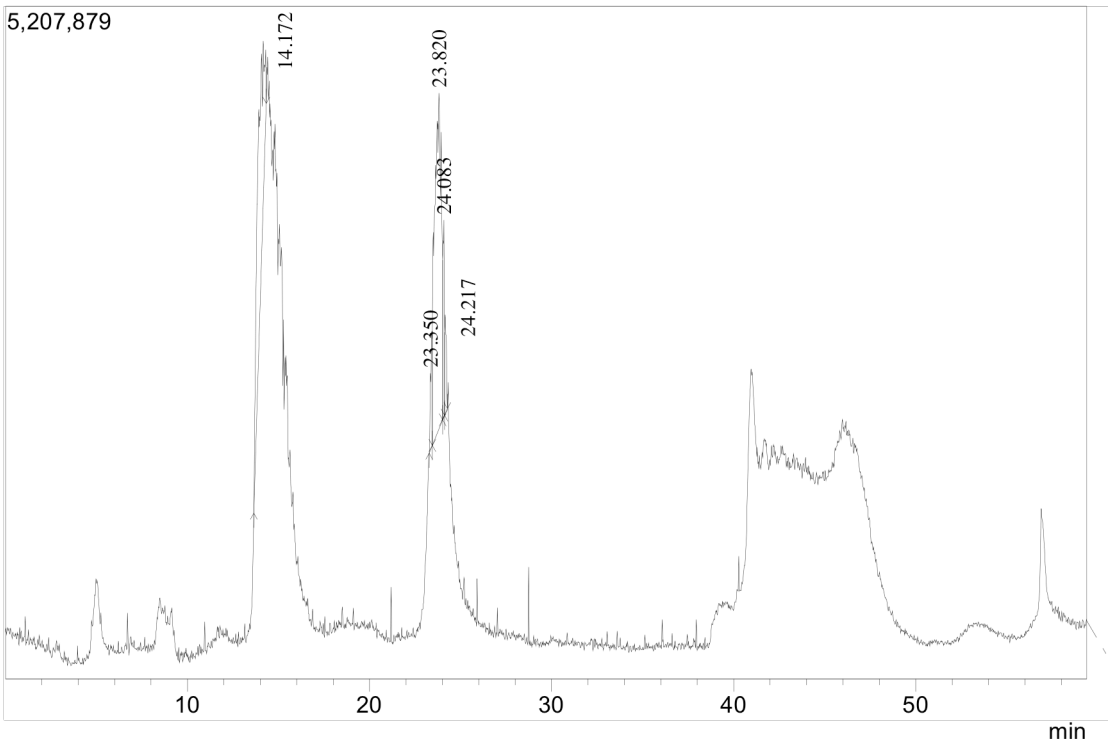


Figure A-15. Mass Data for pH 7.0 Aerobic Photolysis Run

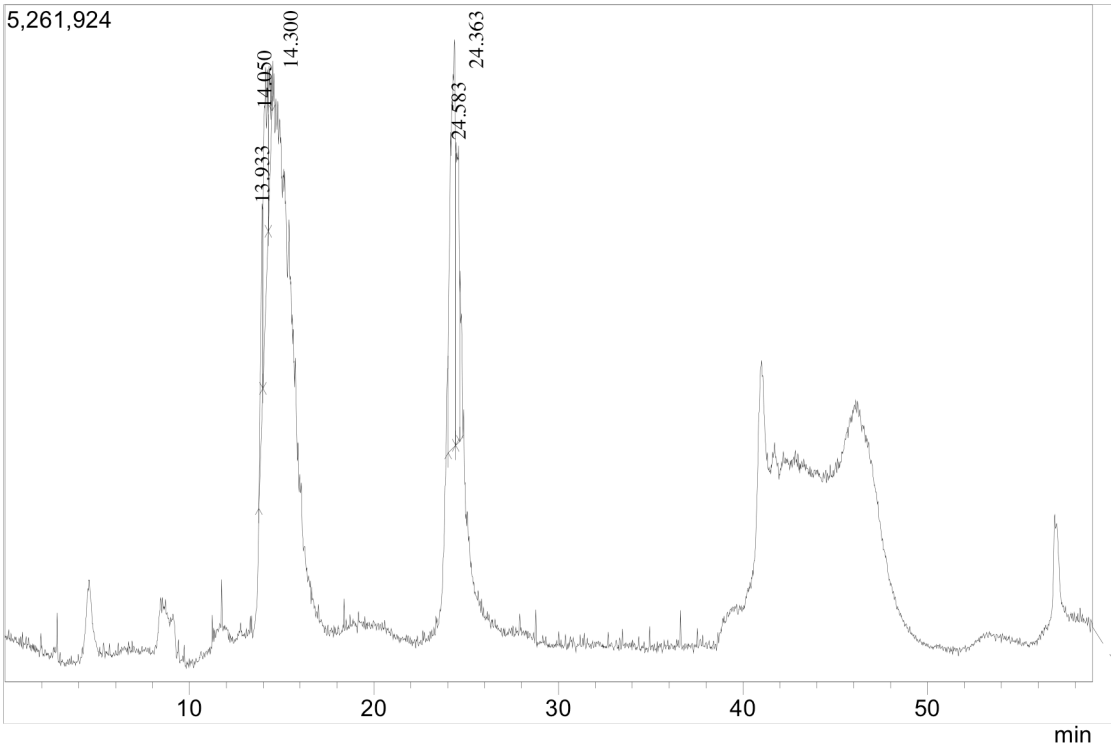


Figure A-16. Mass Data for pH 3.5 Aerobic Photolysis Run

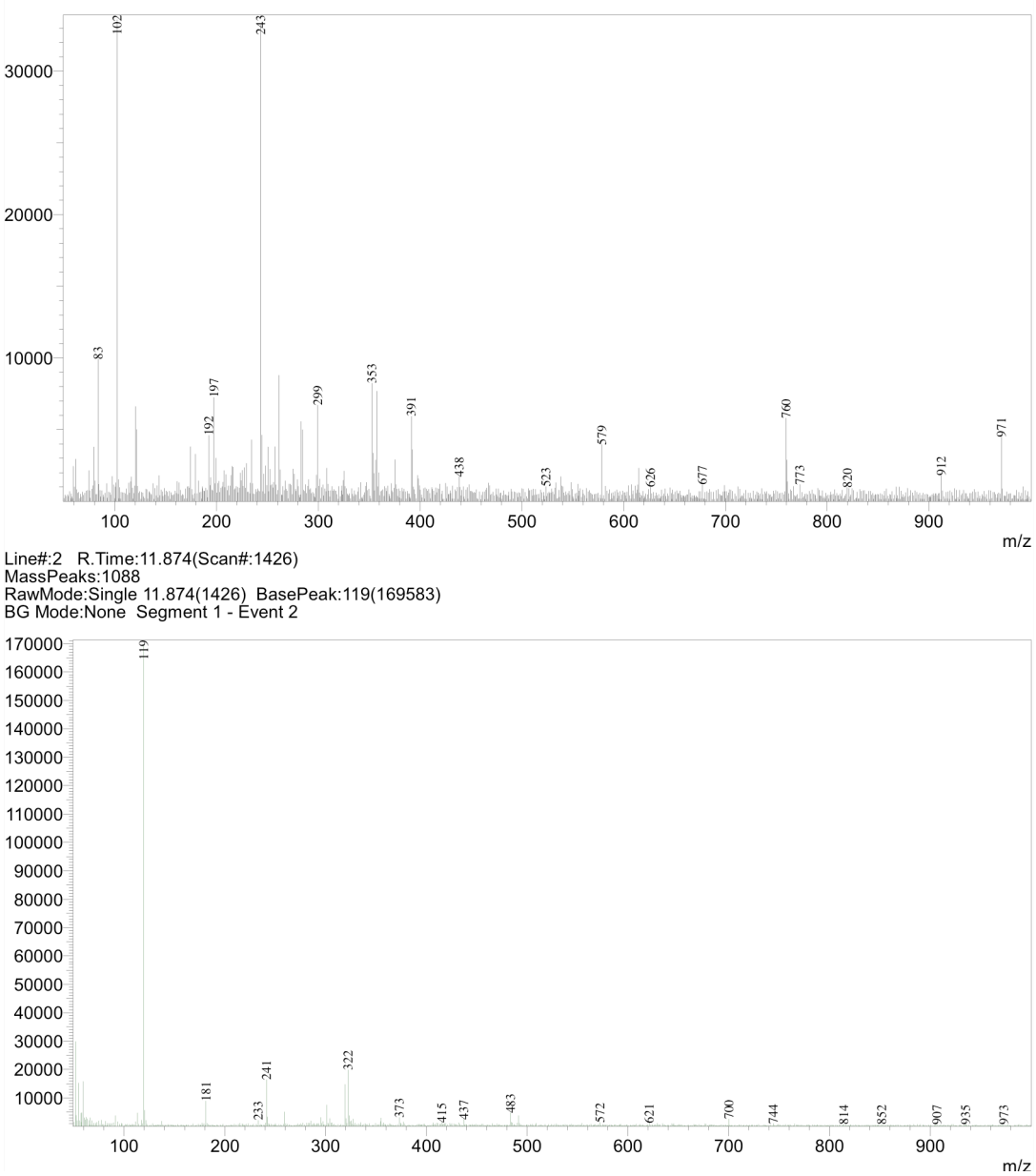


Figure A-17. Mass Data for 11.8 min, pH 7.0 Aerobic Photolysis Run

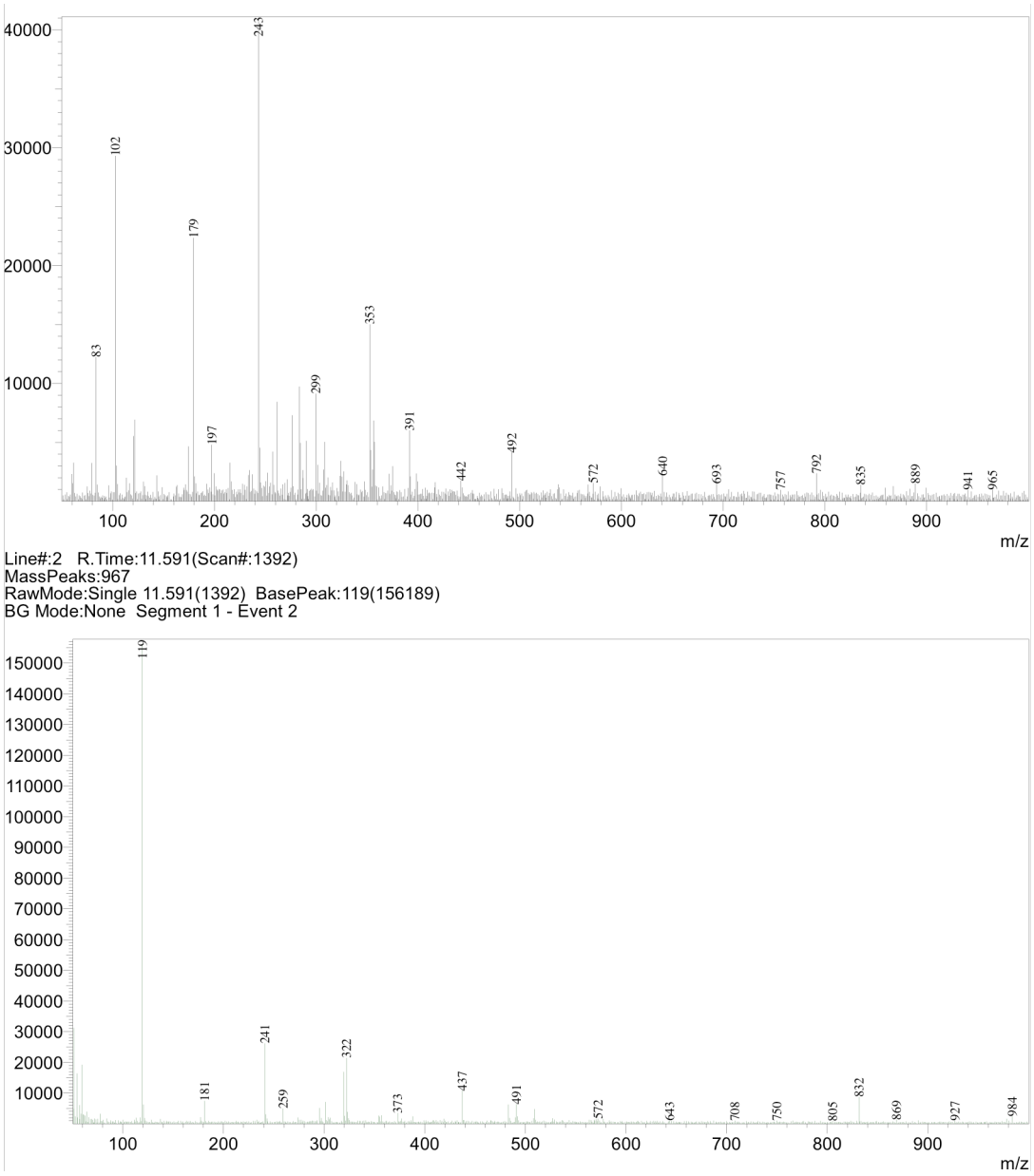


Figure A-18. Mass Data for 11.5 min, pH 3.5 Aerobic Photolysis Run

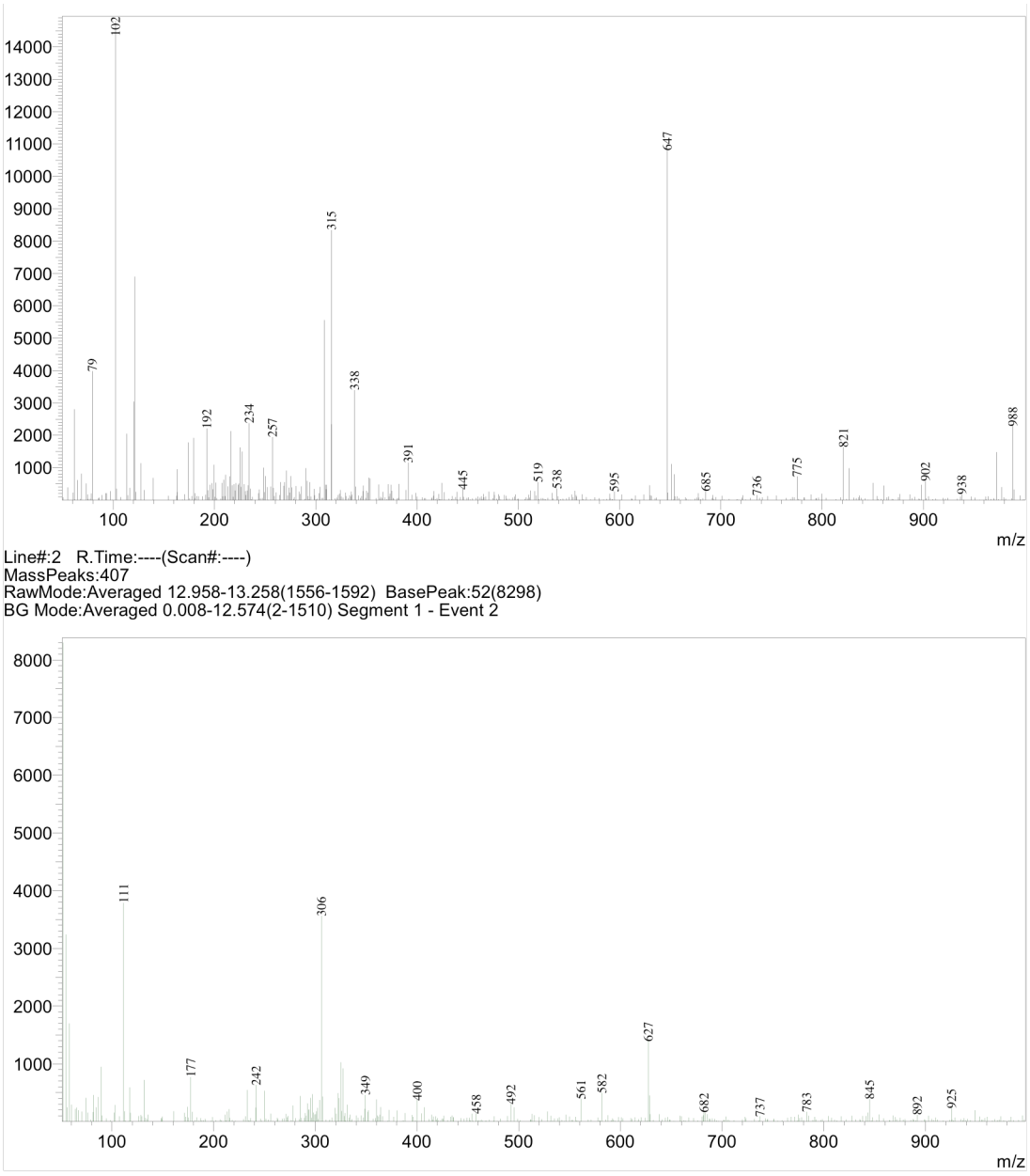


Figure A-19. Mass Data for 12.9-13.3 min, pH 7.0 Aerobic Photolysis Run

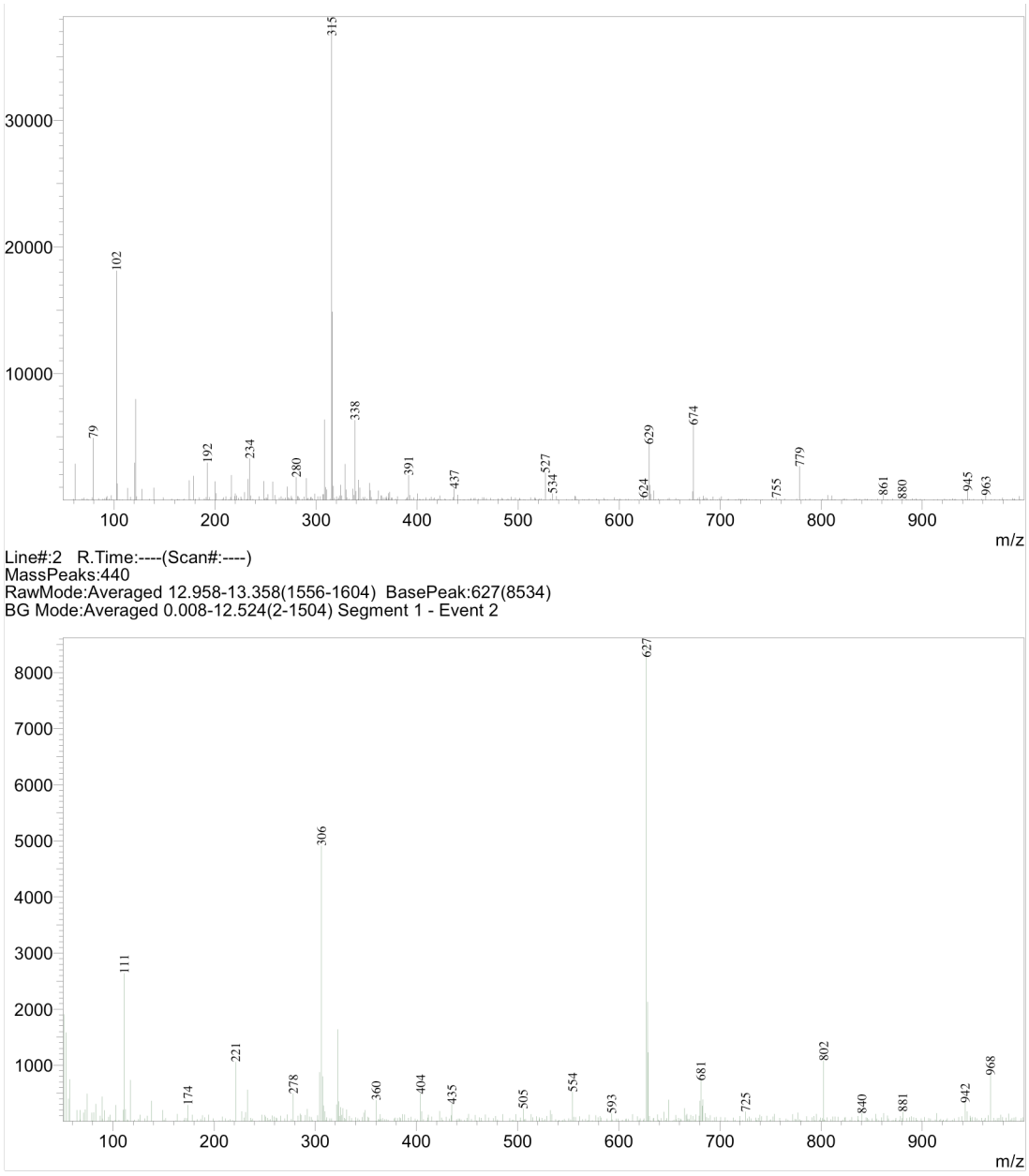


Figure A-20. Mass Data for 12.9-13.3 min, pH 3.5 Aerobic Photolysis Run

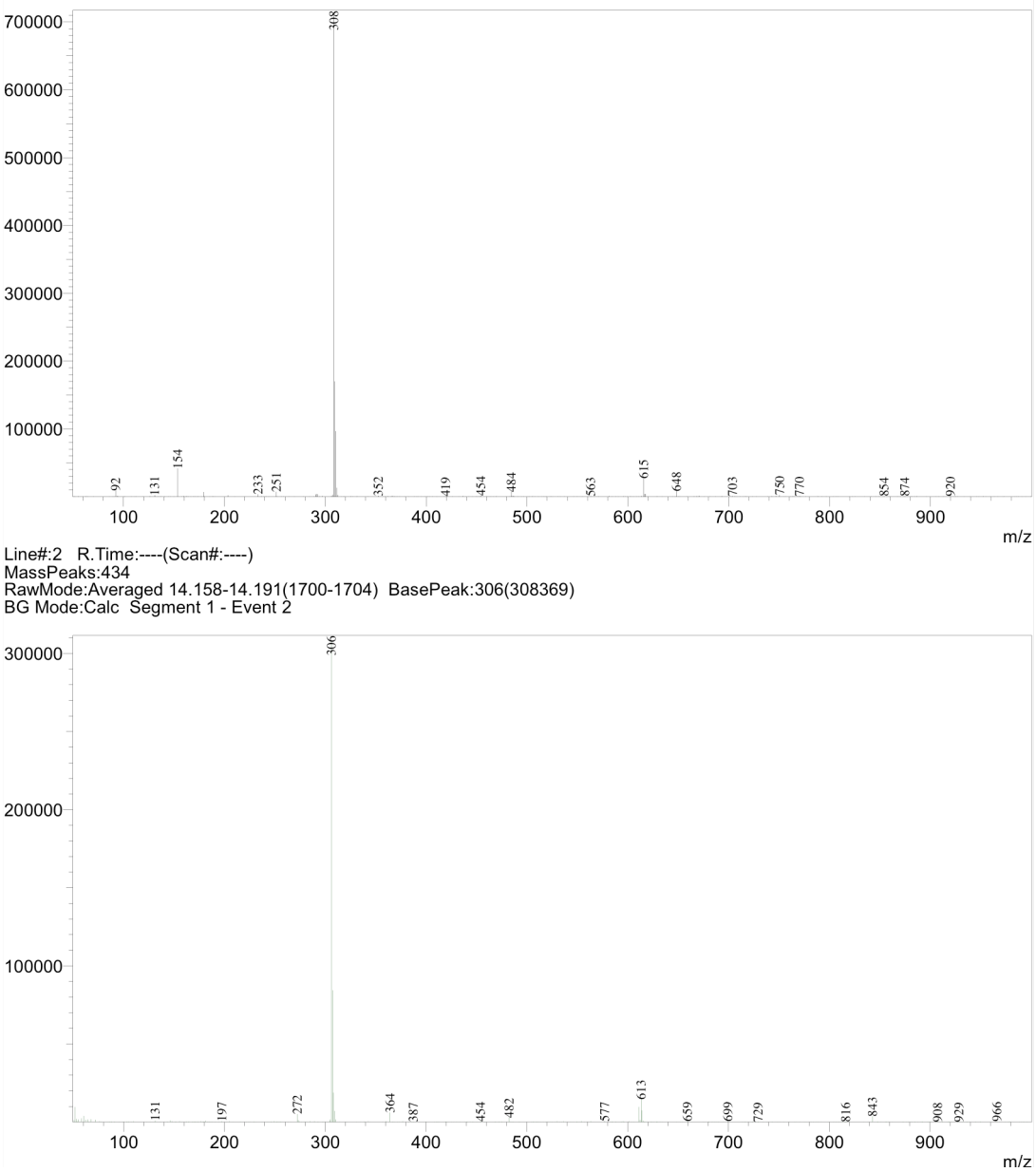


Figure A-21. Mass Data for 14.2 min, pH 7.0 Aerobic Photolysis Run

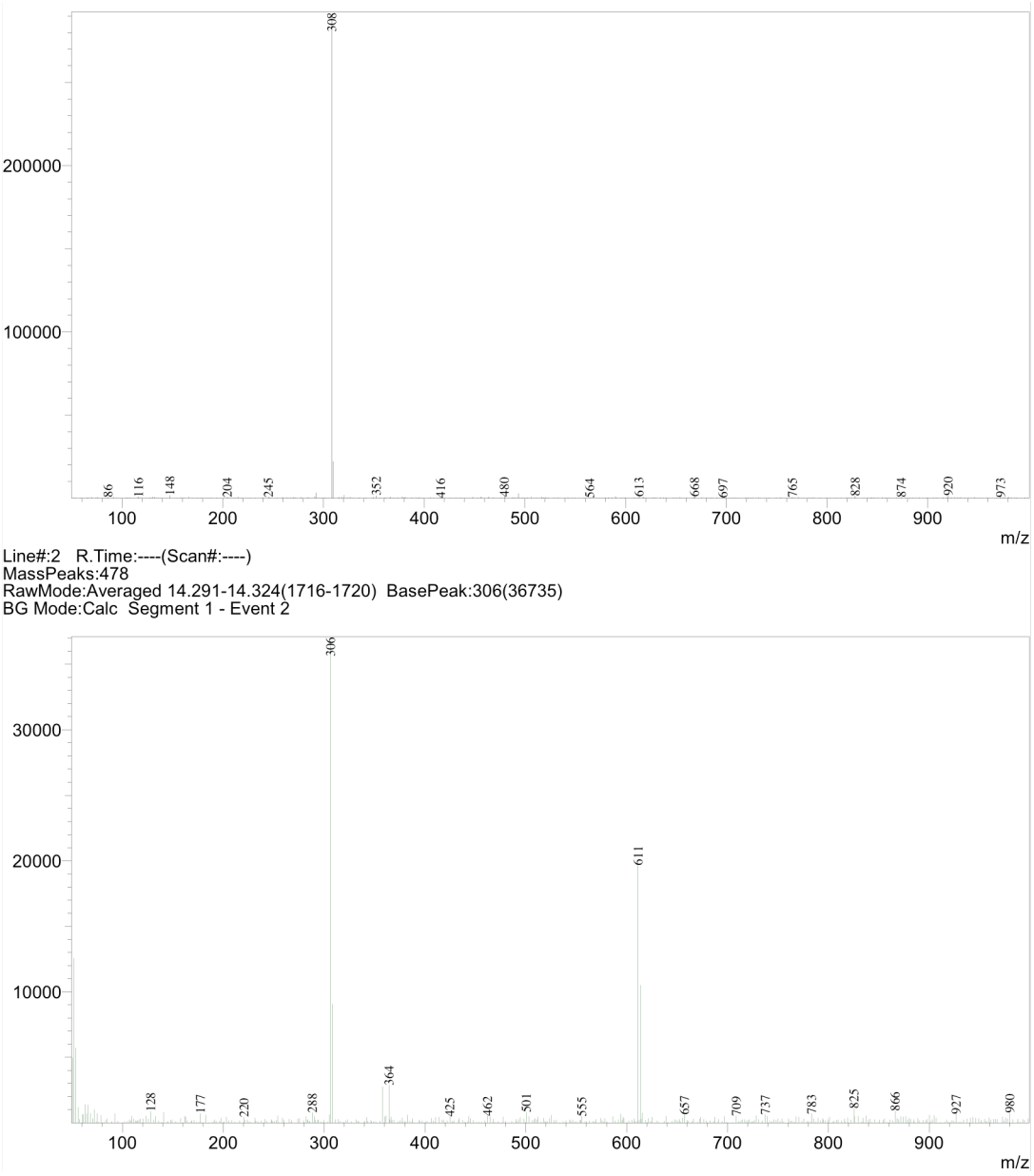


Figure A-22. Mass Data for 14.1 min, pH 3.5 Aerobic Photolysis Run

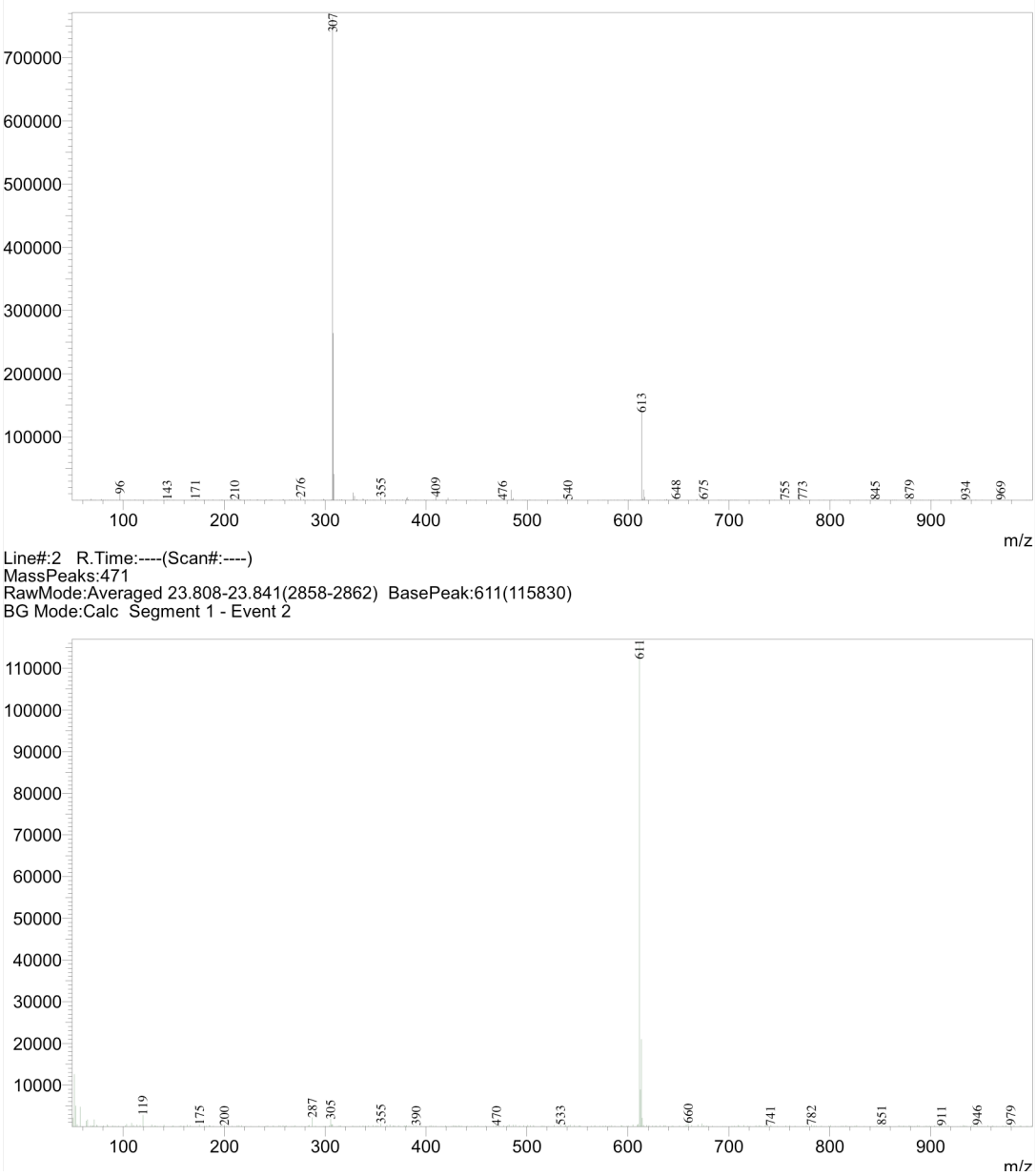


Figure A-23. Mass Data for 23 min, pH 7.0 Aerobic Photolysis Run

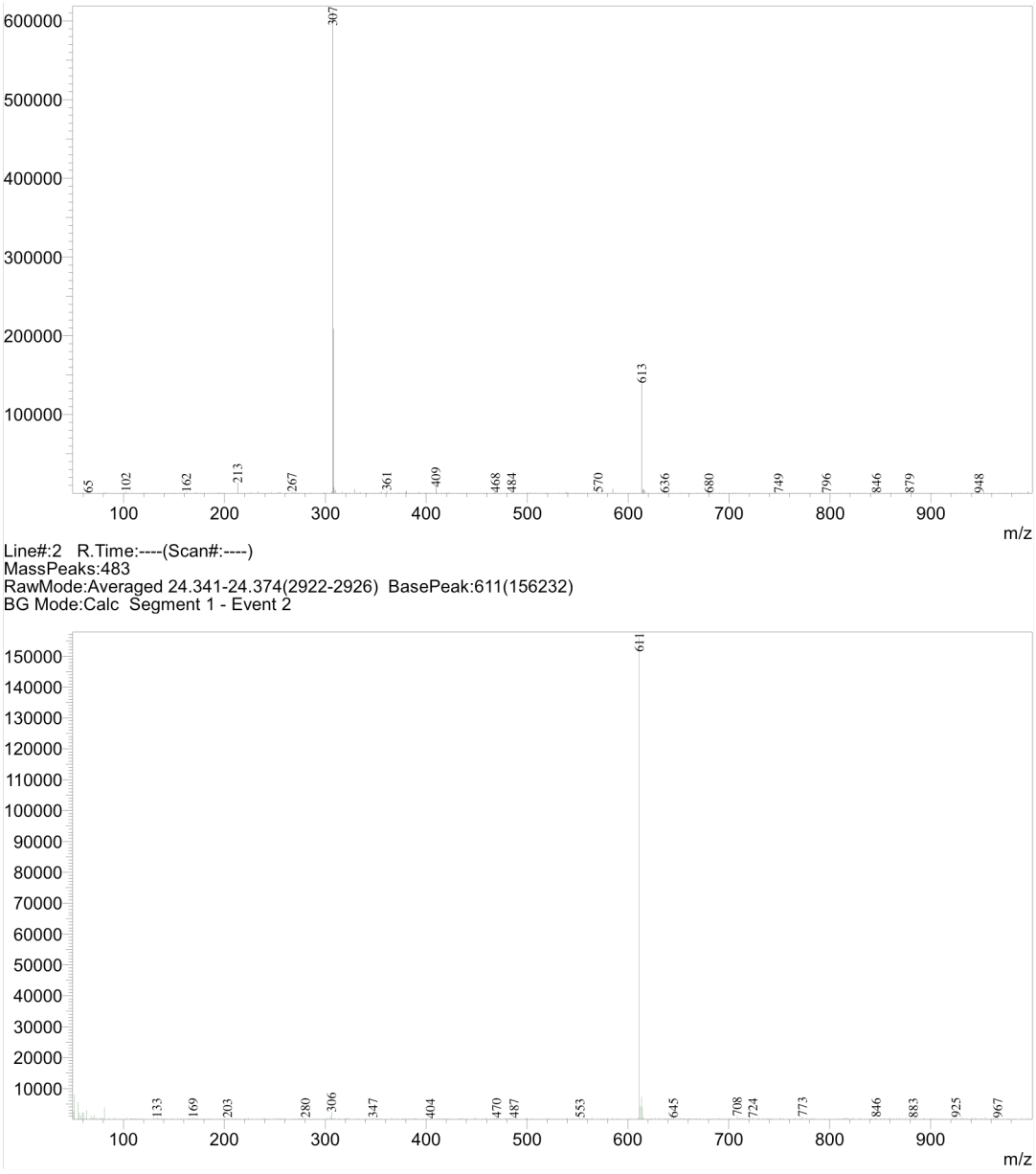


Figure A-24. Mass Data for 24 min, pH 3.5 Aerobic Photolysis Run

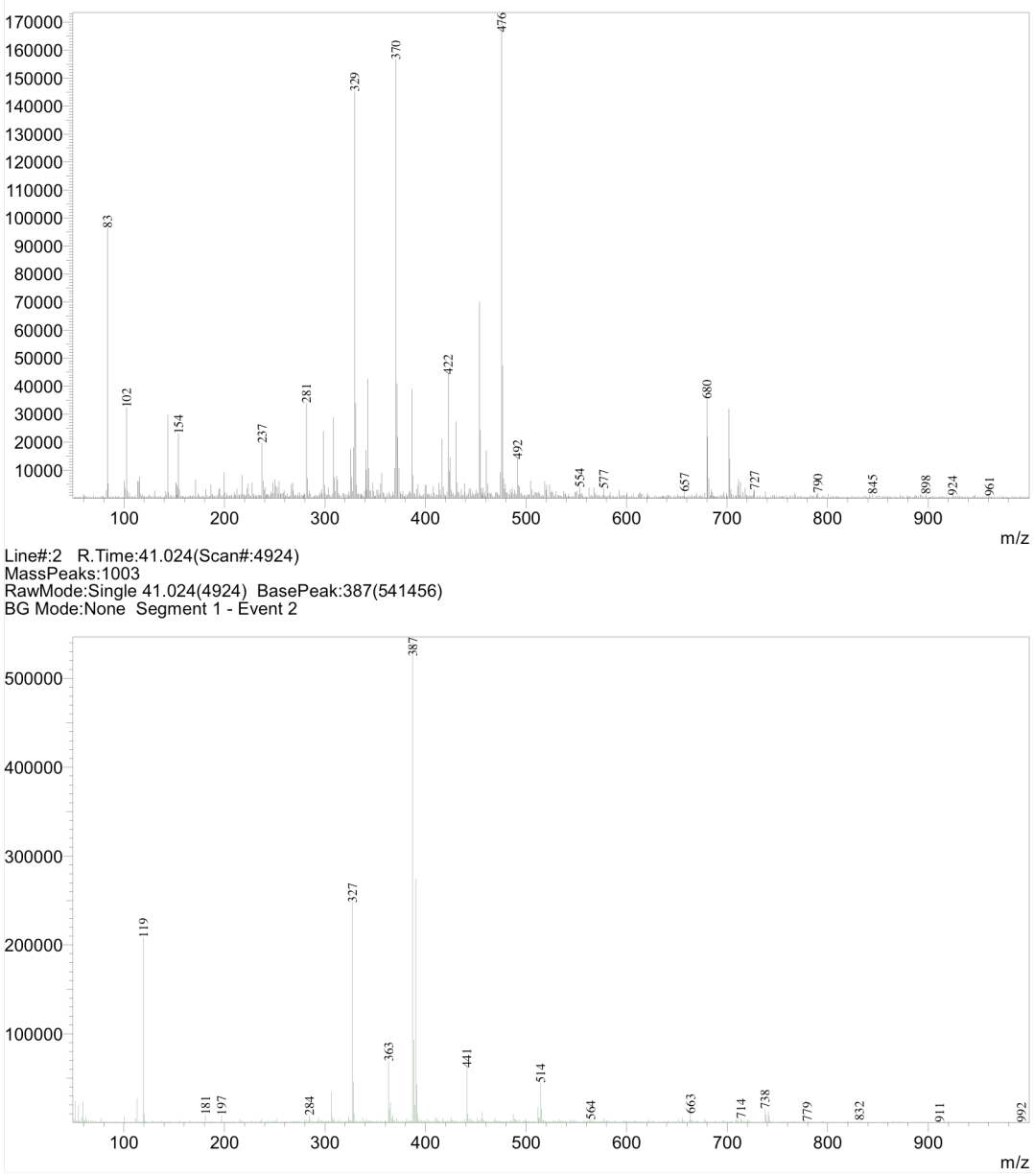


Figure A-25. Mass Data for 41.0 min, pH 7.0 Aerobic Photolysis Run

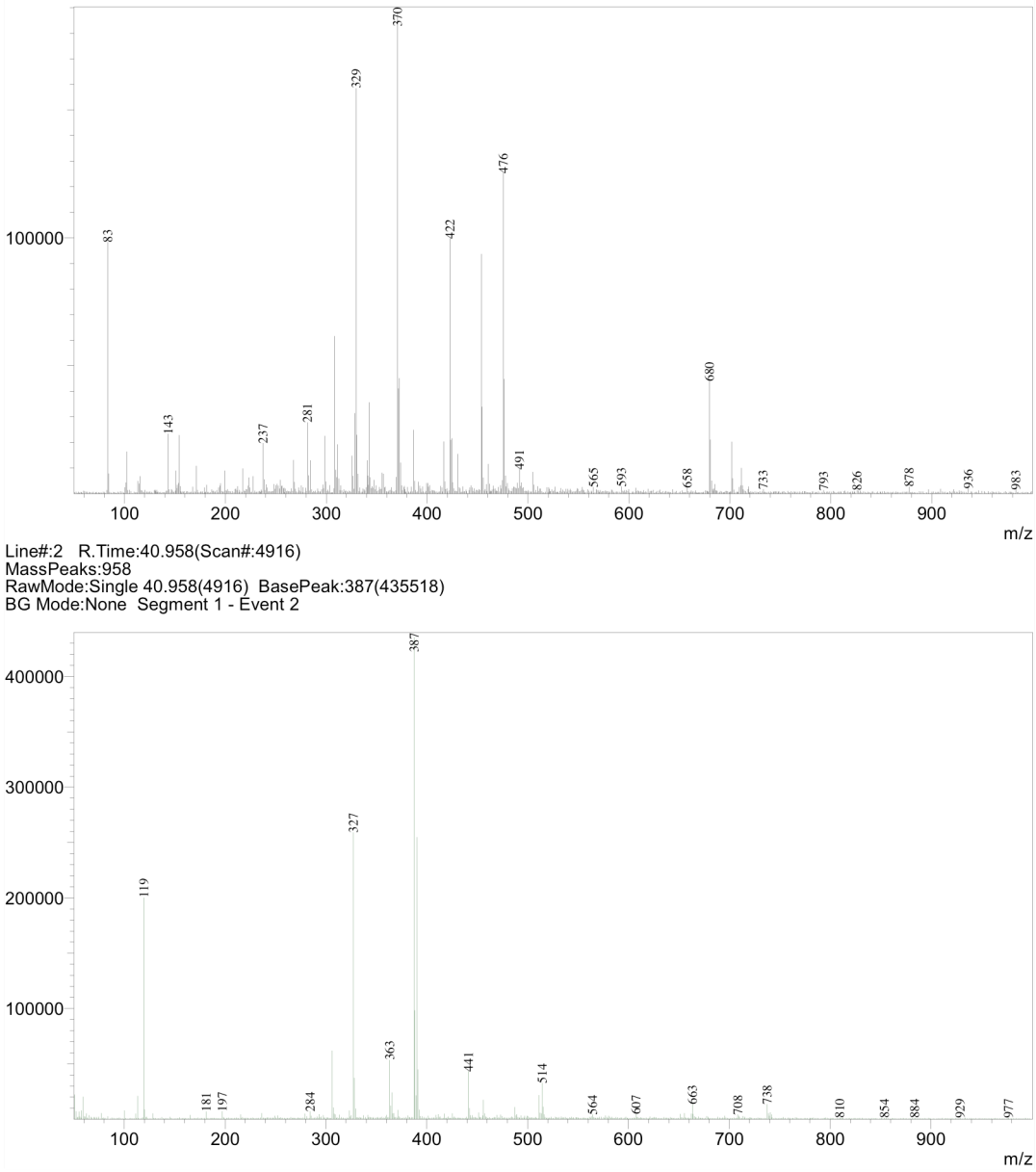


Figure A-26. Mass Data for 40.9 min, pH 3.5 Aerobic Photolysis Run

# References


(1) Wild, C. P. (2005) Complementing the genome with an "exposome": the outstanding challenge of environmental exposure measurement in molecular epidemiology. *Cancer Epidemiol Biomarkers Prev 14*, 1847-1850.

(2) Miller, G. W., and Jones, D. P. (2014) The nature of nurture: refining the definition of the exposome. *Toxicological sciences : an official journal of the Society of Toxicology 137*, 1-2.

(3) Newman, C. A., Resendiz, M. J., Sczepanski, J. T., and Greenberg, M. M. (2009) Photochemical generation and reactivity of the 5,6-dihydrouridin-6-yl radical. *J Org Chem 74*, 7007-7012.

(4) Jacobs, A. C., Resendiz, M. J., and Greenberg, M. M. (2011) Product and mechanistic analysis of the reactivity of a C6-pyrimidine radical in RNA. *J Am Chem Soc 133*, 5152-5159.

(5) Resendiz, M. J., Pottiboyina, V., Sevilla, M. D., and Greenberg, M. M. (2012) Direct strand scission in double stranded RNA via a C5-pyrimidine radical. *J Am Chem Soc 134*, 3917-3924.

(6) Honda, K., Smith, M. A., Zhu, X., Baus, D., Merrick, W. C., Tartakoff, A. M., Hattier, T., Harris, P. L., Siedlak, S. L., Fujioka, H., Liu, Q., Moreira, P. I., Miller, F. P., Nunomura, A., Shimohama, S., and Perry, G. (2005) Ribosomal RNA in

Alzheimer disease is oxidized by bound redox-active iron. *J Biol Chem 280*, 20978-20986.

(7) Tanaka, M., Chock, P. B., and Stadtman, E. R. (2007) Oxidized messenger RNA induces translation errors. *Proc Natl Acad Sci U S A 104*, 66-71.

(8) Calabretta, A., Kupfer, P. A., and Leumann, C. J. (2015) The effect of RNA base lesions on mRNA translation. *Nucleic Acids Res 43*, 4713-4720.

(9) Sekiguchi, T., Ito, R., Hayakawa, H., and Sekiguchi, M. (2013) Elimination and utilization of oxidized guanine nucleotides in the synthesis of RNA and its precursors. *J Biol Chem 288*, 8128-8135.

(10) A. Klungland, R. P., V. Rolseth, Y. Yamada, Y. Ueno, P, Wiik, A. Matsuda, E. Seeberg, S. Bjelland. (2001) 5-Formyluracil and its nucleoside derivatives confer toxicity and mutagenicity to mammalian cells by interfering with normal RNA and DNA metabolism. *Toxicology Letters 119*, 8.

(11) Sang Kook Kim, J. Y. K., Ae Kyeong Baek, and Byung Jo Moon. (2002) Base Pairing Properties of 8-Oxo-7,8-dihydroadenosine in cDNA Synthesis by Reverse Transcriptases. *Bioorg Med Chem Lett 12*, 4.

(12) Sang Kook Kim, S. H. L., Oh-Shin Kwon, and Byung Jo Moon. (2004) DNA · RNA Heteroduplex Containing 8-Oxo-7,8-dihydroguanosine: Base Pairing, Structures, and Thermodynamic Stability. *J Biochem Mol Biol 37*, 6.

(13) Song Cui, Y.-H. K., Cheng-Hao Jin, Sng Kook Kim, Man-hee Rhee, Oh-Shin Kwon, & Byung Jo Moon. (2009) Synthesis and base pairing properties of DNA-RNA heteroduplex containing 5-hydroxyuridine. *BMB Reports*, 7.

(14) Kupfer, P. A., and Leumann, C. J. (2011) Synthesis, base pairing properties and trans-lesion synthesis by reverse transcriptases of oligoribonucleotides containing the oxidatively damaged base 5-hydroxycytidine. *Nucleic Acids Res 39*, 9422-9432.

(15) Calabretta, A., and Leumann, C. J. (2013) Base pairing and miscoding properties of 1,N(6)-ethenoadenine- and 3,N(4)-ethenocytosine-containing RNA oligonucleotides. *Biochemistry 52*, 1990-1997.

(16) Zhang, J., Perry, G., Smith, M. A., Robertson, D., Olson, S. J., Graham, D. G., and Montine, T. J. (1999) Parkinson's Disease Is Associated with Oxidative Damage to Cytoplasmic DNA and RNA in Substantia Nigra Neurons. *The American Journal of Pathology 154*, 1423-1429.

(17) W. Martinet, G. R. Y. D. M., A. G. Herman, and M. M. Kockx. (2004) Reactive oxygen species induce RNA damage in human atherosclerosis. *European Journal of Clinical Investigation 34*, 5.

(18) Akihiko Nunomura, S. C., Kenji Kosaka, Atsushi Takeda, Rudy J. Castellani, Mark A. Smith, and George Perry. (2002) Neuronal RNA oxidation is a prominent feature of dementia with Lewy bodies. *Clinical Neuroscience and Neuropathology 13*, 5.

(19) Chang, Y., Kong, Q., Shan, X., Tian, G., Ilieva, H., Cleveland, D. W., Rothstein, J. D., Borchelt, D. R., Wong, P. C., and Lin, C. L. (2008) Messenger RNA oxidation occurs early in disease pathogenesis and promotes motor neuron degeneration in ALS. *PLoS One 3*, e2849.

(20) Shan, X., and Lin, C. L. (2006) Quantification of oxidized RNAs in Alzheimer's disease. *Neurobiol Aging 27*, 657-662.

(21) Shan, X., Chang, Y., and Lin, C. L. (2007) Messenger RNA oxidation is an early event preceding cell death and causes reduced protein expression. *FASEB J 21*, 2753-2764.

(22) Xiu Shan, H. T., and Chien-liang Glenn Lin. (2003) The Identification and Characterization of Oxidized RNAs in Alzheimer's Disease. *The Journal of Neuroscience 23*, 9.

(23) Akihiko Nunomura, G. P., Miguel A. Pappolla, Ramon Wad, Keisuke Hirai, Shigeru Chiba, and Mark A. Smith. (1999) RNA Oxidation Is a Prominent Feature of Vulnerable Neurons in Alzheimer's Disease. *The Journal of Neuroscience 19*, 6.

(24) Nunomura, A., Honda, K., Takeda, A., Hirai, K., Zhu, X., Smith, M. A., and Perry, G. (2006) Oxidative damage to RNA in neurodegenerative diseases. *J Biomed Biotechnol 2006*, 82323.

(25) Nunomura, A., Chiba, S., Lippa, C. F., Cras, P., Kalaria, R. N., Takeda, A., Honda, K., Smith, M. A., and Perry, G. (2004) Neuronal RNA oxidation is a prominent feature of familial Alzheimer's disease. *Neurobiol Dis 17*, 108-113.

(26) Moreira, P. I., Nunomura, A., Nakamura, M., Takeda, A., Shenk, J. C., Aliev, G., Smith, M. A., and Perry, G. (2008) Nucleic acid oxidation in Alzheimer disease. *Free Radic Biol Med 44*, 1493-1505.

(27) Jorgensen, A., Broedbaek, K., Fink-Jensen, A., Knorr, U., Greisen Soendergaard, M., Henriksen, T., Weimann, A., Jepsen, P., Lykkesfeldt, J., Poulsen, H. E., and

Balslev Jorgensen, M. (2013) Increased systemic oxidatively generated DNA and RNA damage in schizophrenia. *Psychiatry Res 209*, 417-423.

(28) Kharel, P., McDonough, J., and Basu, S. (2016) Evidence of extensive RNA oxidation in normal appearing cortex of multiple sclerosis brain. *Neurochem Int 92*, 43-48.

(29) Weidner, A. M., Bradley, M. A., Beckett, T. L., Niedowicz, D. M., Dowling, A. L., Matveev, S. V., LeVine, H., 3rd, Lovell, M. A., and Murphy, M. P. (2011) RNA oxidation adducts 8-OHG and 8-OHA change with Abeta42 levels in late-stage Alzheimer's disease. *PLoS One 6*, e24930.

(30) Steenken, A. J. S. C. V. a. S. (1990) Pattern of OH Radical Reaction with Adenine and Its Nucleosides and Nucleotides. Characterization of Two Types of Isomeric OH Adduct and Their Unimolecular Transformation Reactions. *J Am Chem Soc 112*, 9.

(31) Berger, J. C. a. M. (1985) Radiation-induced decomposition of the purine bases within DNA and related model compounds. *International Journal of Radiation Biology and Related Studies in Physics, Chemistry, and Medicine 47*, 7.

(32) Ingle, S., Azad, R. N., Jain, S. S., and Tullius, T. D. (2014) Chemical probing of RNA with the hydroxyl radical at single-atom resolution. *Nucleic Acids Res 42*, 12758-12767.

(33) Tiberiu Simandan, J. S., and Thomas A. Dix. (1998) Oxidation of DNA bases, deoxyribonucleosides and homopolymers by peroxyl radicals. *Biochem J 335*, 7.

(34) Nihon Kagakkai, I., Toshio. (1994) Oxidation of Nucleic Acid Related Compounds by the Peroxodisulfate Ion. *The Bulletin of the Chemical Society of Japan 67*, 8.

(35) Adinarayana. (2005) Reaction of substituted pyrimidines with photochemically generated t-BuO* radicals. *Indian Journal of Biochemistry & Biophysics 42*, 5.

(36) Maram Ravi Kumar, M. T. R. a. M. A. (2000) Phophoate radical induced oxidation of pyrimidine bases in aqueous solution. *Indian Journal of Biochemistry & Biophysics 37*, 5.

(37) Crean, C., Geacintov, N. E., and Shafirovich, V. (2008) Intrastrand G-U cross-links generated by the oxidation of guanine in 5'-d(GCU) and 5'-r(GCU). *Free Radic Biol Med 45*, 1125-1134.

(38) Yu Ye, J. G. M., Wenchen Luo, Charles L. Mayne, Anthony J. Shallop, Roger A. Jones, and Cynthia J. Burrows. (2003) Formation of 13C-, 15N-, and 18O-Labeled Guanidinohydantoin from Guanosine Oxidation with Singlet Oxygen. Implications for Structure and Mechanism. *J Am Chem Soc 125*, 2.

(39) Chimin Sheu, P. K., Saeed Khan, and Christopher S. Foote. (2002) Low-Temperature Photosensitized Oxidation of a Guanosine Derivative and Formation of an Imidazole Ring-Opened Product. *J Am Chem Soc 124*, 9.

(40) Foote, C. S. a. C. (1995) Photosensitized Oxygenation of a 7,8-Dihydro-8-oxoguanosine Derivative. Formation of Dioxetane and Hydroperoxide Intermediates. *J Am Chem Soc 117*, 4.

(41) Wenchen Luo, J. G. M., and Cynthia J. Burrows. (2001) The pH-Dependent Role of Superoxide in Riboflavin-Catalyzed Photooxidation of 8-Oxo-7,8-dihydroguanosine. *Org Lett 3*, 4.

(42) Tomaszewska-Antczak, A., Guga, P., Nawrot, B., and Pratviel, G. (2015) Guanosine in a single stranded region of anticodon stem-loop tRNA models is prone to oxidatively generated damage resulting in dehydroguanidinohydantoin and spiroiminodihydantoin lesions. *Chemistry 21*, 6381-6385.

(43) Wenchen Luo, J. G. M., Elliot M. Rachlin, and Cynthia J. Burrows. (2000) Characterization of Spiroiminodihydantoin as a Product of One-Electron Oxidation of 8-Oxo-7,8-dihydroguanosine. *Org Lett 2*, 4.

(44) Wenchen Luo, H. G. M., Elliot M. Rachlin, and Cynthia J. Burrows. (2001) Characterization of Hydantoin Products from One-Electron Oxidation of 8-Oxo-7,8-dihydroguanosine in a Nucleoside Model. *Chem Res Toxicol 14*, 12.

(45) Tanaka, M., Jaruga, P., Kupfer, P. A., Leumann, C. J., Dizdaroglu, M., Sonntag, W. E., and Boon Chock, P. (2012) RNA oxidation catalyzed by cytochrome c leads to its depurination and cross-linking, which may facilitate cytochrome c release from mitochondria. *Free Radic Biol Med 53*, 854-862.

(46) Yu Fen M. Chaw, E. C., Peter Lange, and Robert Shapiro. (1980) Isolation and Identification of Cross-Links from Formaldehyde-Treated Nucleic Acids. *Biochemistry 19*, 7.

(47) Koga, Y., Taniguchi, Y., and Sasaki, S. (2013) Synthesis of the oligoribonucleotides incorporating 8-oxo-guanosine and evaluation of their base pairing properties. *Nucleosides Nucleotides Nucleic Acids 32*, 124-136.

(48) Chauca-Diaz, A. M., Choi, Y. J., and Resendiz, M. J. (2015) Biophysical properties and thermal stability of oligonucleotides of RNA containing 7,8-dihydro-8-hydroxyadenosine. *Biopolymers 103*, 167-174.

(49) Kupfer, P. A., and Leumann, C. J. (2005) RNA abasic sites: preparation and trans-lesion synthesis by HIV-1 reverse transcriptase. *Chembiochem 6*, 1970-1973.

(50) Kupfer, P. A., Crey-Desbiolles, C., and Leumann, C. J. (2007) Trans-lesion synthesis and RNaseH activity by reverse transcriptases on a true abasic RNA template. *Nucleic Acids Res 35*, 6846-6853.

(51) J.O. Kang, K. S. G., G. Cohen. (1993) Methylation of RNA Purine Bases by Methyl Radicals. *Arch Biochem Biophys 306*, 5.

(52) Ougland, R., Zhang, C. M., Liiv, A., Johansen, R. F., Seeberg, E., Hou, Y. M., Remme, J., and Falnes, P. O. (2004) AlkB restores the biological function of mRNA and tRNA inactivated by chemical methylation. *Mol Cell 16*, 107-116.

(53) Satokko Yoshizawa, D. F., Joseph D. Puglisi. (1999) Recognition of the Codon-Anticodon Helix by Ribosomal RNA. *Science 285*, 4.

(54) Lia S. Nakao, E. F., and Ohara Augusto. (2002) Detection of C8-(1-Hydroxyethyl)guanine in Liver RNA and DNA from Control and Ethanol-Treated Rats. *Chem Res Toxicol 15*, 6.

(55) Augusto, L. S. N. a. O. (1998) Nucleic Acid Alkylation by Free Radical Metabolites of Ethanol. Formation of 8-(1-Hydroxyethyl)guanine and 8-(2-Hydroxyethyl)guanine Adducts. *Chem Res Toxicol 11*, 7.

(56) Jolie K. Kwee, M. S. A., Helio A. Stefani, Ohara Augusto. (1998) Cell proliferation induced by 8-oxoguanosine and 8-methylguanosine, two adducts

produced by free radical attack on ribonucleosides and RNA. *Chemico-Biological Interactions 116*, 17.

(57) J. P. Henderson, J. B., J. W. Heinecke. (1999) Chlorination of nucleobases, RNA and DNA by myeloperoxidase: a pathway for cytotoxicity and mutagenesis by activated phagocytes. *Redox Report 4*, 2.

(58) Davies, C. L. H. a. M. J. (2002) Hypochlorite-Induced Damage to DNA, RNA, and Polynucleotides: Formation of Chloramines and Nitrogen-Centered Radicals. *Chem Res Toxicol 15*, 10.

(59) Badouard, C., Masuda, M., Nishino, H., Cadet, J., Favier, A., and Ravanat, J. L. (2005) Detection of chlorinated DNA and RNA nucleosides by HPLC coupled to tandem mass spectrometry as potential biomarkers of inflammation. *J Chromatogr B Analyt Technol Biomed Life Sci 827*, 26-31.

(60) J. P. Gould, J. T. R., and M. G. Miles. (1984) THE KINETICS AND PRIMARY PRODUCTS OF URACIL CHLORINATION. *Water Res 18*, 8.

(61) Jeffrey P. Henderson, J. B., Dianne M. Mueller, and Jay W. Heinecke. (2001) The Eosinophil Peroxidase-Hydrogen Peroxide-Bromide System of Human Eosinophils Generates 5-Bromouracil, a Mutagenic Thymine Analogue. *Biochemistry 40*, 8.

(62) Halina Sierakowska, R. R. S., Zbigniew Dominski, and Ryszard Kole. (1989) Inhibition of Pre-mRNA Splicing by 5-Fluoro-,5-Chloro-, and 5-Bromouridine. *J Biol Chem 264*, 7.

(63) Dennison, J. B., Balakrishnan, K., and Gandhi, V. (2009) Preclinical activity of 8-chloroadenosine with mantle cell lymphoma: roles of energy depletion and inhibition of DNA and RNA synthesis. *Br J Haematol 147*, 297-307.

(64) Christine M Stellrecht, H. V. V., Xiao-Feng Le, Weiqun Mao, and Shujun Shentu. (2014) ATP directed agent, 8-chloro-adenosine, induces AMP activated protein kinase activity, leading to autophagic cell death in breast cancer cells. *Journal of Hematology & Oncology 7*, 12.

(65) Yermilov, V. (1995) Formation of 8-nitroguanine by the reaction of guanine with peroxynitrite in vitro. *Carcinogenesis 16*, 6.

(66) Ma, N., Adachi, Y., Hiraku, Y., Horiki, N., Horiike, S., Imoto, I., Pinlaor, S., Murata, M., Semba, R., and Kawanishi, S. (2004) Accumulation of 8-nitroguanine in human gastric epithelium induced by Helicobacter pylori infection. *Biochem Biophys Res Commun 319*, 506-510.

(67) Akaike, T., Okamoto, S., Sawa, T., Yoshitake, J., Tamura, F., Ichimori, K., Miyazaki, K., Sasamoto, K., and Maeda, H. (2003) 8-nitroguanosine formation in viral pneumonia and its implication for pathogenesis. *Proc Natl Acad Sci U S A 100*, 685-690.

(68) Mitsuharu Masuda, H. N., Hiroshi Ohshima (2002) Formation of 8-nitroguanosine in cellular RNA as a biomarker of exposure to reactive nitrogen species. *Chemico-Biological Interactions 139*, 11.

(69) T. Nguyen, D. B., C. L. Crepsi, B. W. Penman, J. S. Wishnok, and Tannenbaum, S. R. (1992) DNA damage and mutation in human cells exposed to nitric oxide in vitro. *Proc Natl Acad Sci U S A 89*, 5.

(70) Rodrigues, A. F., Roecker, R., Junges, G. M., de Lima, D. D., da Cruz, J. G., Wyse, A. T., and Dal Magro, D. D. (2014) Hypoxanthine induces oxidative stress in kidney of rats: protective effect of vitamins E plus C and allopurinol. *Cell Biochem Funct 32*, 387-394.

(71) Jacquin C. Niles, J. S. W., and Steven R. Tannenbaum. (2000) A Novel Nitration Product Formed during the Reaction of Peroxynitrite with 2′,3′,5′-Tri-O-acetyl-7,8-dihydro-8-oxoguanosine: N-Nitro-N′-[1-(2,3,5-Tri-O-acetyl- -D-erythro-pentofuranosyl)- 2,4-dioxoimidazolidin-5-ylidene]guanidine. *Chem Res Toxicol 13*, 7.

(72) Chatgilialoglu, C., Duca, M., Ferreri, C., Guerra, M., Ioele, M., Mulazzani, Q. G., Strittmatter, H., and Giese, B. (2004) Selective generation and reactivity of 5'-adenosinyl and 2'-adenosinyl radicals. *Chemistry 10*, 1249-1255.

(73) Paul, R., and Greenberg, M. M. (2015) Rapid RNA strand scission following C2'-hydrogen atom abstraction. *J Am Chem Soc 137*, 596-599.

(74) Paul, R., and Greenberg, M. M. (2014) Independent generation and reactivity of uridin-2'-yl radical. *J Org Chem 79*, 10303-10310.

(75) Jacobs, A. C., Resendiz, M. J., and Greenberg, M. M. (2010) Direct strand scission from a nucleobase radical in RNA. *J Am Chem Soc 132*, 3668-3669.

(76) Shaik, R., Ellis, M. W., Starr, M. J., Amato, N. J., and Bryant-Friedrich, A. C. (2015) Photochemical Generation of a C5'-Uridinyl Radical. *Chembiochem 16*, 2379-2384.

(77) Harald Strittmatter, A. D., Urs Schwitter, Bernd Giese. (1999) Differences Between 4'-RNA and 4'-DNA Radicals during Anaerobic and Aerobic Strand Cleavage. *Angew. Chem. Int. Ed 38*, 3.

(78) Joseph J. Dalluge, T. H., Alan E. Sopchik, James A. McCloskey, and Darrell R. Davis. (1996) Conformational flexibility in RNA: the role of dihydrouridine. *Nucleic Acids Res 24*, 7.

(79) Conforti, P. F., Yingling, Y. G., and Garrison, B. J. (2007) Computational studies of ultraviolet ablation of poly(methyl methacrylate). *Journal of Physics: Conference Series 59*, 322-327.

(80) Paul, R., and Greenberg, M. M. (2016) Mechanistic Studies on RNA Strand Scission from a C2'-Radical. *J Org Chem 81*, 9199-9205.

(81) Roy, S., and Caruthers, M. (2013) Synthesis of DNA/RNA and their analogs via phosphoramidite and H-phosphonate chemistries. *Molecules 18*, 14268-14284.

(82) Martin, D. B. D. a. J. C. (1991) A useful 12-I-5 triacetoxyperiodinane (the Dess-Martin periodinane) for the selective oxidation of primary or secondary alcohols and a variety of related 12-I-5 species. *J. Am. Chem. Soc. 113*, 11.

(83) Khan, A. T., Khan, M. M., and Adhikary, A. (2011) Tetrabutylammonium tribromide (TBATB): a mild and efficient catalyst for O-isopropylidenation of carbohydrates. *Carbohydr Res 346*, 673-677.

(84) Manetto, A., Georganakis, D., Leondiadis, L., Gimisis, T., Mayer, P., Carell, T., and Chatgilialoglu, C. (2007) Independent generation of C5'-nucleosidyl radicals in thymidine and 2'-deoxyguanosine. *J Org Chem 72*, 3659-3666.

(85) Peter Stanetty, H. K., and Mark Mihovilovic. (1992) Directed ortho lithiation of phenylcarbamic acid 1,1-dimethylethyl ester (N-BOC-aniline). Revision and improvements. *J. Org. Chem. 57*, 5.

(86) Huan Zhu, M. H., Gerard L. Bannenberg, Peter Moldeus, Howard G. Shertzer. (1996) Effects of glutathione and pH on the oxidation of biomarkers of cellular oxidative stress. *Arch Toxicol 70*, 6.

(87) Zhang, H., Hay, E. B., Geib, S. J., and Curran, D. P. (2013) Radical Cyclizations of Cyclic Ene Sulfonamides Occur with β-Elimination of Sulfonyl Radicals to Form Polycyclic Imines. *J. Am. Chem. Soc. 135*, 16610-16617.

(88) Gilbert, M. F. a. B. C. (1986) Radical Reactions of Carbohydrates. Part 6. An Electron Spin Resonance. Study of the Reaction of the Hydroxyl Radical with Some Lactones derived from Sugars and with Ascorbic Acid. *J Chem Soc Perkin Trans II*, 9.

(89) Calvin J. Emanuel, M. N., Carla Ferreri, and Chryssostomos Chatgilialoglu. (1999) Kinetics of 2′-Deoxyuridin-1′-yl Radical Reactions. *J. Am. Chem. Soc. 121*, 2.

(90) Keri A. Tallman, C. T., Dong Jin Yoo, and Marc M. Greenberg. (1997) Release of Superoxide from Nucleoside Peroxyl Radicals, a Double-Edged Sword? *Journal of the American Chemical Society 120*, 7.

(91) Schumperli, M. T., Hammond, C., and Hermans, I. (2012) Reactivity of alpha-amino-peroxyl radicals and consequences for amine oxidation chemistry. *Phys Chem Chem Phys 14*, 11002-11007.

(92) Dibble, T. S. (2002) Mechanism and dynamics of the CH2OH + O2 reaction. *Chemical Physics Letters 355*, 8.

(93) Gabriel da Sliva, J. W. B. (2009) Role of the a-hydroxyethylperoxy radical in the reactions of acetaldehyde and vinyl alcohol with HO2. *Chemical Physics Letters 483*, 5.

(94) E. M. Evleth, C. F. M., M. T. Rayez, J. C. Rayez, W. Forst. (1993) Theoretical Characterization of the Reaction of HO2 with Formaldehyde. *J. Phys. Chem. 97*, 6.

(95) Ive Hermans, J.-F. M., Thanh Lam Nguyen, Pierre A. Jacobs, and Jozef Peeters. (2005) Kinetics of a-Hydroxy-alkylperoxyl Radicals in Oxidation Processes. HO2•-Initiated Oxidation of Ketones/Aldehydes near the Tropopause. *J. Phys. Chem. A 109*, 9.

(96) Domingo, J. M. A. a. V. M. (2005) Mechanism for the Gas-Phase Reaction between Formaldehyde and Hydroperoxyl Radical. A Theoretical Study. *J. Phys. Chem. A 109*, 9.

(97) Sakakura, A., Kawajiri, K., Ohkubo, T., Kosugi, Y., and Ishihara, K. (2007) Widely useful DMAP-catalyzed esterification under auxiliary base- and solvent-free conditions. *J Am Chem Soc 129*, 14775-14779.

(98) Xu, S., Held, I., Kempf, B., Mayr, H., Steglich, W., and Zipse, H. (2005) The DMAP-catalyzed acetylation of alcohols--a mechanistic study (DMAP = 4-(dimethylamino)pyridine). *Chemistry 11*, 4751-4757.

(99) V. A. Efimov, A. L. K., O. G. Chakhmakhcheva. (1993) Dipentafluorophenyl carbon-a reagent for the synthesis of oligonucleotides and their conjugates. *Nucleic Acids Research 21*, 8.

(100) Srivastava, S. C., Pandey, D., Srivastava, N. P., and Bajpai, S. P. (2011) RNA synthesis by reverse direction process: phosphoramidites and high purity RNAs and introduction of ligands, chromophores, and modifications at 3'-end. *Curr Protoc Nucleic Acid Chem Chapter 3*, Unit3 20.

(101) Suresh C. Srivastava, D. P., Naveen P. Srivastava, Satya P. Bajpai. (2010) WO 2010/027512 A2.

(102) Suresh C. Srivastava, N. P. S. (2011) US 2011/0137010 A1.

(103) Suresh C. Srivastava, N. P. S. (2015) WO 2015/039053 A2.

(104) Zaramella, S., and Bonora, G. M. (1995) The Application of H-Phosphonate Chemistry in the HELP Synthesis of Oligonucleotides. *Nucleosides, Nucleotides and Nucleic Acids 14*, 809-812.

(105) Zhu, X.-F., Williams, H. J., and Ian Scott, A. (2003) An Improved Transient Method for the Synthesis ofN-Benzoylated Nucleosides. *Synthetic Communications 33*, 1233-1243.

(106) Gholam H. Hakimelahi, Z. A. P., Kelvin K. Ogilvie. (1982) New catalysts and procedures for the dimethoxytritylation and selective silylation of ribonucleosides. *Can. J. Chem. 60*, 8.

(107) Al-Oudat, B., Salyer, A., Trabbic, K., and Bryant-Friedrich, A. (2013) 3'-Modified oligodeoxyribonucleotides for the study of 2-deoxyribose damage in DNA. *Bioorg Med Chem Lett 23*, 854-859.

(108) Yanli Xu, H. J., Zhenjun Yang, Liangren Zhang, Lihe Zhang. (2009) Synthesis and biological evaluation of novel neamine–nucleoside conjugates potentially targeting to RNAs. *Tetrahedron 65*, 12.

(109) Wexselblatt, E., Katzhendler, J., Saleem-Batcha, R., Hansen, G., Hilgenfeld, R., Glaser, G., and Vidavski, R. R. (2010) ppGpp analogues inhibit synthetase activity of Rel proteins from Gram-negative and Gram-positive bacteria. *Bioorg Med Chem 18*, 4485-4497.